

ORGANICS ON MARS

- Laboratory studies of organic material under simulated martian conditions -

Proefschrift

ter verkrijging van

de graad van Doctor aan de Universiteit Leiden,
op gezag van de Rector Magnificus Dr. D. D. Breimer,
hoogleraar in de faculteit der Wiskunde en
Natuurwetenschappen en die der Geneeskunde,
volgens besluit van het College voor Promoties
te verdedigen op donderdag 26 januari 2006

klokke 16.15 uur

door

Inge Loes ten Kate

geboren te Rotterdam in 1976

Promotiecomissie

Promotores	Prof. Dr. P. Ehrenfreund Prof. Dr. Ir. M. C. M. van Loosdrecht
Referent	Dr. J. D. Rummel
Overige leden	Prof. Dr. J. Bada Prof. Dr. E. F. van Dishoeck Dr. B. H. Foing Prof. Dr. Ir. J. G. E. M. Fraaije Dr. J. R. C. Garry Prof. Dr. P. T. de Zeeuw

The studies presented in this thesis were performed at the Leiden Institute of Chemistry and Leiden Observatory, departments of the Faculty of Mathematics and Natural Sciences, Leiden University, the Netherlands; the European Space Research and Technology Centre (ESTEC) of the European Space Agency (ESA), Noordwijk, the Netherlands; and at the Department of Biotechnology of the Faculty of Applied Sciences, University of Technology Delft, the Netherlands.

The study described in this thesis was supported by the Bio-Science Initiative of Leiden University.

Financial support by the European Space Research and Technology Centre (ESTEC) of the European Space Agency (ESA), Stichting Ruimteonderzoek Nederland (SRON), and the Leids Kerkhoven-Bosscha Fonds is gratefully acknowledged.

Printed by Optima Grafische Communicatie, Rotterdam.
ISBN: 90-8559-132-5

Contents

CHAPTER 1	7
General introduction	
CHAPTER 2	25
Investigating complex organic compounds in a simulated Mars environment	
CHAPTER 3	47
Amino acid photostability on the martian surface	
CHAPTER 4	63
The effects of martian near surface conditions on the photochemistry of amino acids	
CHAPTER 5	73
Analysis and survival of amino acids in martian regolith analogues	
CHAPTER 6	95
The behaviour of halophilic archaea under martian conditions	
CHAPTER 7	109
Nederlandse samenvatting	
Reference list	123
Curriculum vitae	141
Nawoord	143
Additional publications	145

Chapter 1

General introduction

This thesis describes the results of laboratory investigations of the reactions of certain amino acids and microorganisms under simulated martian surface conditions. An overview of the current state of knowledge of the planet Mars is given in this chapter. Furthermore the rationale behind the investigations is described. The research and its results are summarised at the end of this chapter.

1. MARS

Mars, named after the Roman god of War, is the fourth planet in our Solar System as seen from the Sun, with an average distance of 227.9 million kilometres (1.52 astronomical units, AU), see Fig. 1.

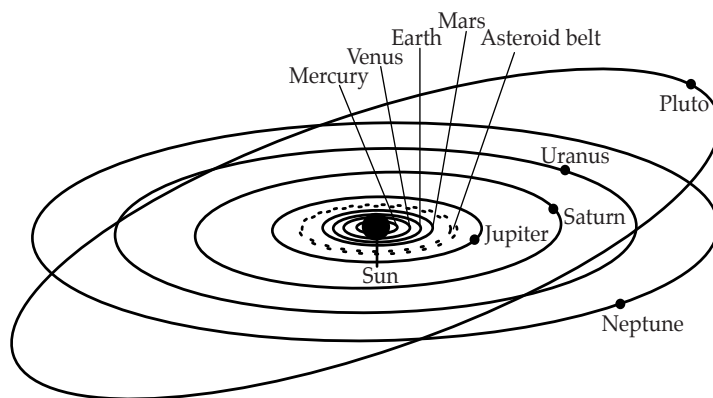


Fig. 1. Schematic overview of the Solar System (not on linear scale).

With a diameter of 6794 km, approximately half the size of the Earth, Mars is the seventh largest planet in the Solar System. Mars' orbit is much more elliptical than the Earth's, causing among other things a large temperature difference between perihelion and aphelion (the closest point towards and furthest point away from the sun). The average temperature on the surface is around 218 K (-55 °C), and can vary between 140 K (-133 °C) on the poles in winter and 300 K (+27 °C) around the equator on the day side in summer. Table 1 gives a comparison of characteristic parameters of the present day Mars and Earth. Fig. 2 shows a Hubble picture of Mars.

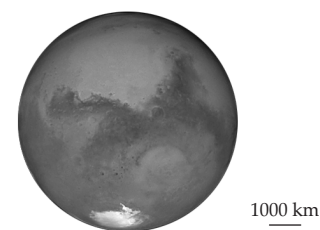


Fig. 2. Mars during its closest approach to Earth in 60,000 years. This picture was taken in August 2003 by the Hubble Space Telescope in orbit around the Earth, and is the most detailed view of Mars ever taken from Earth. Visible features include the south polar cap in white at the image bottom, the circular Huygens crater just to the right of the image centre, Hellas Impact Basin - the large light circular feature at the lower right, planet-wide light highlands dominated by many smaller craters, and large sweeping dark areas dominated by relatively smooth lowlands. Credit: J. Bell (Cornell U.), M. Wolff (SSI) *et al.*, STScI, NASA.

Table 1. Characteristic parameters of Mars and the Earth[§]

Characteristics	Mars	Earth
Equatorial radius	3397 km	6378 km
Approximate mass	0.64×10^{24} kg	5.97×10^{24} kg
Surface gravity	3.71 m s^{-2}	9.80 m s^{-2}
Average density	3933 kg m^{-3}	5515 kg m^{-3}
Mean distance from the Sun	227.9 million km (1.52 AU)	149.6 million km (1 AU)
Orbital eccentricity	0.09	0.02
Orbital period	686.98 days	365.26 days
Rotational period	24 h 37 min	23 h 56 min
Surface temperature	mean: 210 K (-63 °C); range: 140 K to 300 K (-133 °C to +25 °C)	mean: 288 K (15 °C); range: 184 K to 330 K (-89 °C to +57 °C)
Atmospheric composition (main gases, % by moles)	95.3% CO ₂ , 2.7% N ₂ , 1.6% Ar, 0.15% O ₂ , 0.08% CO, 0.03% H ₂ O	78.1% N ₂ , 20.9% O ₂ , 0.9% Ar, traces CO ₂ , CH ₄ , Ne, He, Kr, H
Atmospheric pressure	average 6.36 mbar (4-9 mbar)	average at sea level 1014 mbar
Number of satellites	2 (Phobos, Deimos)	1 (Moon)

[§]<http://nssdc.gsfc.nasa.gov/planetary/factsheet/marsfact.html>

The current state of knowledge about Mars has been obtained in several ways. Observations of the atmosphere and surface have been made by ground and space based telescopes. Meteorites that are believed to be of martian origin are analysed

for their chemical and geochemical composition. These meteorites are called SNC meteorites, named after the collection site of the first three meteorites believed to be from Mars (Shergotty, Nakhla and Chassigny). Moreover, Mars has been visited by many spacecraft (orbiters and landers), with varying degrees of success (see Table 2, p. 16,17). These close investigations have shown that our neighbouring planet has had an interesting history and that it likely harbours water in its subsurface.

2. MARS' INTERIOR

Mars has a relatively low density (3933 kg m^{-3}) compared to the other terrestrial planets (Earth (5515 kg m^{-3}), Venus (5243 kg m^{-3}) and Mercury (5427 kg m^{-3})), suggesting a relatively large fraction of lighter elements, such as sulphur.

Core

Like the Earth's, the martian core is assumed to consist mainly of iron and small amounts of nickel. Various compositional models suggest a core with a radius between 1500 and 2000 km and fractional mass of 15 to 30 %. However, from what is currently known of the geophysical and geochemical composition of Mars, various compositions could be possible, ranging from a nearly pure iron core comprising 15 % of the planet's mass, or a iron-nickel core of ~40 % of Mars' radius, to a core containing 34 weight% sulphur, constituting 24 % of the planet's total mass and 60 % of its radius (Schubert *et al.*, 1992, Longhi *et al.*, 1992, and references in both).

Observations from the Magnetometer and Electron Reflector (MAG-ER) instrument on the Mars Global Surveyor (MGS) showed that Mars currently does not have a global magnetic field. However, these observations suggest that Mars may have had a magnetic field in the distant past. This magnetic field would have been caused by an active core dynamo (Acuña *et al.*, 2001) that ceased to operate ~ 4 Gyr (10^9 year) ago (Acuña *et al.*, 1999). However, regions with a small magnetic field still exist. These fields are caused by the interaction of the solar wind with the atmosphere (Connerney *et al.*, 2001), and by magnetised crust that formed when Mars still had a global magnetic field (Acuña *et al.*, 1999).

Like Earth, Mars is influenced by the gravitational pull of the Sun. This causes a solid body tide with a bulge toward and away from the Sun. However, for Mars this bulge is much smaller than for the Earth. By measuring this bulge in the Mars gravity field, the flexibility (also called the solar tidal deformation) of Mars can be determined. As measured by Mars Global Surveyor (MGS) radio tracking, this deformation shows that it is large enough to rule out a solid iron core and indicates that at least the outer part of the core is liquid (Yoder *et al.*, 2003).

Mantle and crust

The thickness of the mantle and the crust can only be estimated from indirect evidence, which leads to quite some variation between the existing models. The thickness of the mantle is estimated to be 1500 to 2100 km (Schubert *et al.*, 1992). The mantle can be subdivided into an upper part (900-1100 km

thick) and a lower part (from the base of the upper part to the core). The estimates for the thickness of the crust vary widely between values of 9 km and 130 km for the Hellas basin only, and between 28 and 150 km for a global average. Models based on the composition of the SNC meteorites, however, predict that the densities used for these thickness estimates are much too low (Schubert *et al.*, 1992, Longhi *et al.*, 1992, and references therein).

The elemental composition of the mantle and the crust is estimated to be 36.8 to 44.4 % silicon dioxide (silica, SiO_2), 0.1 to 0.3 titanium dioxide (TiO_2), 3.0 to 6.4 % aluminium oxide (Al_2O_3), 0.4 to 0.8 % chromium oxide (Cr_2O_3), 27.4 to 32.7 % magnesium oxide (MgO), 15.8 to 26.8 % iron oxide (FeO), 0.1 to 0.5 % manganese oxide (MnO), 2.4 to 5.2 % calcium oxide (CaO), 0.1 to 1.4 % sodium oxide (Na_2O), 0.001 to 0.9 % water (H_2O) and 60 to 1200 part per million potassium (K). In addition, a range of minor and trace elements is present in the martian mantle (Longhi *et al.*, 1992, and references therein). The mineralogical composition of Mars is somewhat similar to that of the Earth; the most abundant mineral in the upper mantle is olivine ($(\text{Mg,Fe})_2\text{SiO}_4$) and the next most abundant is orthopyroxene ($(\text{Mg,Fe})\text{SiO}_3$) (Longhi *et al.*, 1992, Mustard *et al.*, 2005).

3. MARS' SURFACE

The history of Mars can be subdivided into three periods, the Noachian, the Hesperian, and the Amazonian, in chronologi-

cal order. These periods represent the major periods of geologic activity and are named after the surface region formed during that period (Tanaka *et al.*, 1992). From a geology point-of-view Mars is very different from the Earth. Mars has two very different hemispheres, with an abrupt change in elevation of 2-5 km kilometres between the old and heavily cratered highlands of the southern hemisphere and the younger, less cratered northern lowlands, a phenomenon known as hemispheric dichotomy (Smith *et al.*, 1999). The majority of the southern highlands are formed during the Noachian period. The northern lowlands, are mostly covered by lava flows and sediments of late Hesperian and Amazonian age (Tanaka *et al.*, 1992). The surface of Mars has more distinguished features, such as the volcano Olympus Mons (with a height of 24 km the largest mountain in the Solar System), Tharsis (a 4000 km long bulge with an elevation of 10 km), and Valles Marineris (a system of canyons with a depth between 2 and 7 km). Finally, Hellas Planitia, a 6 km deep impact crater with a 2000 km diameter, can be found in the southern hemisphere. Recent high resolution observations show channels indicative of past water flows on Mars, see Fig. 3. A molten rocky mantle and a thin crust build up the surface of Mars. Four major processes have shaped planet Mars in the past: plate tectonics, volcanism, impact cratering and erosion.

Plate tectonics

Recent observations have shown that the regional crustal magnetic field in Meridiani has characteristics that are, on Earth, unique to plate tectonics. This supports the idea that the crust of Mars is composed of plates formed in an early era,

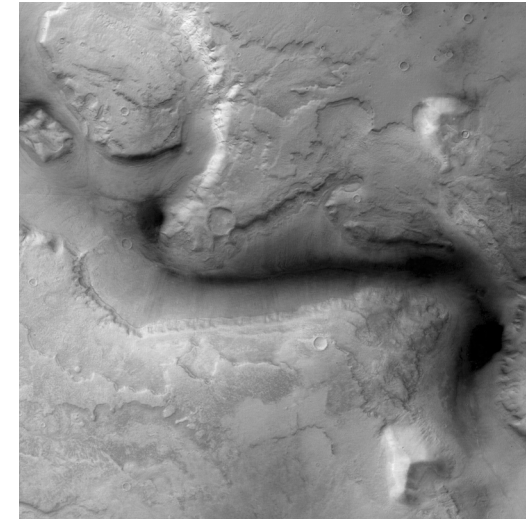


Fig. 3. Past water channels on Mars. This picture was taken by the High Resolution Stereo Camera (HRSC) onboard ESA's Mars Express orbiter, in colour and 3D, in orbit 18 on 15 January 2004 from a height of 273 km. The location is east of the Hellas basin at 41° South and 101° East. The area is 100 km across, with a resolution of 12 m per pixel, and shows a channel (Reull Vallis) once, almost certainly, formed by flowing water. The landscape is seen in a vertical view, North is at the top. Credits: ESA/DLR/FU Berlin (G. Neukum).

in the presence of a core dynamo. However, the thickness and size of the southern highland crust have led to ceasing plate motions, by growing beyond a critical fraction (0.5) of the planet's surface (Connerney *et al.*, 2005; Lenardic *et al.*, 2004; Banerdt *et al.*, 1992).

Volcanoes

Mars has the largest shield volcanoes in the solar system. Shield volcanoes are tall volcanoes with broad summit areas and low-sloping sides. The large scale of these volcanoes is caused by the fact that Mars lacks plate tectonics. Mars also has a wide range of other volcanic features, including large volcanic cones, unusual patera structures (flat, ash-shield volcanoes), mare-like volcanic plains, and a number of other smaller features. Volcanic features appear mostly in three regions. The largest part of those volcanoes can be found in Tharsis, consisting of 12 large volcanoes and a number of smaller ones, among which Olympus Mons and Alba Patera. Alba Patera is the largest volcanic structure on Mars, an area with a low elevation, but a large caldera, over 1500 km in diameter. A much smaller cluster of three volcanoes lies in Elysium, and a few paterae form the third region near the Hellas impact basin. New data from the High Resolution Stereo Camera (HRSC) onboard Mars Express indicate very recent volcanic activity, suggesting that the volcanoes are potentially still active today. The data show repeated activation and resurfacing of five major volcanoes, with phases of activity as young as two million years (Neukum *et al.*, 2004).

Impact cratering

Impact cratering is observed on the surface of all terrestrial planets. On Mars, craters occur in all sizes, from a few meters up to thousands of kilometres in diameter, like giant basins as Hellas, 2400 km, and Argyre, 1792 km across. More craters appear on the southern highlands than on the northern low-

lands, which may imply that the southern areas are older than the northern. The southern cratered highlands are thought to have formed around 3.5-4 Gyr ago; the northern lowlands were assumed to be much younger, through dating by extrapolating recent lunar and terrestrial impact rates to Mars. Recent studies, however, imply that this method may have caused an underestimation of the age, and that the northern lowlands are probably of the same age as the southern highlands (Chappelow and Sharpton, 2005).

Erosion

On the surface of Mars several erosive processes play a role, such as weathering, mass wasting by creep or land sliding, precipitation-driven runoff, erosion by ground water seepage, and wind-induced (aeolian) erosion and deposition. Several regions on Mars show topographic features that are suggested to have resulted from aeolian erosion, such as large-scale linear grooves and ventifacts (microscale pits in rocks) (e.g. Bridges *et al.*, 1999). Aeolian dust may be composed of fine-grained surface materials, like weathered rock particles and regolith, as well as material injected in the atmosphere by impacts and volcanic eruptions. Deposition of dust forms features like dunes and crater filling. Although Mars has a very thin atmosphere large dust storms occur on the surface. These dust storms are produced by high velocity seasonal winds correlated with solar heating of the surface and lead to high surface erosion. A recently discovered form of water erosion by the Mars Orbiter Camera (MOC) on MGS is the so-called gully (see section 5).

Soil

The surface of Mars is covered by a fine soil (see Fig. 4) that contains silicon, iron, aluminium, magnesium, calcium, titanium and is relatively rich in sulphur and chlorine, compared to terrestrial soils. Mars' red colour is caused by oxidation of iron in the soil and in rocks, when exposed to oxidants formed among others by photochemistry in the atmosphere. These and other oxidants are present in the soil as well, and may be one of the causes of the lack of organic material (e.g. Yen *et al.*, 2000). High concentrations of minerals, such as



Fig. 4. The surroundings of the Sagan Memorial Station on Mars, as observed by Mars Pathfinder. The big rock on the fine grained soil on the right is called Yogi and just to its left is the robot Sojourner Rover taking measurements of it. Other now-famous rocks are also visible including Barnacle Bill. Credit: IMP Team, JPL, NASA.

chlorine and sulphur salt-minerals, magnetically active minerals and jarosite (see section 5) have been detected. On the other hand, the soil seems to lack carbonates and clay minerals. (For reviews see Squyres *et al.*, 2004 a, b; Banin, 2005, and references therein; Yen *et al.*, 2005).

4. MARS' ATMOSPHERE

The major component (95.3 %) of the martian atmosphere is carbon dioxide (CO_2 , Kuiper, 1955). Other major gases in Mars' atmosphere are nitrogen, argon, oxygen and carbon monoxide (Owen, 1992). Water is a minor constituent, varying between 10 and 1000 parts per million (ppm, Encrenaz *et al.*, 2004a). Several other trace gases have been detected in the martian atmosphere, including hydrogen peroxide (20-50 parts per billion (ppb), Clancy *et al.*, 2004; Encrenaz *et al.*, 2004b) and methane (CH_4 , 5 ppb, Krasnopolsky *et al.*, 2004; Formisano *et al.*, 2004). The detection of CH_4 is debated, but important, due to its relation to biological processes and to non-equilibrium geochemistry. In contrast to the Earth's atmosphere, the martian atmosphere does not contain a significant amount of ozone (O_3 , 40-200 ppb, Owen, 1992), which acts on Earth as protection against ultraviolet radiation. The surface pressure ranges from 9 mbar in deep basins to 1 mbar at the top of Olympus Mons, with an average of 7 mbar, which is still thick enough for strong winds and dust storms to occur. There is a weak greenhouse effect, just enough to raise the surface temperature by a few degrees. This temperature rise is not sufficient to establish and maintain a surface

temperature where liquid water can exist. If the temperature is high enough for water-ice to melt, the atmospheric pressure is so low that water-ice directly evaporates. It is thought that Mars had a much denser atmosphere in the past. Due to its small mass and weak gravity Mars was not able to retain its atmosphere. Sputtering by solar wind may have additionally eroded the atmosphere, since Mars has lost its global magnetic field and corresponding protective magnetosphere. Mars' small size and lack of plate tectonics and active volcanoes prevent the CO₂ that is locked as carbonates, from being recycled back into the atmosphere. The current CO₂ cycle is predominantly caused by the seasonal condensation and sublimation in the polar regions (Owen, 1992).

5. WATER ON MARS

Polar ice caps

Mars has ice caps at the north and south pole, both growing and receding with the seasons. The north pole has a residual summer cap consisting of nearly 100 % water-ice, covered by a seasonal cap of CO₂ ice (Feldman *et al.*, 2003; Byrne and Ingersoll, 2003), and is surrounded by sand dunes. The south pole consists of layered deposits thought to be composed of dust and a mixture of CO₂ ice and water-ice (Bibring *et al.*, 2004; Titus *et al.*, 2003). Like the north pole, the south pole is covered with a seasonal CO₂ cap. The residual cap on the south pole shows a wider variety of geologic features than the cap on the north pole, indicating an asymmetry in the polar climates of Mars (Thomas *et al.*, 2000).

Equatorial regions

In 2002 the High Energy Neutron Detector, the Neutron Spectrometer and the Gamma-Ray Spectrometer on board Mars Odyssey identified hydrogen rich regions in both poles as well as in regions closer to the equator. Modelling suggests that tens of centimetres thick water-ice rich layers, similar to permafrost layers on Earth, exist in these regions, buried beneath hydrogen-poor soil (Mitrofanov *et al.*, 2002; Feldman *et al.*, 2002; Boynton *et al.*, 2002). The existence of such permafrost layers underneath the surface has been suggested already since the Viking missions (Bianchi and Flamini, 1977).

As described earlier, a gully can be formed by water flow, for example caused by the melting of snow deposits on the poles (Christensen, 2003). Most of the gullies detected on Mars are found in the south, occurring in regional clusters within the walls of a few impact craters, south polar pits and martian valleys (see Fig. 5). Their appearance can be explained by processes associated with ground water seepage and surface runoff. Also shallow and deep aquifers in the martian subsurface are thought to play a role in the formation of the gullies (Heldmann and Mellon, 2004). From the lack of impact craters overlaying the gullies and the relationship of the gullies to the underlying ground, the gullies are estimated to be relatively young, younger than a million years (Malin and Edgett, 2000).

Both Spirit and Opportunity discovered haematite at the surface of Mars, a mineral that on Earth is usually formed in the presence of water. Furthermore the instruments on Oppor-

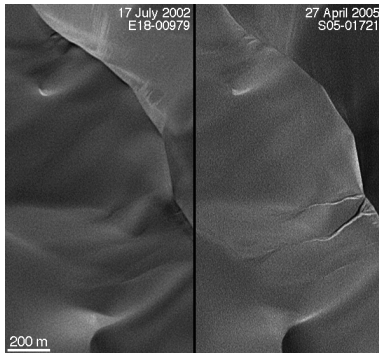


Fig. 5. Formation of a gully. This pair of images is taken by the Mars Orbiter Camera (MOC) onboard the Mars Global Surveyor. The images show a couple of gullies that have been formed during ~ 1.4 Mars years on a dune in an unnamed crater in the Hellespontus region, west of Hellas Basin. The 2002 image was obtained with the incident sunlight coming from a lower angle, relative to the horizon, than the 2005 image. If the gullies would have been present in 2002 their appearance would have been sharper and more pronounced than they are in the 2005 image. Credit NASA/JPL/MSSS/ASU

tunity detected high levels of sulphate salts (jarosite, an iron sulphate mineral), which on Earth would normally form in water. Opportunity also found rocks containing small spherules, nicknamed Blueberries, and indentations that point to modification by liquid water (Klingelhöfer *et al.*, 2004; Rieder *et al.*, 2004; Squyres *et al.*, 2004c).

6. LIFE ON MARS

From what is known on Earth, life needs water and life is sensitive to ultraviolet radiation. The absence of liquid water at the surface of Mars and the strong radiation environment, caused by the thin atmosphere and the lack of ozone, make Mars hostile to known terrestrial life. Several attempts have been undertaken to search for life on or from Mars. The Viking mission (see Table 2) was designed to search for evidence of life, as was the failed Beagle 2 mission. On Earth the martian meteorite ALH84001 has been examined for organic material and fossils of early, very small life forms (McKay *et al.*, 1996). Recent investigations by the Opportunity Rover in Meridiani Planum show aqueous and aeolian depositions in regions that were dry, acidic and oxidising. The measurements suggest that Meridiani Planum may have been habitable during at least part of the interval when the depositions took place (Knoll *et al.*, 2005).

The Viking Mission

The Viking mission consisted of two spacecraft, Viking 1 and Viking 2, both composed of an orbiter and a lander (Soffen, 1977). Viking 1 landed on July 20, 1976 at Chryse Planitia (22.48° N, 49.97° W), and Viking 2 at Utopia Planitia on September 3, 1976 (47.97° N, 225.74° W). The main goals of the mission were to obtain high resolution images of the martian surface, to characterise the structure and composition of the atmosphere and surface, and to search for evidence of life (Biemann *et al.*, 1977). The biology experiments initially could have pointed to life in the martian soil. Based on these results

the presence of a process that would destroy organic material in the near surface environment has been suggested. The results of the molecular analysis experiment, however, pointed towards the absence of organic compounds in the martian soil (see section 7). For a more in-depth description of the Viking missions see Chapter 2.

ALH 84001

Meteorite ALH84001, named after its discovery location Allan Hills on Antarctica, is thought to come from Mars. In 1996 it was reported that ALH84001 contained possible evidence for life on Mars, in the form of biogenic fossils, polycyclic aromatic hydrocarbons (PAHs) and magnetite (Fe_3O_4) (McKay *et al.*, 1996). This claim has been the subject of intense debates (Jull *et al.*, 1998), but more recently conclusions have been drawn that the fossils are probably artefacts and that magnetite and PAHs found within ALH84001 are terrestrial contamination (Barrat *et al.*, 1999), or have been produced inorganically, without biological influences (Kirkland *et al.*, 1999; Golden *et al.*, 2000; Thomas-Keprta *et al.*, 2001, 2002; Zolotov and Shock, 2000).

Future endeavours for life detection

Mars may have had better conditions to host life in the past. If life would have existed on the surface or in the near subsurface, remnants of this extinct life may be still present. From Earth it is known that life can survive under extreme conditions; early life on Mars could also have evolved into extreme life forms still present in the subsurface or underneath rocks. In the near future several missions will be launched to land

on the surface in order to conduct life-detection experiments. The Phoenix lander is designed to land in the north polar region (2007), the Mars Science Laboratory is to be launched in 2009, and ExoMars, the first European Mars rover is foreseen to be launched in 2011. These landers and rovers are expected to carry suites of instruments that are able to detect organic material in the ppb/ppt range and possible traces of life on Mars. In the context of these missions 'planetary protection' issues, such as contamination of martian soil with terrestrial bacteria, have to be evaluated (Rummel and Billings, 2004).

7. RATIONALE AND TOPIC OF THIS RESEARCH

As described in the previous section no organic material or any remnants have been detected on the surface of Mars. Organic material has, however, been detected in the interstellar medium (Millar, 2004; Ehrenfreund and Charnley, 2000; and references in both), in comets (see Crovisier, 2004, for a review), meteorites (Sephton, 2002; Botta and Bada, 2002; and references in both) and interplanetary dust particles (Schramm *et al.*, 1989; Flynn, 1996). A major source of organic material on the primitive Earth and Mars could have been delivered from space via comets and small interplanetary dust particles (e.g. Chyba *et al.*, 1990). Mars had a history of being bombarded like the Earth, with an estimated annual planet-wide amount of organic material, incorporated in dust particles, impacting intact on the surface in the order of 10^6 kg per year (Flynn, 1996). This extramartian material provides one

possible source of organic material on the surface of Mars. Endogenous production of organic material on Mars cannot be excluded. Several mechanisms for endogenous production of organic material on early Earth have been suggested, such as lightning, coronal discharge, UV radiation, and atmospheric shocks. Some of these processes could have played a role on early Mars as well (Chyba and Sagan, 1992).

The fact that no organic material has been detected on the surface of Mars leads to several questions:

- » Is infalling extramartian material overheated or burned during atmospheric entry?
- » Is extramartian material delivered intact, but destroyed on the surface by UV radiation?
- » Are there oxidising processes occurring in/on the surface that destroy organics?
- » What role does water play in the destruction of organic material?
- » Can organic material be detected underneath the martian surface or within rocks?
- » Were the Viking instruments sensitive enough?

It is possible that the Viking GCMS may have failed to detect certain types of organic material. Glavin *et al.* (2001) reported that the pyrolysis products (mainly ethylamine) of several million bacterial cells per gram of martian soil, would have fallen below the detection limits of the Viking GCMS, which had already been suggested by Klein (1978, 1979), but was never confirmed with experimental data. For a review see Klein *et al.* (1992). Benner *et al.* (2000) concluded that organic

molecules, such as benzenecarboxylates, oxalates and perhaps acetates are likely to have been formed on the martian surface via oxidation of impacted organic material. These compounds are not directly detectable by GCMS. Instruments with higher sensitivity (in the ppt range) using higher pyrolysis temperatures may be more successful in the future to pick up the signature of trace organics.

Next to the in-situ research as carried out by the Viking landers, Earth-based laboratory research and theoretical work has tried to answer some of these questions. A few related projects are briefly described. Oró and Holzer (1979) investigated the photolytic degradation of glycine, adenine and naphthalene adsorbed on powdered quartz, under UV radiation from a mercury discharge lamp (~245-275 nm) at room temperature (25 °C), 10 °C and 4 °C. They also investigated the oxidative effect of the presence of oxygen during irradiation. Their results indicate that only naphthalene breaks down significantly due to UV radiation, and that glycine and adenine only degrade in the presence of oxygen, implying that in the presence of oxygen, UV exposure enhances the oxidative degradation of the examined compound. Stoker and Bullock (1997) investigated photolytic degradation of glycine under UV radiation from a xenon lamp (~200-800 nm), when mixed with a Mars soil analogue under a Mars-like atmosphere. From their experiments they concluded that, even in the absence of oxidants, the surface conditions are severe enough to break down organic compounds at a faster rate than the rate at which they arrive at the surface. Yen *et al.* (2000) showed that, under a simulated martian atmosphere, superoxide radicals form on Mars-analogue surface minerals

when exposed to UV radiation. These radicals could play an important role in destroying organic material on the surface. Quinn *et al.* (2005a,b) have investigated the photochemical stability of carbonates under simulated Mars conditions as well as the aqueous decomposition of organic compounds in martian soils. From these experiments it is concluded that soil and water-ice may serve as a sink for photochemically produced oxidising species resulting in accelerated organic decomposition kinetics during wetting events. Their results also suggest that the apparent absence of carbonate deposits on the martian surface could be due to UV photodecomposition of calcite.

The research described in this thesis focuses on the stability of organic material on the surface of Mars, where UV radiation, atmosphere and temperature play a role. It is practically impossible to fully recreate planetary conditions in the laboratory. However, one of the advantages of experimental work is that simultaneously occurring effects may be studied separately, thus allowing us to investigate individual processes that give crucial insights into the complex multiparameter destruction processes of organics on Mars.

8. OUTLINE OF THIS THESIS

The search for organic molecules and traces of life on Mars has been a major topic in planetary science for several decades. 26 years ago Viking, a mission dedicated to the search for life on Mars, detected no traces of life. The search for ex-

tinct or extant life on Mars is the future perspective of several missions to the red planet. In order to determine where and what those missions should be looking for, laboratory experiments under simulated Mars conditions are crucial.

Chapter 2 describes experiments that are performed in support of future Mars missions. Besides the description of the experiments, the experimental hardware and set-up, this paper also gives the scientific rationale behind those experiments. The historical background of the search for life on Mars is outlined, followed by a description of the Viking Lander biology and molecular analysis experiments and their results, as well as a summary of possible reasons why no organic compounds have been detected. An overview on future missions is given stressing the relation between space missions and laboratory simulations.

Experiments performed to study the stability of thin films of two amino acids against UV irradiation are described in **Chapter 3**, together with a technical description of the equipment. The data obtained through these experiments are used to predict the survival time of these compounds on and in the martian regolith. We show that thin films of glycine and D-alanine are expected to have a half-life of 22 ± 5 hours and of 4 ± 2 hours, respectively, when irradiated with Mars-like UV flux levels. Fig. 6 shows the infrared (IR) spectra of glycine and D-alanine and the destruction after ~ 50 hours of UV irradiation. A model of amino acids embedded in the regolith with a mixing ratio of 1 ppb, shows that they would survive for as long as 10^7 years, when considering UV effects only.

Chapter 4 contains follow-up experiments to Chapter 3, describing the measured effects of two parameters, a CO₂ atmosphere and low temperature, on the destruction rate of amino acids when irradiated with Mars-like UV radiation. We measured the destruction rate of ~300 nm thick polycrystalline films of glycine deposited on silicon substrates, when irradi-

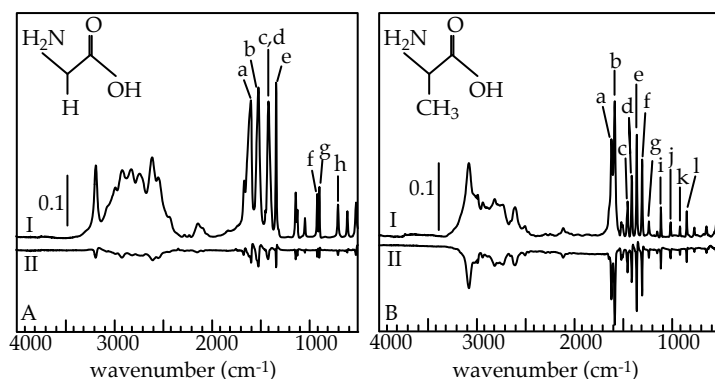


Fig. 6. The IR spectra of (A) solid glycine and (B) solid D-alanine in the range 4000-500 cm⁻¹ measured with a resolution of 4 cm⁻¹. Two spectra are shown, (I) is recorded before irradiation with a deuterium discharge lamp, and (II) is obtained by subtracting the spectrum of the unirradiated compound from the spectrum recorded after ~50 hours of irradiation. Our lamp spectrum has a ~25 times lower integrated flux than the UV flux in equatorial regions on Mars in the same wavelength range. The vertical scale bars show the infrared absorption in absorption units.

ated with UV (190-325 nm) in vacuum (~10⁻⁷ mbar), in a CO₂ atmosphere (~7 mbar), or when cooled to 210 K. The results show that the presence of a 7 mbar CO₂ atmosphere does not affect the destruction rate of glycine and that cooling the sample to 210 K (average Mars temperature) lowers the destruction rate by a factor of 7. A thin layer of water representative for martian conditions may have been accreted on the glycine film, but did not measurably influence the destruction rate. Our results form a basis for the understanding of more complex processes occurring on the martian surface, in the presence of regolith and other reactive agents. Low temperatures may enhance the stability of amino acids in certain cold habitable environments, which may be important in the context of the origin of life.

We have investigated the intrinsic amino acid composition of two analogues of martian soil, JSC Mars-1 and Salten Skov in **Chapter 5**. A Mars simulation chamber has been built and used to expose samples of these analogues to temperature and lighting conditions similar to those found at low-latitudes on the martian surface. The effects of the simulated conditions have been examined using high performance liquid chromatography (HPLC). Exposure to energetic UV light in vacuum at room temperature appears to cause a modest increase in the concentration of certain amino acids within the materials. This is interpreted as resulting from the degradation of microorganisms. The irradiation of samples at low temperature (210 K) in the presence of a 7 mbar CO₂ atmosphere showed a modest decrease in the amino acid content of the soil samples. It is probable that residual water, present in the chamber and

introduced with the CO₂ atmosphere, was adsorbed on the mineral surfaces. Adsorbed water is key to the generation of reactive species on mineral grains, leading to the destruction of amino acids. This implication supports the idea that reactive chemical processes involving H₂O are at work within the martian soil. Furthermore, we have demonstrated that an analogue such as Mars-1, which is used as a spectral and physical match to a nominal average martian soil, is inappropriate for a life-science study in its raw state.

Chapter 6 focuses on the response of halophilic archaea to Mars-like conditions, such as low pressure, UV radiation and low temperatures. 'Halophiles' form a class of bacteria and archaea that live in environments with high salt concentrations, in the order of ten times higher than the salt concentration of ocean water. Mars is widely thought to have had liquid water present at its surface for geologically long periods. The progressive desiccation of the surface has likely led to an increase in the salt content of remaining bodies of water. If life had developed on Mars, then some of the mechanisms evolved in terrestrial halophilic bacteria to cope with high salt content may have been shared by martian organisms. We have exposed samples of the halophilic archaea *Natronorubrum* sp. strain HG-1 to conditions of UV radiation that are similar to those of the present-day martian environment. Furthermore, the effects of low temperatures and low pressure have been investigated. The results, obtained by monitoring growth curves by both optical and cell-counting methods, indicate that the present UV radiation at the surface of Mars is a significant hazard for this organism. Exposure of

the cells to high vacuum inactivates ~50 % of the cells. Freezing to -20 °C and -80 °C kills ~80 % of the cells. When desiccated and embedded in a salt crust cells are somewhat more resistant to UV radiation than when they are suspended in an aqueous solution. The cell inactivation by UV radiation is wavelength dependent. Exposure to UV-A (longward of 300 nm) has no effect on the cell viability. Comparing irradiation using UV-B (250-300nm) to irradiation using UV-C (195-250 nm) indicates that UV-C is the most lethal to *Nr.* strain HG-1. Exposure to UV-B for a duration equivalent to ~80 hours of noontime equatorial illumination on the surface of Mars inactivated the proliferating capabilities of more than 95 % of the cells. From these experiments it can be concluded that *Nr.* strain HG-1 would not be a good model organism to survive on the surface of Mars, even when embedded in salt crystals.

Table 2. Chronology of Mars Exploration †

Mission name	Launch data	Goal
Marsnik 1 (Mars 1960A)	10 October 1960	Attempted mars fly by (launch failure)
Marsnik 2 (Mars 1960B)	14 October 1960	Attempted mars flyby (launch failure)
Sputnik 22	24 October 1962	Attempted mars flyby
Mars 1	1 November 1962	Mars flyby (contact lost)
Sputnik 24	4 November 1962	Attempted mars lander
Mariner 3	5 November 1964	Attempted mars flyby
Mariner 4	28 November 1964	Mars flyby
Zond 2	30 November 1964	Mars flyby (contact lost)
Zond 3	18 July 1965	Lunar flyby, mars test vehicle
Mariner 6	25 February 1969	Mars flyby
Mariner 7	27 March 1969	Mars flyby
Mars 1969A	27 March 1969	Attempted mars orbiter (launch failure)
Mars 1969B	2 April 1969	Attempted mars orbiter (launch failure)
Mariner 8	8 May 1971	Attempted mars orbiter (launch failure)
Cosmos 419	10 May 1971	Attempted mars orbiter/lander
Mars 2	19 May 1971	Mars orbiter/ attempted lander
Mars 3	28 May 1971	Mars orbiter/ lander
Mariner 9	30 May 1971	Mars orbiter (partner mission with Mariner 8)
Mars 4	21 July 1973	Mars flyby (attempted mars orbiter)

Mission name	Launch data	Goal
Mars 5	25 July 1973	Mars orbiter
Mars 6	5 August 1973	Mars lander (contact lost)
Mars 7	9 August 1973	Mars flyby (attempted mars lander)
Viking 1	20 August 1975	Mars orbiter and lander
Viking 2	9 September 1975	Mars orbiter and lander
Phobos 1	7 July 1988	Attempted mars orbiter and Phobos lander
Phobos 2	12 July 1988	Mars orbiter and attempted Phobos lander
Mars Observer	25 September 1992	Attempted mars orbiter (contact lost)
Mars Global Surveyor	7 November 1996	Mars orbiter
Mars 96	16 November 1996	Attempted mars orbiter/landers
Mars Pathfinder	4 December 1996	Mars lander and rover
Nozomi (Planet B)	3 July 1998	Mars orbiter
Mars Climate Orbiter	11 December 1998	Attempted mars orbiter
Mars Polar Lander	3 January 1999	Attempted mars lander
Deep Space 2 (DS2)	3 January 1999	Attempted mars penetrators
2001 Mars Odyssey	7 April 2001	Mars orbiter
Mars Express / Beagle 2	2 June 2003	Mars orbiter and attempted lander
Spirit (MER A)	10 June 2003	Mars rover
Opportunity (MER B)	7 July 2003	Mars rover

*<http://nssdc.gsfc.nasa.gov/planetary/factsheet/marsfact.html>

Chapter 2

Investigating complex organic compounds in a simulated Mars environment

The search for organic molecules and traces of life on Mars has been a major topic in planetary science for several decades. 26 years ago Viking, a mission dedicated to the search for life on Mars, detected no traces of life. The search for extinct or extant life on Mars is the future perspective of several missions to the red planet, for example Beagle 2, the lander of the Mars Express mission. In order to determine what those missions should be looking for, laboratory experiments under simulated Mars conditions are crucial. This review paper describes ongoing experiments that are performed in support of future Mars spacecraft missions. Besides the description of the experiments, the experimental hardware and set-up, this paper also gives the scientific rationale behind those experiments. The historical background of the search for life on Mars is outlined, followed by a description of the Viking Lander *biology* and *molecular analysis experiments* and their results, as well as a summary of possible reasons why no organic compounds have been detected. A section about organic compounds in space discusses the organic molecules we will use in simulation experiments. The set-up is discussed briefly in the following section. We conclude with an overview on future missions stressing the relation between these missions and our laboratory experiments. The research described in this article has been developed as part of a Mars Express Recognised Cooperating Laboratory RCL, and for planned future Mars missions such as the PASTEUR lander.

Inge Loes ten Kate, Richard Ruitkamp, Oliver Botta, Bernd Lehmann, Cesar Gomez Hernandez, Nathalie Boudin, Bernard H. Foing, Pascale Ehrenfreund
International Journal of Astrobiology 2003; 1(4):387-399

1. MARS, THE HISTORICAL PERSPECTIVE

For centuries humankind has been curiously watching the night sky with its stars and planets. One of the fundamental questions has always been if there is life beyond the Earth. Mars, the next planet further out in the solar system has always played a major role in this context (see Table 1).

In 1892 Camille Flammarion published a book called, “La Planète Mars et ses Conditions d’Habitabilité”. It contained a compilation of all credible telescope observations of Mars carried out until then, and Flammarion’s main conclusion was that Mars has dry plains and shallow seas, and that it is obviously habitable. He also speculated about canals built

by a higher civilisation than the one on Earth. This speculation was probably built on the apparent “discovery” of canals by Giovanni Schiaparelli in 1877, who thought that he saw a geometric network of straight canals appearing in pairs. When Percival Lowell heard about the canals on Mars he got so excited that he immediately started to build his own observatory. Even before he started his observations he stated that the canals could be nothing else than the result of the work of very intelligent beings. His observations showed that the canal network was too regular to be natural, so he concluded that they should have been created by a species more advanced than humans. Furthermore he published that the polar caps seen on the planet could be nothing else than water-ice and that the dark spots seen along the canals were growth of vegetation. His theories were widely accepted until Lowell started writing about similar canals on Venus, which were very soon afterwards proven not to exist. Very recently Sheehan and Dobbins (2002) published that Lowell narrowed the lens of his telescope that far that he created an ophthalmoscope, with which he saw the reflection of his own eyeball. Nevertheless, several of his martian theories lasted for decades.

Even in 1961, only a few years before the first space mission was launched to Mars, de Vaucouleurs published still some of Lowell’s ideas. In his ‘The Physics of the Planet Mars’, de Vaucouleurs wrote that Mars had a 85 mbar nitrogen atmosphere, was cold, but with a tolerable surface temperature, had seasonal changes probably due to vegetation, and that the polar ice caps are not composed of frozen CO₂ but of water-ice.

Table 1. Main characteristic parameters of Mars[§]

Average distance from the Sun	227.9 million km (1.52 AU)
Length of year	686.98 days
Length of day	24 h 37 min
Temperature	-133 °C to +27 °C (av. -60 °C)
Atmosphere	95.3 % CO ₂ , 2.7 % N ₂ , 1.6 % Ar, 0.15 % O ₂ , 0.08 % CO, 0.03 % H ₂ O
Atmospheric pressure	7 mbar (~1/100 th of Earth’s)
Gravitational acceleration	3.68 m s ⁻² (0.375 × g _{Earth})
Solar constant	43 % of Earth’s
Solar UV	190 – 280 nm

2. MARS DURING THE SPACE AGE

In 1960 the Soviet Union started a new era in the exploration of Mars, by sending a spacecraft, Mars 1960A, to Mars. Unfortunately this mission and seven of its successors failed, making the US' mission Mariner 4 in 1965 the first mission to reach Mars. Mariner 4, looking at Mars from a distance of 9,846 km, sent back data suggesting that Mars looked similar to the Moon, with a cratered surface (Chapman *et al.*, 1969). Also a surface atmospheric pressure of 4.1 to 7.0 mbar could be estimated and no magnetic field was detected. Mariner 6 and 7, launched in 1969, did more detailed research and revealed that the surface of Mars is very different from the surface of the Moon, in contrast to the results of Mariner 4. Furthermore the spacecraft showed a south polar cap predominantly composed of CO₂, and a atmospheric surface pressure between 6 and 7 mbar (e.g. Herr *et al.*, 1970). In 1971 the Soviet Union sent two spacecraft to Mars, Mars 2 and 3. In spite of the failing of the landers, the orbiters sent back new data that enabled creation of surface relief, temperature and pressure maps, and gave information on the martian gravity and magnetic fields (e.g. Marov and Petrov, 1973). The data led to the following discoveries:

- » mountains up to 22 km
- » H₂O in the upper atmosphere
- » surface temperatures of 163 to 286 K
- » surface pressures of 5.5 to 6 mbar
- » water vapour concentrations 5000 times less than in Earth's atmosphere

- » the base of the ionosphere starting at 80 to 110 km altitude
- » grains from dust storms as high as 7 km in the atmosphere.

The first detailed images of the volcanoes, Vales Marineris, the polar caps and the moons Phobos and Deimos, were delivered by Mariner 9 (e.g. Veverka *et al.*, 1974). This spacecraft, launched in 1971, also revealed new data on global dust storms, the tri-axial figure of Mars, the rugged gravity field and evidence for surface Aeolian activity. In 1973, two partly successful Soviet missions were launched, Mars 5 and 6, that revealed more data on the surface and the atmosphere, followed by the Viking missions in 1975 (see next section). After more than a decade two Phobos missions were launched by the Soviet Union in 1988. Unfortunately both missions failed due to communication problems, one after two, one after nine months.

The next completely successful mission to the red planet, the Mars Pathfinder Mission, was launched in 1997, and landed in the Ares Vallis region at 19.33 °N, 33.55 °W. Using a small rover to drive around on the surface, many atmospheric and surface data were obtained (e.g. Golombek, 1997). Some rocks at the landing site appeared to be high in silica, unlike what was expected from the martian meteorites found on Earth. Rounded pebbles and grooved rocks suggested liquid water in the past. The elemental composition of the soil appeared to be similar to the landing sites of Viking 1 and 2. Whirlwinds that probably mix dust into the atmosphere and cause the

so-called gardening of the soil, were analysed. Early morning water-ice clouds, which evaporated when the temperature rose, were detected in the lower atmosphere, as well as abrupt temperature fluctuations.

After Pathfinder six missions were launched of which the Japanese Nozomi-planetB mission is still on its way and will arrive in 2003. The only two missions that succeeded in reaching Mars were Mars Global Surveyor (MGS), launched in 1996, and 2001 Mars Odyssey. MGS showed the possible presence of water on Mars by imaging relatively young landforms and gullies. This spectacular result was endorsed by the results of the Mars Odyssey mission that found large quantities of hydrogen and water-ice just underneath the surface of Mars (Mitranov *et al.*, 2002; Feldman *et al.*, 2002; Boynton *et al.*, 2002). The results of these missions have put the search for possible life in a completely new perspective.

3. THE VIKING MISSION

The Viking mission consisted of two spacecraft, Viking 1 and Viking 2, each composed of an orbiter and a lander (Soffen, 1977). The main goals of the mission were to obtain high resolution images of the martian surface, to characterise the structure and composition of the atmosphere and surface, and to search for evidence of life. Viking 1 was launched on August 20, 1975 and entered Mars orbit on June 19, 1976. The first month of orbiting was used to find appropriate landing sites for the Viking Landers. On July 20, 1976 the Viking 1 Lander landed at Chryse Planitia (22.48 °N, 49.97 °W). Viking 2 was

launched September 9, 1975 and arrived at Mars on August 7, 1976. The Viking 2 Lander landed at Utopia Planitia (47.97 °N, 225.74 °W) on September 3, 1976.

3.1 Lander Experiments

The Viking landers (Fig. 1) carried several experiments onboard, among which a biological and a molecular analysis experiment. These experiments had as their main purpose the search for life related organic molecules and organisms.

Biological investigations and results

The biology experiment searched for the presence of martian organisms by looking for metabolic products. To perform this search the experiment was equipped with three instruments that incubated samples of the martian surface under varying environmental conditions, the gas exchange (GEx) experiment, the pyrolytic release (PR) or carbon assimilation experi-

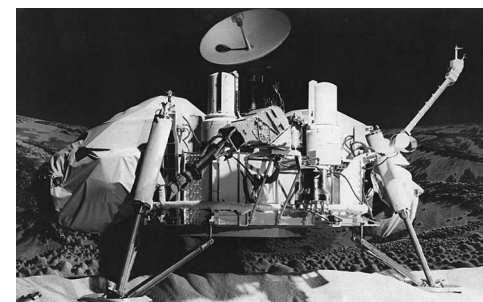


Fig. 1: Viking lander

ment, and the labelled release (LR) experiment (Biemann *et al.* 1977; Klein, 1978).

The GEx experiment measured the production of CO₂, N₂, CH₄, H₂, and O₂ and the uptake of CO₂ by soil samples (Oyama and Berdahl, 1977). A sample was sealed and purged with He, followed by incubation with a mixture of He, Kr, and CO₂. Thereafter a nutrient solution was added and the sample was incubated. At intervals, samples of the atmosphere were taken and analysed by a gas chromatograph with a thermal conductivity detector. The experiments were performed in two modes, the "humid" and the "wet" mode.

In the "humid" mode the nutrient medium, composed of a mixture of organic compounds and inorganic salts, was added without soil contact, and the soil was only exposed to the water vapour in the atmosphere. The results showed that some CO₂ and N₂ was released from the soil and that oxygen was produced rapidly after humidification. This rapid production of oxygen, in combination with the facts that (a) adding water in a later stage did not cause further release of oxygen, and (b) oxygen was also released from a sterilised sample (145 °C for 3.5 hours), clearly excludes a biological explanation of the results.

In the "wet" mode the nutrient made contact with the soil. The results from the "wet" mode confirmed results of the "humid" mode (Klein, 1978), because (a) the release of CO₂ also occurred in sterile samples, and (b) the CO₂ production rate slowed down, when the used nutrient was replaced with fresh nutrient.

The PR experiment was designed to detect the photosynthetic or chemical fixation of ¹⁴CO₂ or ¹⁴CO or both (Horowitz *et al.*, 1977). Soil samples were incubated in the presence of an atmosphere of ¹⁴CO or ¹⁴CO₂, some with and some without simulated sunlight. After several days of incubation each sample was heated to 120 °C to remove the ¹⁴CO and ¹⁴CO₂ that had not reacted. Next, the soil was pyrolysed at 650 °C and organic products were collected in an organic vapour trap. Finally, the trap was heated to combust any organic material to CO₂ and any evolved radioactive gas was measured. The results showed that heating the samples to 175 °C strongly reduced the reaction of ¹⁴CO and ¹⁴CO₂ with the sample, although heating to 90 °C did not have any effect. The data suggested that the reaction proceeded better in light, but storage of the soil within the spacecraft (in the dark) for four months did not affect the reaction.

The LR experiment used radio-respirometry to detect metabolic processes (Levin and Straat, 1977, 1981). This was done by adding an aqueous nutrient solution labelled with radioactive carbon (¹⁴C) to the soil sample. The atmosphere over the samples was continuously monitored to detect any radioactive gases released from these non-volatile nutrients. The LR produced the most controversial results. The results showed the rapid release of labelled gas upon addition of the nutrients. After an initial high peak, the gas production quickly dropped to a level where no further gas production could be detected. At that point 90 % of the nutrients was still left. When the samples were heated to moderate temperatures (40-50 °C) the reaction slowed down, whereas raising

the temperature to 160 °C caused the reaction to end. The reactions in the soil stopped as well when the samples were stored at the spacecraft for four months.

Molecular analysis experiments and results

The main purpose of the molecular analysis experiments of the Viking landers was to investigate whether or not organic compounds were present at a significant concentration at the surface of Mars (Biemann *et al.*, 1977). The soil analyses were performed using a gas-chromatograph mass-spectrometer (GCMS) with a high sensitivity, high structural specificity, and broad applicability to a wide range of compounds. A stepwise heating process vaporised substances from the surface material. Using $^{13}\text{CO}_2$, the released volatiles were then brought towards the gas-chromatographic (GC) column, where, using hydrogen as a carrier gas, the substances were separated. After hydrogen was removed, the residual stream moved into the mass spectrometer (MS), which created a mass spectrum (masses from 12 to 200 amu) every 10 seconds for the 84 minutes of the gas chromatogram. For atmospheric measurements, gases were directly introduced into the MS, bypassing the GC column.

In the four samples taken from surface and subsurface material from both landing sites, no organic compound, of martian origin, containing more than two carbons, were present at levels in the parts per billion (ppb) range and no one- and two-carbon-containing compounds at parts per million (ppm) level (Biemann *et al.*, 1977). Furthermore, no traces of meteoritic material were found (Biemann and Lavoie, 1979).

3.2 Conclusions from the Viking experiments

The results of the molecular analysis experiments clearly pointed towards the absence of organic compounds in the martian soil. Several explanations have been proposed, all pointing towards the suggestion that the production and infall rate of organic material is much smaller than the destruction rate.

The biology experiments initially could have pointed to life in the martian soil, especially the data of the LR experiments. However, in combination with the other results and when considering the non-detection of any organic compound in the upper soil made people search for a non-biological explanation. Based on these results the presence of a destructive oxidising agent, such as a metalperoxide or a superoxide, in the soil is suggested.

Recent experiments indicate that the pyrolysis products generated from several million bacterial cells per gram of martian soil would not have been detected at the ppb level, by the molecular analysis experiment (Glavin *et al.*, 2001). This has already been suggested by Klein (1978, 1979), but it was never confirmed with experimental data. Other research concluded that organic molecules, such as benzenecarboxylates, oxalates and perhaps acetates are likely to have been formed on the martian surface via oxidation of delivered organic material (Benner *et al.*, 2000). These compounds were very difficult for Viking to detect.

4. ORIGIN OF ORGANIC COMPOUNDS ON MARS

Early Earth and Mars may have been seeded with organic material from meteorites and comets, which have survived the impact. Such molecules may have been destroyed, altered or displaced into deeper soil layers, where they are protected against radiation and oxidation. The continuous, planet-wide meteoritic mass influx on Mars is estimated between 2700 and 59000 ton year⁻¹. This is equivalent with a meteoritic mass accretion rate between 1.8×10^{-5} to 4×10^{-4} g m⁻² year⁻¹. (Flynn and McKay, 1990)

4.1 Organic matter in asteroids, comets, and planetary satellites

Evidence for solid organic material on the surfaces of solar system bodies comes from astronomical and spacecraft observations. Three main groups of objects are important in this context: low albedo asteroids, which populate mainly the outer part of the asteroid belt, comets, and planetary satellites with low albedo surface features. The cause of the low albedos of these objects is believed to be the presence of macromolecular carbon bearing molecules (kerogen-like material), elemental carbon, and other opaque minerals (e.g. magnetite).

Low-albedo asteroids are thought to be the main source of most carbonaceous chondrites. They have largely featureless spectra, and their albedos are similar to the C-bearing, dark carbonaceous chondrites. Thus, C and also P- and D-type asteroids are thought to contain organic carbon and/or

complex organic compounds in their regolith (Cronin *et al.*, 1988). Comparisons of telescopic reflectance spectra of C and G type asteroids with laboratory reflectance spectra of carbonaceous meteorites showed a close match when the Murchison samples were heated to 900 °C (Hiroi *et al.*, 1993). A spectroscopic survey of primitive objects in the solar system and a comparison of these spectra to laboratory samples that included meteorite powder, tar sand, carbon lampblack, coal and synthetic graphite provided an upper limit of 3 % organic carbon on the surfaces of main belt asteroids (Luu *et al.*, 1994). Comets are thought to contain significant amounts of organic compounds (Kissel and Krueger, 1987). Estimates are in the range of 23 wt% for the complex organic refractory material and 9 wt% for the extremely small carbonaceous particles (Greenberg, 1998).

A recently discovered class of solar system bodies is the Centaurs, small bodies with orbits crossing those of the outer planets (Yeomans, 2000). In contrast to the featureless reflectance spectra of low-albedo asteroids in the main belt, one object in this class, 5145 Pholus, shows an unique absorption pattern in its reflectance spectrum. This pattern can be explained by the presence of a common silicate (olivine), a refractory solid complex of organic molecules (tholin), water and methanol ices, and carbon in the form of partially processed remnants of the original interstellar organic material on its surface (Cruikshank *et al.*, 1998). The spectrum is so well fit by a rigorous model that includes all of the basic components of comets, that it seems reasonable to assume that Pholus is the nucleus of an inactive comet.

Titan, the largest moon of Saturn, has a thick atmosphere with a surface pressure of 1.5 bar and an average surface temperature of 95 K. An orange-coloured haze of aerosol particles prevents a direct view onto the surface. Laboratory experiments have shown that this haze is spectroscopically similar to the mixture of organic material known as "tholin", which has been produced by photochemical experiments in the laboratory (McDonald *et al.*, 1994). Tholins yield amino acids upon acid hydrolysis, indicating the possibility of aqueous organic chemistry on Titan if liquid water is present for significant periods of time. In addition, because of its large inventory of organic compounds, including hydrocarbons and nitriles, detected in its atmosphere, Titan is considered a natural laboratory for prebiotic organic chemistry, with the main difference to the early Earth being the average surface temperature over time (Sagan *et al.*, 1992).

4.2 Meteorites

Laboratory evidence for the presence of organic compounds on other solar system bodies comes primarily from the research on carbonaceous chondrites, which are the most primitive meteorites in terms of their elemental composition. These meteorites contain up to 3 weight % of organic carbon, the majority of which is bound in an insoluble component. The soluble fraction can be obtained by treating a crushed meteorite sample with a series of solvents of different polarity, which leads to the presence of complex mixtures of compounds in the individual extracts. The total soluble fraction of CI(1) and CM(2) chondrites was estimated to contain 30-40 %

of the total carbon (Hayes, 1967), which is probably an upper limit due to the additional dissolution of inorganic salts in the polar solvents (Cronin and Chang, 1993).

The insoluble fraction of carbonaceous chondrites is composed of macromolecular matter that is commonly referred to as "kerogen-like" material (Gardinier *et al.*, 2000). Kerogen is insoluble macromolecular organic matter, operationally defined as the organic residue left after acid demineralisation of a rock. The study of organic compounds in this phase is similar to their analysis in coal, oil shale and petroleum source rocks and involves the dissolution of the mineral fraction of the rock by attack with HCl in combination with HF (Robl and Davis, 1993). The structure of the macromolecular carbon, the "polymer-like" component in the insoluble carbon fraction, is not well characterised. Based on pyrolytic release studies, Zinner (1988) calculated a formula of $C_{100}H_{48}N_{1.8}O_{12}S_2$ for this material in Murchison. Results from ^{13}C -NMR spectroscopic measurements of partially demineralised samples also suggest that polycyclic aromatic rings are an important structural feature in the insoluble carbon of the Murchison, Orgueil and Allende meteorites (Cronin *et al.*, 1987). However, these measurements also suggest that this material contains abundant aliphatic substituents that are probably bridging the aromatic units. All these features point to a resemblance of the meteoritic macromolecular carbon to aromatic terrestrial kerogens.

The soluble fraction of the organic matter in carbonaceous chondrites can be obtained by extracting powdered meteorite samples with solvents of varying polarity. About one third of this soluble fraction is comprised of polycyclic aromatic

Table 1. Abundances of water-soluble organic compounds found in meteorites (Botta and Bada, 2002). Amino acids concentrations have been determined for several CI and CM chondrites. All other data are for the CM chondrite Murchison (except the aromatic hydrocarbons and the fullerenes).

Compound Class	Concentration (ppm)
Amino Acids	
CM meteorites	17-60
CI meteorites	~ 5 ^{a)}
Aliphatic hydrocarbons	> 35
Aromatic hydrocarbons	3319 ^{b)}
Fullerenes	> 100 ^{c)}
Carboxylic acids	> 300
Hydroxycarboxylic acids	15
Dicarboxylic acids & Hydroxydicarboxylic acids	14
Purines & Pyrimidines	1.3
Basic N-heterocycles	7
Amines	8
Amides	
linear	> 70
cyclic	> 2 ^{d)}
Alcohols	11
Aldehydes & Ketones	27
Sulphonic acids	68
Phosphonic acids	2

^{a)} average of the abundances in the CI carbonaceous chondrites Orgueil and Ivuna (Ehrenfreund *et al.*, 2001a); ^{b)} for the Yamato-791198 carbonaceous chondrite (Naraoka *et al.*, 1988); ^{c)} 0.1 ppm estimated for C₆₀ in Allende (Becker *et al.*, 1994); ^{d)} Cooper and Cronin, 1995.

hydrocarbons (PAHs) with carboxylic acids and fullerenes present at abundances of one order of magnitude less. All other compound classes, including the biologically relevant amino acids and nucleobases, are present in concentrations of 1–100 ppm (see Table 1).

More than 70 extraterrestrial amino acids and several other classes of compounds including carboxylic acids, hydroxycarboxylic acids, sulphonic and phosphonic acids, aliphatic, aromatic and polar hydrocarbons, fullerenes, heterocycles as well as carbonyl compounds, alcohols, amines and amides have been detected in the CM meteorite Murchison as well as in other carbonaceous chondrites (see Table 1). Several amino acids that are extremely rare on Earth, such as α -aminoisbutyric acid (AIB) and isovaline, were found to be among the most abundant amino acids in several CM type carbonaceous chondrites (Botta *et al.*, 2002). In contrast, the CI carbonaceous chondrites Orgueil and Ivuna showed only high abundances of glycine and β -alanine. Only very low abundances of AIB, isovaline and other more complex amino acids were detected, which indicates that these meteorites originated on a parent body with an entirely different chemical composition or a different thermal evolution (Ehrenfreund *et al.*, 2001). Fig. 2 shows that the relative amino acid composition in the martian meteorites is close to identical to the terrestrial samples, and that these two sample sets differ significantly from the amino acid composition of the carbonaceous chondrites.

In all organisms on Earth, only the L-enantiomers (left-handed forms) of chiral amino acids are incorporated into proteins and enzymes. In contrast, abiological synthesis of chiral amino acids always yields a 1:1 mixture of the D- and

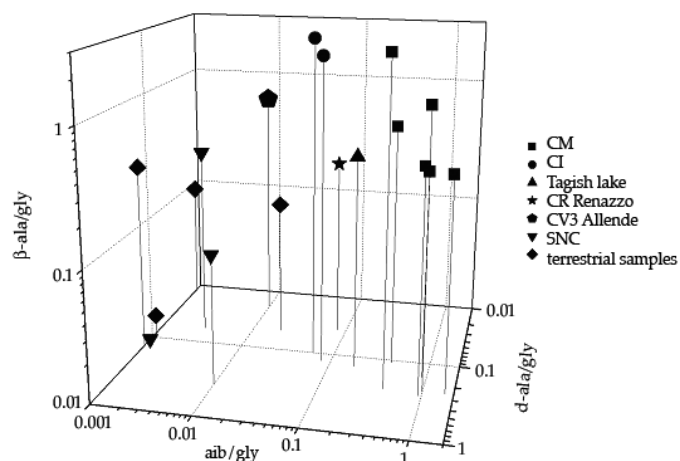


Fig. 2. 3-dimensional logarithmic diagram of the amino acid abundance ratios AIB/Gly, D-Ala/Gly and β -Ala/Gly. In this diagram the following samples are compared:

- » CM (Murchison, Murray, Mighei, Nogoya, Essebi, LEW90500), CI (Orgueil, Ivuna), CR (Renazzo), and CV3 (Allende) type carbonaceous chondrites and the Tagish Lake meteorite
- » three SNC (Shergotty, Nakhla, Chassigny-type) martian meteorites (ALH84001, ETAA79001 and Nakhla)
- » four terrestrial samples (Murchison soil, Nile Delta sediment, Tatahouine soil, Antarctic ice)

Note: the AIB/Gly ratios for Renazzo, Allende, martian meteorites, Tagish Lake, as well as all terrestrial samples are upper limits due to the non-detection of AIB in these samples. Also, the D-Ala/Gly ratios in Renazzo and Allende as well as the β -Ala/Gly in all martian meteorites are upper limits. Abbrev.: AIB: α -aminoisobutyric acid, β -Ala: β -alanine, D-Ala: D-alanine, Gly: glycine (Botta *et al.*, 2002).

L-enantiomers (a racemic mixture). Therefore, the molecular architecture of these compounds provides a powerful tool to discriminate between biological and non-biological origins of amino acids in meteorites. Until recently, all chiral amino acids (e.g. alanine or isovaline) in meteorite extracts were found to be present as racemic mixtures, which indicates an abiotic origin and therefore the presence of indigenous extraterrestrial amino acids. Enantiomeric excesses of the L-enantiomer of the two diastereoisomers of 2-amino-2,3-dimethylpentanoic acid (DL- α -methylisoleucine and DL- α -methylalloisoleucine) as well as isovaline, were found in Murchison hot-water extracts (Cronin and Pizzarello, 1997). Both are non-biological amino acids that, due to their molecular architecture, are not prone to racemisation (the conversion of an enantiomerically pure compound into a racemic mixture).

The content of N-heterocyclic compounds in meteorites was investigated by Schwartz and coworkers about 25 years ago. They found the pyrimidine uracil, a monocyclic aromatic ring containing two nitrogen atoms, in the Murchison, Murray and Orgueil meteorites in concentrations between 37 and 73 ppb (Stoks and Schwartz, 1979). Later, the purines adenine, guanine, xanthine and hypoxanthine, which are bicyclic rings with four nitrogen atoms and slightly different substitution patterns, were found in the same meteorites at abundances between 542 and 1649 ppb (Stoks and Schwartz, 1981). Finally, several other N-heterocyclic compounds, including 2,4,6-trimethylpyridine, quinoline, isoquinoline, 2-methylquinoline and 4-methylquinoline, were positively identified in the formic acid extract of the Murchison meteorite

(Stoks and Schwartz, 1982). Higher derivatives of quinolines and isoquinolines have also been detected in this meteorite (Krishnamurthy *et al.*, 1992).

Generally, meteoritic organic matter is enriched in deuterium, and distinct groups of organic compounds show isotopic enrichments of carbon and nitrogen relative to terrestrial matter (Irvine, 1998). These enriched isotope values, especially for deuterium, can be traced back to the isotopic fractionation associated with the very low temperatures in the interstellar medium, where the precursors (e.g. HCN, NH₃, and carbonyl compounds for the amino acids) formed by gas phase ion-molecule reactions and reactions on interstellar grain surfaces (for reviews see Smith, 1992; Herbst, 1995).

4.3 ALH84001

In 1996 it was reported that the martian meteorite ALH84001 (Fig. 3) contained possible evidence for life on Mars. It has been argued that this meteorite showed biogenic fossils (McKay *et al.*, 1996). The PAH component of meteorites has been invoked, as an integral part of the claim that the martian meteorite ALH84001 contains extinct microbial life, a claim that is currently the subject of intense debate (e.g. Jull *et al.*, 1998). Examination of carbonate globules and bulk matrix material of ALH84001 using laser absorption mass spectrometry indicated the presence of an organic component of high molecular weight, which appears to be extraterrestrial in origin (Becker *et al.*, 1999a).

Later research by Barrat *et al.* (1999) on the Tatahouine me-

eteorite, a non-martian meteorite that fell in 1931 in Tunisia, showed similar features as found in ALH84001, which were definitely formed on Earth. Kirkland *et al.* (1999) demonstrated that the bacteria-shaped objects as seen in ALH84001 can be formed without any biology being involved. This conclusion was also drawn by Golden *et al.* (2000), who published that “carbonates with chemical zoning, composition, size, and appearance similar to those in ALH84001 can be achieved by purely inorganic means and at a relatively low temperature”. Also Zolotov and Shock (2000) get to a similar conclusion, that, based on thermochemical calculations, the PAHs in ALH 84001 (and the proportions of the various PAH species) could reasonably have been produced inorganically, without biological influences.

Thomas-Keppta *et al.* (2001, 2002) continued the research, started by McKay *et al.* (1996), on carbonate globules and characterised a subpopulation of magnetite (Fe₃O₄) crystals,

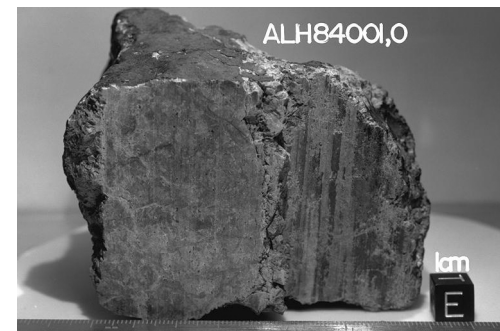


Fig. 3. ALH84001, picture courtesy NASA

which were found chemically and physically identical to terrestrial magnetites produced by the magnetotactic bacteria strain MV-1. The crystals are both single-domain, chemically pure and have both a crystal habit called truncated hexa-octahedral, which on Earth are exclusively produced biogenically. They suggested that the magnetite crystals were likely produced by a biogenic process and thus interpreted these results as evidence of life. Further research implied that approximately 25% of the magnetite crystals embedded in ALH 84001 is identical to terrestrial biogenic magnetite.

4.4 Possible destruction mechanisms on the martian surface

Since the science results of the Viking mission several scenarios have been proposed to explain the absence of organic matter in the martian soil. Biemann *et al.* (1977) suggested that the organic compounds would be destroyed by a combination of short wavelength UV, and oxygen, H₂O₂, metaloxides, or other oxidising agents. These oxidising agents in combination with short wavelength UV cause organics to be removed much faster than by UV alone, and are even destructive in the dark. The oxidising agent hypothesis is the most important one, although there are also arguments against it. The major reasons for this hypothesis are described below (see also Bullock *et al.*, 1994).

(a) In the Viking experiments (see section 3.1) the soil released O₂ when humidified in GEx (Oyama and Berdahl, 1977, 1979), but when the samples were wetted with nutrient solution no

additional O₂ was released. On the other hand during wetting a slow evolution of CO₂ occurred, indicating oxidation of organics by an oxidising agent. When the samples were heated to 145 °C the amount of O₂ was reduced by 50 % but not eliminated.

(b) The GCMS in the molecular analysis experiment did not detect organics in surface and below-surface samples, although there are at least two mechanisms that could produce organics, meteoritic infall, estimated by Flynn and McKay (1990), and UV production (Biemann *et al.*, 1977).

(c) The LR experiment showed a rapid release of ¹⁴CO₂ when samples were wetted with aqueous nutrient medium containing ¹⁴C. This rapid release was completely removed by heating to 160 °C for 3 hours and partially destroyed when heated to 40-60 °C. The sample stayed unaffected by storage at 18 °C for short time, but was lost after 2-4 months at that temperature.

Bullock *et al.* (1994) proposed that H₂O₂ is a good candidate for the thermally labile oxidant that produced rapid evolution of ¹⁴CO₂. This assumption is based on the results of the Viking LR experiments and experiments performed after Viking. Hunten (1979) suggested that H₂O₂, which could be the source of the oxidants in the LR experiments, is produced in the atmosphere by photochemical reactions at a rate of 2×10^9 molecules cm⁻² sec⁻¹. Huguenin *et al.* (1979) and Huguenin (1982) have suggested that chemisorbed H₂O₂ is produced by frost weathering of olivine. In the same year Oyama and Berdahl (1979) reproduced the LR experiment by reacting

formate with H_2O_2 and $\gamma\text{-Fe}_2\text{O}_3$ mixed with martian surface minerals. They also duplicated the slow CO_2 production in the LR and GEx experiments with a mixture of $\gamma\text{-Fe}_2\text{O}_3$ and formate. These findings were endorsed by Ponnampereuma *et al.* (1977), who also found a $^{14}\text{CO}_2$ production when the Viking nutrient mixture was added to $\gamma\text{-Fe}_2\text{O}_3$.

However, there are also arguments against H_2O_2 . Levin and Straat (1981) published that 1) H_2O_2 reacted also with other compounds in nutrients than formate, meaning that the H_2O_2 hypothesis did not account for the fact that only one compound in LR was oxidised to CO_2 ; and 2) H_2O_2 is much more thermally labile than the oxidant in LR nutrient. Other arguments against the H_2O_2 hypothesis are the short lifetime of only 10^4 seconds against UV destruction on the martian surface and that H_2O_2 alone cannot explain the thermally stable GEx results.

Another explanation in the oxidant hypothesis was given by Yen *et al.* (2000), who proposed “that superoxide radical ions (O_2^-) are responsible for the chemical reactivity of the martian soil”. This was concluded from laboratory experiments on the formation of O_2^- on Mars, which is expected to form readily on mineral grains at the surface. Addition of water to O_2^- produces O_2 , HO_2^- and OH . This explains the release of O_2 during humidification and injection of water into the martian soil samples by Viking, and is consistent with the decomposition of organic nutrients in the Viking experiments. The absence of organic compounds can as well be explained by the presence of O_2^- , and is likely caused by decomposition of oxygen radi-

cals and by the products of O_2^- reactions with the atmospheric water vapour.

A substantial fraction of ~ 140 molecules that have been identified in interstellar and circumstellar regions are organic in nature (Ehrenfreund and Charnley, 2000). Large carbon-bearing molecules (such as polycyclic aromatic hydrocarbons (PAHs), fullerenes, and unsaturated chains) are also thought to be present in the interstellar medium. The presence of large aromatic structures is evidenced by infrared observations of the interstellar medium in our galaxy and in extragalactic environments (Tielens *et al.*, 1999). A variety of complex aromatic networks is likely to be present on carbonaceous grains (see Henning and Salama (1998) for a review).

The total annual influx of organic material from space (IDPs, meteorites, etc) on Mars is estimated at approximately 300 tons per year (Chyba and Sagan, 1992). This influx will most likely consist of the above mentioned large aromatic networks, PAHs, fullerenes, as well as non-aromatic structures, like carboxylic acids, and amino acids.

Another theory for the fact that Viking did not find organic material is the destruction of organics by UV radiation. Stoker and Bullock (1997) have performed several laboratory experiments on organic degradation under simulated martian UV conditions. These experiments show an organic decomposition rate of $8.7 \times 10^{-4} \text{ g m}^{-2} \text{ yr}^{-1}$. This rate exceeds the upper limit of infalling organics, $4 \times 10^{-4} \text{ g m}^{-2} \text{ yr}^{-1}$. This leads to the conclusion that the organic compounds, which reach the martian surface as constituents of infalling micrometeorites,

are likely destroyed by UV breakdown as rapidly as they are added.

Non-aromatic organic structures will be destroyed by UV radiation (Ehrenfreund *et al.*, 2001b). Polycyclic aromatic structures on the other hand are more resistant to UV radiation. The PAH quaterrylene is among the largest of its class measured under space simulated conditions. Stable cations are formed when PAHs are subjected to Lyman- α UV radiation (10.2 eV) in inert matrices but there is no spectroscopic evidence of fragmentation (Ruiterkamp *et al.*, 2002). Since the martian atmosphere is opaque for radiation with energies higher than 6.5 eV (190 nm), all Lyman- α radiation will be absorbed. Thus PAHs with a high molecular mass, such as quaterrylene, are expected to survive the radiation environment on Mars. From Earth based tests with the Viking instruments (Biemann *et al.*, 1977) it is shown that Viking should have been capable of detecting these molecules. This implies that other (chemical) mechanisms of destruction such as oxidation may also effect PAHs exposed to the martian atmosphere.

5. MARS SIMULATION CHAMBER

5.1 Rationale

It is unclear why no traces of impacting organics have been found by Viking. It is likely that organic compounds are destroyed on the exposed surface, but may survive when protected in greater depth of martian dust and soil. In order to

determine the stability of specific organic compounds, laboratory simulations are a crucial step to understand chemical pathways on the martian surface.

In this context an experimental programme was developed at the European Space Research and Technology Centre of ESA, ESTEC, and Leiden University. The experimental research work includes the investigation of organic molecules subjected to simulated martian atmospheres. An atmospheric simulation chamber in combination with a solar simulator is used to collect data on the combined effects of UV photo-processing, atmospheric conditions and the presence/absence of oxidising agents on organic molecules. All those described effects will be studied independently and in combination in order to get insights in the individual processes and their interactions on organics in the martian soil. The organic compounds represent analogues for abundant meteoritic and cometary molecules and entail aliphatic and aromatic hydrocarbons, fullerenes, amino acids and nucleobases and carbonaceous solids.

5.2 Technical set-up

The Mars Simulation Chamber (MSC), used for the experiments, is an 80 cm long, 60 cm high vacuum chamber, which will be filled with a simulated Mars atmosphere. It is equipped with 17 flanged portholes and a hinged door that allow access to the interior of the chamber (Fig. 4 and 5). These flanged portholes are used for different purposes. To allow clean sample handling two differentially pumped rub-

ber gloves, isolated from the exterior by two O-ring sealed hinged blinds, were mounted on two ports at the side of the chamber. Above the gloves is another flange, which is used as a control window. A solar simulator fitted with a 1 kW Xenon lamp and CaF_2 window is mounted perpendicular to the experiment plane, above the top port with a quartz window.



Fig. 4. The Mars simulation facility at ESTEC.

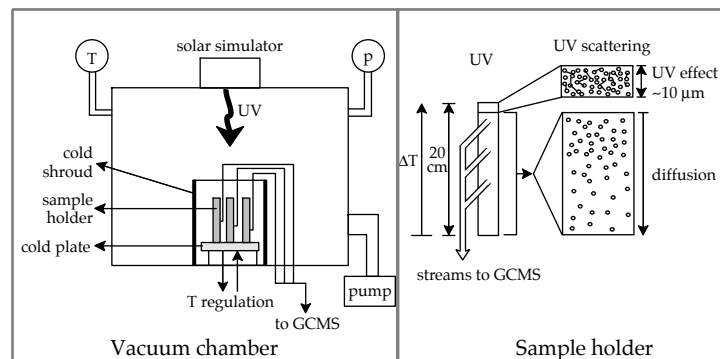


Fig. 5. Schematic outline of the Mars simulation chamber.

The remaining flanges are used as feed-through flanges that allow controlled access of cryogenic fluids to the cold plate and shroud in the chamber, sampling of the interior gas by a GCMS apparatus and the introduction of gases into the chamber.

A turbo molecular pump, backed by a rotary vane pump is connected to the chamber. The rotary vane pump is isolated from the chamber by a liquid nitrogen cold trap. The pumps can be separated from the chamber by an electric gate valve. An ion gauge and a pirani gauge monitor the pressure in the chamber.

The atmosphere in the chamber can be varied in pressure and in composition. The pressure maintained by the above mentioned pumps varies from $\sim 5 \times 10^{-6}$ mbar to ambient pressure. To simulate the current martian atmosphere we use a mixture

of N₂ (2.7 % volume), Ar (1.6 % volume), O₂ (1000 volumetric ppm), CO (500 volumetric ppm), H₂O (100 volumetric ppm), CO₂ (rest of mixture). This gas mixture is transferred into the chamber as a premixed atmosphere, from gas tanks placed next to the chamber. The electromagnetic radiation environment can be changed in intensity and in spectral composition by means of a deuterium lamp with a spectral range of 115-600 nm, that can be mixed in with the solar simulator. This allows us to simulate other eras in the martian or terrestrial history.

The organic samples are introduced in the chamber in six sample holders (Fig. 5), fastened onto a copper ground-plate that allows temperature control by means of slush solutions that are pumped through the plate. The sample containers are 20 cm long stainless steel tubes with a diameter of 1.5 cm, which can be sealed with an o-ringed stopper. Three sample sites allow in-situ measurements of the volatiles at three different heights in the containers, by means of stainless steel streams connected to a GCMS. The containers are welded to copper base-plates that are screwed onto the copper ground plate.

The temperature of the medium in the chamber can be cooled by means of a cold shroud positioned around the sample containers. Feed-through lines enable the cooling medium to enter the cold shroud, allowing the temperature of the gases inside the chamber to be set between liquid nitrogen temperatures and room temperature. The temperature of the sample holders can be set within the same range.

The experimental protocol comprises three parts: (1) preparation of the chamber, (2) setting the experimental parameters, and (3) in situ and post-processing measurements of the samples. During the preparation phase, sample tubes are filled with a mixture of martian soil simulant, JSC-1 (Allen *et al.*, 1998, 2000), organic compounds and oxidising agents, and are attached to the copper ground-plate. The feed through lines for the GCMS are connected to the sample holders and the chamber is pumped down to $\sim 5 \times 10^{-6}$ mbar. After closing the main gate valve the chamber is now filled with the simulation gases to a pressure of ~ 7 mbar. The experimental parameters that must be set prior to irradiation are the chamber temperature cycle, the sample temperature cycle and the in situ measurement protocol. During irradiation samples are taken from the volatiles inside the sample containers and fed to the GCMS in an automated fashion. Post-processing analysis of the samples by means of high performance liquid chromatography is performed with a Shimadzu HPLC system, equipped with a fluorescence detector, a diode array detector and an auto-injector. All equipment used in the experiments, such as the transfer lines, sample holders, but also the soil analogues, will be sterilised (3 hours at 500 °C) before use.

5.3 Complex organic samples

Specific organics will be embedded in either porous or compact martian soil analogues or quartz beads. The recessed surface in the sample trays will be deep in order to simulate the effects of the various processes on organics according to their depth in the soil analogues.

Samples will be adsorbed on martian soil analogues and quartz beads before exposure in the vacuum chamber. For these investigations, the sample holders will be charged with organic samples, such as,

1. simple aliphatic species, like pentane, hexane, octane
2. simple aromatic species, like benzene, naphthalene, biphenyl
3. oxygen bearing species, like methanol, formic acid
4. nitrogen bearing species, like acetonitrile, propanetrile
5. simple amino acids, like glycine, alanine
6. stable PAH molecules, like tribenzo(a,g,m)coronene, hexa-peri-benzocoronene, ovalene
7. reactive PAHs, like dibenzo(a,j)tetracene, pentacene, bisanthene
8. aza-, oxo-, thio-PAHs (since N and O are abundant elements in space)
9. PAH isomers, like benzo(a)pyrene / benzo(k)fluoranthene
10. fullerenes C_{60} , C_{70} and some of their hydrogenated compounds, as well as exohedral compounds with Na, K, Mg
11. carbonaceous solids, like AC, or HAC
12. kerogens and solid bitumens of different initial origin

5.4 Experimental approach

The following experiments will be simulated in the vacuum chamber:

- A. The effects of the martian atmosphere
The chamber will be filled with gases simulating the

evolution of the martian atmosphere (CO_2 , N_2 and Ar and traces of O_2 and CO). In order to simulate the clement phase of Mars' early atmosphere, pressures of 1-15 bars of CO_2 have been reported.

- B. The effect of UV irradiation on organic molecules embedded in the soil

The solar UV flux may penetrate into the martian soil down to a few mm due to scattering. We intend to simulate the UV irradiation with microwave discharge lamps and deuterium lamps, which can be attached to the vacuum chamber. Filters will be used to simulate the variation of the solar UV flux between 190-280 nm according to the O_3 content in the martian atmosphere.

- C. The effect of oxidation on organic molecules in the soil

As oxidising agents we intend to use mostly H_2O_2 , which will yield CO and CO_2 that escape the samples while breaking aliphatic bonds. Additionally, O_3 (present in the martian atmosphere) will be added as gas in the chamber in order to study oxidation effects. The O_3 fixation on Earth in the ground has been estimated to be 0.07 cm s^{-1} and therefore O_3 may be of relevance for the martian soil.

- D. The effect of thermal cycling on the surface

We shall reproduce the thermal (e.g. 180-280 K) cycling, and measure the evolution and thermal degradation products of embedded organics. In the higher temperature range, the sublimation rates of the more volatile compounds will be significant.

6. FUTURE MISSIONS

Below, several Mars missions that will be launched in the near future are briefly described. All these missions will include instruments capable of searching for evidence of water and of early (or even present) life.

Mars Express

Mars Express (ESA) will be launched in June 2003. Its main goal is to study the cycle of water from orbit and drop a lander (Beagle 2) on the martian surface. The Mars Express orbiter is equipped with seven scientific instruments and will perform remote sensing experiments to investigate the martian atmosphere, internal structure and mineralogy. The Beagle 2 lander will perform experiments in exobiology and geochemistry. Although the orbiter has a range of sophisticated instruments on board as well, only the lander instruments will be described here, since the lander instruments are directly related to the research performed with the Mars Simulation Chamber.

In the gas analysis package (GAP) CO₂ is generated by heating samples of soil or rock in the presence of oxygen. Under the conditions used in this experiment package all forms of carbon convert to CO₂, either by decomposition (carbonates) or by combustion. The carbon isotopic composition of the CO₂ will be measured with a mass spectrometer. This mass spectrometer will also study other elements and look for methane in samples of the atmosphere.

In addition to several environmental sensors, the main instrument package on the Beagle 2 lander is the PAW instrument

package, which is mounted at the end of a robotic arm. It consists of several small instruments.

- » Two stereo cameras to construct a 3D model of the area within reach of the robotic arm.
- » A microscope with a resolution of 4 µm, to reveal the shape and size of dust particles, the roughness and texture of rock surfaces and the microscopic structure of rocks.
- » A Mössbauer spectrometer to investigate the mineral composition of rocks and soil by irradiating rock and soil surfaces with gamma rays, and then measuring the spectrum of the gamma rays reflected back.
- » An X-ray spectrometer to measure the amounts of elements in rocks by bombarding exposed rock surfaces with X-rays.
- » A mole (PLUTO for PLANetary Underground TOol) to collect soil samples from underneath rocks for return to the GAP.
- » A corer/grinder to drill down 4 mm to acquire a sample of rock powder for analysis in the GAP.

2003 Mars Exploration Rovers

The NASA 2003 Mars Exploration Rovers mission will be launched in 2003 as well. The mission consists of two identical rovers, landing at different sites, which can drive up to 100 meters a day to search for evidence of liquid water in the past. Rocks and soil will be analysed with five different instruments on each rover: a panoramic camera, a miniature thermal emission spectrometer, a Mössbauer spectrometer, an alpha particle X-ray spectrometer, and a microscopic imager.

2005 Mars Reconnaissance Orbiter

The Mars Reconnaissance Orbiter (MRO) will make high-resolution measurements of the surface from orbit. It will be equipped with a visible stereo imaging camera (HiRISE) with a resolution of 20-30 cm and a visible/near-infrared spectrometer (CRISM) to study the surface composition. Also on board will be an infrared radiometer, an accelerometer, and a shallow subsurface sounding radar (SHARAD).

Its main goals will be collecting data on, gravity field, evidence of past or present water, weather and climate, landing sites for future missions.

PREMIER

PREMIER (Programme de Retour d'Echantillons Martiens et Installation d'Expériences en Réseau) is a French (CNES) programme with two goals:

- * participation in the Mars sample return project (MSR) through a co-operation with NASA
- * deployment of a network of martian landers in co-operation with European partners (NetLander project)

The science goals of PREMIER are to reveal new data on the historical and contemporary geology, climate, and biology.

The 2009 NETLANDER mission

The CNES-Europe NetLander Mission will consist of a network of 4 geophysical and meteorological landers and is part of the PREMIER mission.

This mission will allow to study :

- » Deep internal structure
- » Global atmospheric circulation

- » Planetary boundary layer phenomena
- » Subsurface structures at the km scale, down to water rich layers
- » Surface mineralogy and local geology
- » Alteration processes and surface/atmosphere interaction

Aurora

In the frame of the Aurora programme, ESA is performing assessment studies of two Flagship and two Arrow missions., Flagship missions are major milestones to advance the scientific and technical knowledge in preparation for a human mission. Arrow missions are less complex and cheaper technology missions intended to reduce the risk involved in the more complex Flagship flights. The approved Flagship mission studies are the Exo-Mars Mission and the Mars Sample Return Mission.

The Exo-Mars mission

The Exo-Mars mission, an exobiology mission, searching for life outside the Earth, will investigate the martian biological environment before other landings take place. The mission will consist of an Orbiter and a Rover. Its payload will include a drilling system, as well as a sampling and handling device integrated with the package of scientific instruments.

The Mars Sample Return mission.

The mission is composed of a vehicle that will deliver a descent module and an Earth re-entry vehicle into a Mars orbit. The descent module will carry a landing platform equipped

with a sample collecting device and an ascent vehicle. This ascent vehicle will return a small container with the sample into a low altitude circular Mars orbit for a rendezvous with the Earth re-entry vehicle. The re-entry capsule containing the sample will be returned on a ballistic trajectory into the Earth's atmosphere.

7. PERSPECTIVES

The Mars Simulation Chamber (MSC) is used to validate measurements to be made by Beagle 2, and other future spacecraft missions to Mars. Using the MSC we will try to answer a range of questions on the subject of the apparent absence of organic compounds on Mars. Techniques to be used include gas analysis, environmental sensors, HPLC, spectroscopy and other analytical techniques.

We shall also assess the sensitivity of instruments for the detection of minerals and organic compounds of exobiological relevance in martian analogue soils (mixed under controlled conditions with traces of these organics). The results concerning the simulation of complex organics on Mars, as well as lander instrument chamber simulations will be included in a database to serve for the interpretation of Beagle 2 data and other future Mars missions.

The following questions, concerning ground-based measurements, will be examined in this project.

~ There is obviously organic material delivered to Mars by meteorites and IDP's - why do we not see it?

The effects of several oxidising agents will be examined as well as the chemical processing of surface samples due to a combination of parameters.

~ It is assumed that the organic material is destroyed by oxidising agents - what is their penetration depth in the regolith?

During the experiments we will estimate the depth to which it is necessary to drill, in order to find intact organics.

~ Water has been found by the Mars Odyssey orbiter - what is the influence of water on the destruction and reaction pathways of organics?

Until a few years ago it was only assumed that there was perhaps water on Mars close to the surface. Since the presence of water in this depth has now been confirmed by the Mars Odyssey, its effect on the organic material in the soil cannot be neglected.

The results of the experiments can also provide constraints for the observations from orbit, such as spectroscopy of minerals, measurements of the water cycle, frost and subsurface water, the CO₂ cycle, and the landing site selection.

ACKNOWLEDGEMENTS

For this research we would like to acknowledge the following institutes:

- » the Vernieuwingsimpuls of the NWO (Netherlands Organisation for Scientific Research)
- » the Leiden University BioScience Initiative
- » ESA/ESTEC
- » SRON - Space Research Organisation, the Netherlands.

Chapter 3

Amino acid photostability on the martian surface

In the framework of international planetary exploration programmes several space missions are planned that will search for organics and bio-signatures on Mars. Previous attempts have not detected any organic compounds in the martian regolith. It is therefore critical to investigate the processes that may affect organic molecules on and below the planet's surface. Laboratory simulations can provide useful data about the reaction pathways of organic material at Mars' surface. We have studied the stability of amino acid thin films against ultraviolet (UV) irradiation, and we use those data to predict the survival time of these compounds on and in the martian regolith. We show that thin films of glycine and D-alanine are expected to have a half-life of 22 ± 5 hours and of 3 ± 1 hours, respectively, when irradiated with Mars-like UV flux levels. Modelling shows that the half-lives of the amino acids are extended to the order of 10^7 years when embedded in regolith. These data suggest that subsurface sampling must be a key component of future missions to Mars dedicated to organic detection.

Inge Loes ten Kate, James R. C. Garry, Zan Peeters, Richard Quinn, Bernard H. Foing, Pascale Ehrenfreund
Meteoritics and Planetary Science 2005; 40(5):1185-1193

1. INTRODUCTION

In the apparent absence of biogenic processes on the martian surface, exogenous delivery of organic material must be taken into account. Organic compounds are present in certain classes of meteorites as well as in comets (Ehrenfreund *et al.*, 2002). Intact extraterrestrial delivery of such organic material could have been a significant factor in determining the organic make-up of early Earth and Mars (Pierazzo and Chyba, 1999; Ehrenfreund *et al.*, 2002). Flynn and McKay (1990) have estimated that the mass of meteoritic material reaching the surface of Mars is between 1.63×10^{-6} and 7.36×10^{-8} kg m⁻² yr⁻¹. The major carbon component in carbonaceous meteorite samples is in the form of insoluble organic macromolecules. In the soluble fraction of such samples more than 70 extraterrestrial amino acids have been identified in addition to many other organic compounds, including N-heterocycles, carboxylic acids, sulphonic and phosphonic acids, and aliphatic and aromatic hydrocarbons (Botta and Bada, 2002; Sephton, 2002, and references therein). The total abundance of all amino acids in the Murchison meteorite was determined to be 17-60 ppm by Botta and Bada (2002). Ehrenfreund *et al.* (2001a) determined that the average of the amino acid abundance in the CI carbonaceous chondrites Orgueil and Ivuna is 5 ppm. If burial processes are ignored, then unaltered carbon compounds should accumulate with an annual flux of ~ 15 ng m⁻² yr⁻¹. This flux level should yield detectable concentrations after a geologically brief period. However, the Viking gas chromatograph-mass spectrometer (GCMS), which had an average detection limit on the order of part per billion (ppb),

failed to find organic compounds that had not been identified as background contaminants (Biemann *et al.*, 1977). It is thus thought that some process may be at work on Mars that destroys the infalling organic matter, and gaseous oxidizing agents have been postulated as encouraging the destruction of meteoritically delivered organic matter. However, impacting organic matter may be displaced into deeper regolith layers and thus be protected from radiation and oxidation. It is therefore possible that organic meteoritic material is destroyed on the exposed surface, but may survive when protected at depth. The detection of organic material arising from either biotic or abiotic sources, as well as the characterization of oxidants at the martian surface (Zent and McKay, 1994), are among the main goals of future Mars missions.

Laboratory simulations are a crucial step in understanding the chemical pathways on the martian surface (ten Kate *et al.*, 2003). Organic compounds that are abundant in meteorites such as carbonaceous chondrites are a logical target for those experiments since they may have accumulated to form significant deposits on the martian surface via exogenous delivery (Bland and Smith, 2000). We therefore have examined the photostability of the simpler amino acids, given their well-characterized properties and their ubiquitous presence in meteoritic samples. This paper discusses photostability measurements on two amino acids, glycine and D-alanine, exposed to Mars-like UV radiation. D-alanine is used in this study to prevent biological contamination of the samples; the issue of chirality will not be addressed in this paper. The experimental section describes our simulation chamber, as

well as the UV sources used for the irradiation studies. Also described are the experimental procedure and the characterisation of thin films. In the results section we report on the IR spectroscopy of irradiated amino acids samples. Furthermore we tabulate the half-lives and UV destruction cross sections calculated from different experiments and predict the values for martian insolation intensity.

2. EQUIPMENT AND EXPERIMENTAL PROCEDURE

The amino acids glycine (99.7% purity, Merck) and D-alanine (98% purity, Sigma) were ground using a pestle and mortar. The powders were loaded into a vacuum sublimation system that holds a set of four silicon discs at a distance of 15 cm above a resistively heated copper oven. Each disc (24 mm diameter, 0.8 mm thick) was polished on both circular faces and permanently fixed to a steel backing ring, with an inner diameter of 1 cm, large enough for the beam of an infrared spectrometer to pass through. Four copper straps, one per disc, have embedded magnets to hold the silicon discs above the sublimation oven and permit the discs to be handled without touching their coated faces.

The sublimation took place under vacuum, at a typical pressure $<3 \times 10^{-4}$ mbar and at an oven temperature between 150 and 175 °C. During the deposition process the layer thickness was monitored using standard laser interferometry. A schematic drawing of the arrangement is shown in Fig. 1. Absolute thickness of the layers was obtained from atomic force microscopy (AFM, Zeiss AxioPlan 2) scans, which also

showed that the films formed as solid pore-free layers of nanocrystals. The sublimation rate of the solid amino acid, and hence the layer thickness, was controlled by moderating the

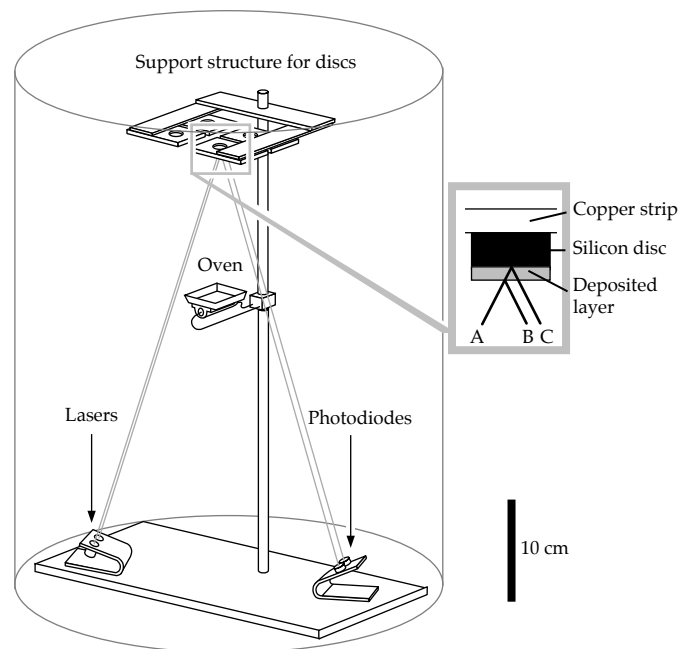


Fig. 1. A schematic drawing of the sublimation chamber, showing the laser geometry. The film thickness can be estimated from the interference arising from the optical path difference taken by rays AC and AB.

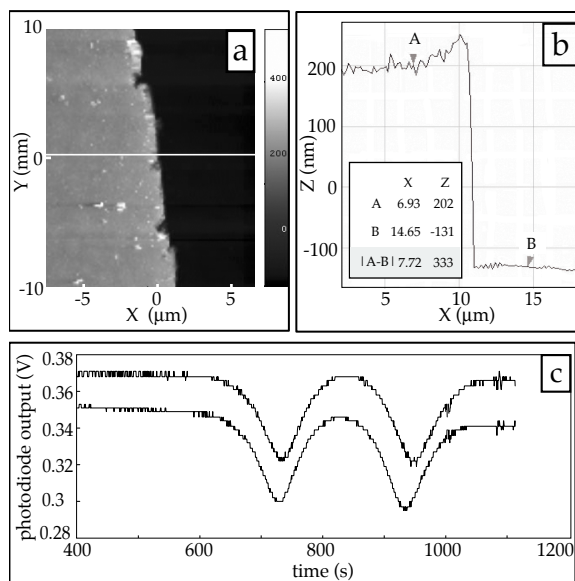


Fig. 2. (a) AFM image of a solid D-alanine layer; the light grey part on the left side is the D-alanine layer, the dark part on the right is the silicon disc on which the layer is deposited. (b) A height profile measurement of the layer along the horizontal line plotted in 2a. (c) The corresponding interferogram from the layer deposition, with two traces showing deposition on the edge (upper trace) and on the centre of the disc (lower trace).

oven heater current. A limited amount of H₂O molecules may be trapped in the amino acid films during deposition, this will be discussed later.

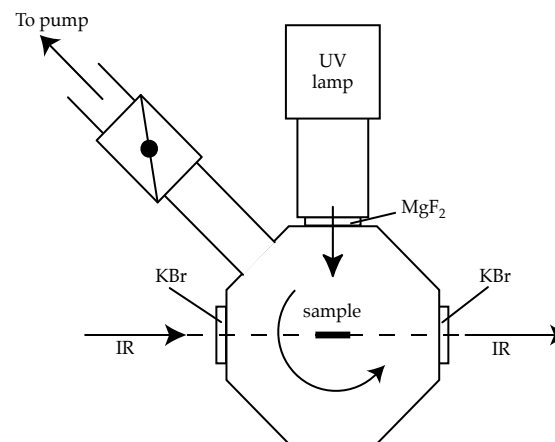


Fig. 3. A schematic drawing of the simulation chamber.

The charts in Fig. 2 show the data for a ~330 nm thick D-alanine layer along with representative data that show that two areas on the disc experience near-identical deposition rates. The thickness of the layer is calculated from the number of interference fringes in the interferogram, not from the absolute voltage of the photodiode output.

Although four discs can be coated simultaneously in the sublimation chamber, only one can be accommodated in the simulation chamber, which is shown schematically in Fig. 3.

The body of this small stainless steel chamber is equipped with four ports and a rotary feedthrough. A mounting stage is fixed to the internal end of the feedthrough, and the copper support tabs of the silicon discs can be clamped to this stage.

One of the ports is equipped with a polished magnesium fluoride (MgF_2) window, to admit the light from the UV lamps. On the opposite face of the chamber a clear window is mounted with which the disc's alignment can be verified. The remaining two ports on the chamber hold potassium bromide (KBr) windows that allow the beam from a Fourier Transform infrared (FTIR) spectrometer to pass through the chamber. By turning the rotary feedthrough on the chamber, the disc can be exposed first to UV radiation, and then to the beam of the FTIR spectrometer. Before, during, and after the irradiation phase, absorption spectra were taken using an Excalibur FTS-4000 infrared spectrometer (BioRad) in the range 4000 to 500 cm^{-1} at 4 cm^{-1} resolution.

2.1 UV sources

Two UV sources have been used for the experiments. A microwave-excited hydrogen flow lamp (Ophos) with an average flux of 4.6×10^{14} photons $\text{s}^{-1} \text{cm}^{-2}$ is used to provide UV light between 120 and 180 nm. The flux of this lamp was measured by solid-state actinometry as described by Cottin *et al.* (2003) and has an estimated uncertainty of 25%. The second UV source is a deuterium discharge lamp (Heraeus-Noblelight, DX 202, range 190-400 nm). This lamp's output was measured before and after each experiment with a UV sensor

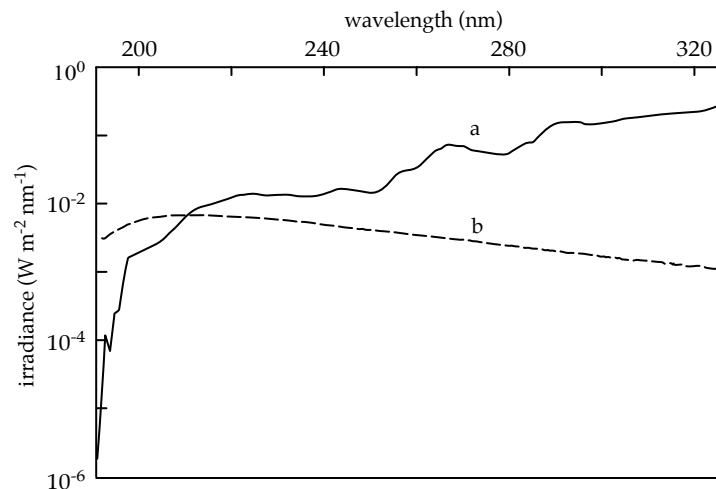


Fig. 4. A comparative chart of the irradiance of the surface noon lighting at the equator of Mars (from Patel *et al.*, 2002) (a), and the light delivered at the working distance of 145 mm from the discharge region of the deuterium lamp (b).

(Solartech model 8.0) that displayed the integrated intensity over the range from ~ 245 nm to ~ 265 nm (half-peak sensitivity, full-width). From the known response curve, the irradiance spectrum provided by Heraeus in arbitrary units could be transformed to give spectral irradiance in absolute units. Similarly, the UV sensor could be used to calculate the absolute irradiance spectrum as a function of distance from the lamp. In Fig. 4 the irradiance of the deuterium lamp is shown for a distance of 145 mm from the lamp's discharge point. At

this distance, and over the range of 190 nm to 325 nm, the lamp generates $4.9 \pm 1 \times 10^{13}$ photons $\text{s}^{-1} \text{cm}^{-2}$ and delivers an intensity of $40 \pm 5 \mu\text{W cm}^{-2}$. If this intensity is compared to the predicted noontime equatorial insolation at Mars' surface in a low atmospheric dust scenario (Patel *et al.*, 2002), then the deuterium lamp provides $\sim 4\%$ of the UV experienced on Mars in the range of 190 nm to 325 nm. The spectral profile of the lamp is deficient in the longer wavelengths compared to the solar spectrum. The spectrum of this lamp is shown in Fig. 4 along with a curve showing the lighting spectrum as expected to exist on Mars.

2.2 Experiments

Two sets of experiments have been performed using two amino acids. In the first set of experiments we used the hydrogen flow lamp as a light source. From those experiments, photo-destruction rates of solid glycine and D-alanine can be calculated. The discs were irradiated with the hydrogen flow lamp for 2.5 hours and IR absorption spectra of the layers were recorded during this period. In the second set of experiments the deuterium discharge lamp was used; this lamp has a lower total power output than the hydrogen lamp and longer exposures (> 40 h) were needed to cause measurable destruction. During all of the experiments the irradiation chamber was pumped continuously and had an average internal pressure of 4×10^{-6} mbar.

An early concern was that the layer material may be lost by sublimation during irradiation of the disc. Thus, a separate

experiment was conducted to measure the *in situ* temperature of the silicon disc during the irradiation process with both the hydrogen lamp and the deuterium lamp. A Pt100 temperature sensor was glued to the illuminated face of the disc and showed that while lit and under high vacuum the temperature of the disc increased by no more than 2°C over the course of a three-hour hydrogen lamp exposure and by no more than 10°C during a 65-hour deuterium lamp exposure. These temperature rises are far below the sublimation temperatures of 150 to 175°C found for the glycine and D-alanine powders in our sublimation chamber at similar pressures. Also a separate 28-hour experiment has been performed to measure the effect of high vacuum (4×10^{-6} mbar) alone on D-alanine and no change in the layer's absorption spectrum could be seen.

UV spectra of the glycine and D-alanine thin films have been recorded with a Varian Cary 3 Bio UV-Visible spectrophotometer (see Fig. 7). The thin films were deposited on MgF_2 windows, because of its transparency in the short wavelength range, from 120 to 7000 nm. Silicon is not transparent for wavelengths shorter than 1000 nm.

3. RESULTS

We have measured IR spectra of glycine and D-alanine sublimated as thin films onto silicon substrate discs. To confirm the obtained absorption data and perform band assignments the glycine spectra were compared with spectra for glycine in KBr pellets as measured by Ihs *et al.* (1990), Uvdal *et al.*

Table 1. Band assignments and wavenumbers (in cm^{-1}) of some spectral features of the IR spectra of glycine and D-alanine. The labels refer to the peaks in Fig. 5.

Label	Glycine	D-alanine
	Wavenumber	Wavenumber
	Band assignment ^a	Band assignment ^a
a	1599	1623
	$\nu_{\text{as}}(\text{COO})$ ^{b,c,d}	$\delta(\text{NH}_3)$ ^{e,g} , $\nu_{\text{as}}(\text{COO})$ ^g
b	1519	1587
	$\delta_{\text{s}}(\text{NH}_3)$ ^{b,c,d}	$\nu_{\text{as}}(\text{COO})$ ^{e,f,g} , $\delta(\text{NH}_3)$ ^g
c	1446	1456
	$\delta_{\text{sc}}(\text{CH}_2)$ ^{b,c,d}	$\delta_{\text{as}}(\text{CH}_3)$ ^{e,g}
d	1414	1414
	$\nu_{\text{s}}(\text{COO})$ ^{b,c,d}	$\nu_{\text{s}}(\text{COO})$ ^e
e	1336	1360
	$\rho_{\text{w}}(\text{CH}_2)$ ^{b,c,d}	$\delta_{\text{a}}(\text{CH}_3)$ ^g
f	916	1307
	$\rho_{\text{r}}(\text{CH}_2)$ ^d	$\delta(\text{CH})$ ^{f,g}
g	896	1239
	$\delta_{\text{sc}}(\text{CC})$ ^d	$\beta(\text{NH}_3)$ ^g
h	703	1115
	$\rho_{\text{r}}(\text{COO})$ ^d	$\rho(\text{NH}_3)$ ^g
i		1015
		$\nu_{\text{s}}(\text{CCNC})$ ^g
j		919
		$\nu_{\text{a}}(\text{CCNC})$, $\rho(\text{CH}_3)$ ^g
k		850
		$2\nu(\text{CCNC})$, $\rho(\text{CH}_3)$ ^g

^a Approximate description of the band assignment: $\nu_{\text{as/sr}}$ asymmetric/symmetric stretching; $\beta_{\text{as/sr}}$ asymmetric/symmetric bending; $\delta_{\text{as/sr}}$ asymmetric/symmetric deformation; δ_{sc} scissoring mode; $\rho_{\text{w/r}}$ wagging/rocking mode.

^b Ihs *et al.* (1990); ^c Uvdal *et al.* (1990); ^d Rosado *et al.* (1998); ^e Cao and Fischer (1999); ^f Cao and Fischer (2000); ^g Rozenberg *et al.* (2003).

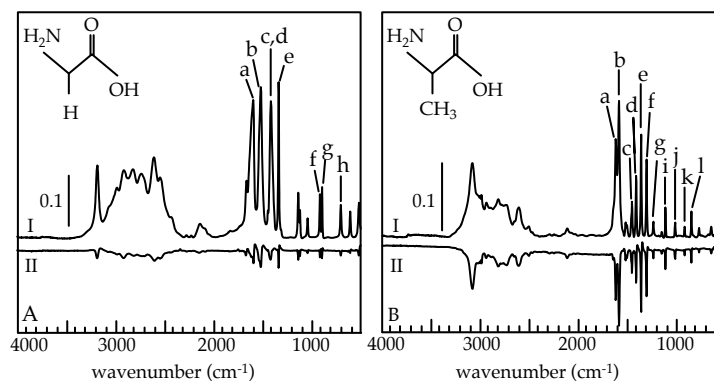


Fig. 5. The IR spectra of (A) solid glycine and (B) solid D-alanine in the range $4000\text{--}500\text{ cm}^{-1}$, measured with a resolution of 4 cm^{-1} . Two spectra are shown, (I) is recorded before irradiation with a deuterium discharge lamp, and (II) is obtained by subtracting the spectrum of the unirradiated compound from the spectrum recorded after 48.3 h (for glycine) and 50.2 h (for D-alanine) of irradiation. The vertical scale bars show the infrared absorbance in arbitrary units. The identification of the peaks can be found in Table 1.

(1990) and Rosado *et al.* (1998). The D-alanine spectra were compared with spectra of L-alanine in KBr pellets determined by Cao and Fischer (1999, 2000) and Rozenberg *et al.* (2003). IR spectra of D- and L-alanine are similar, because chirality does not effect IR spectroscopy (Yamaguchi *et al.*, 2005).

In Fig. 5 glycine and D-alanine infrared absorption spectra before irradiation are shown together with a trace showing the changes in their spectra after ~ 48 hours of irradiation with

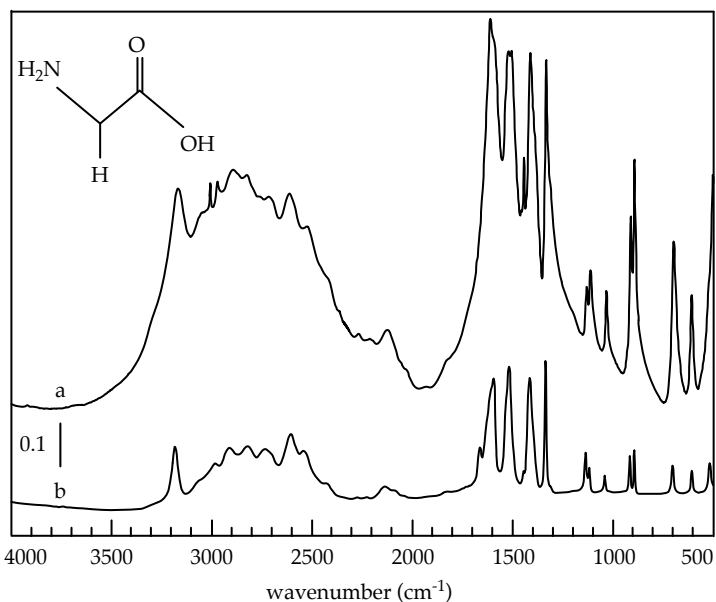


Fig. 6. The IR spectra of (a) glycine in a KBr pellet and (b) solid glycine on a silicon disc, in the range 4000-500 cm^{-1} , measured with a resolution of 4 cm^{-1} . The vertical scale bar shows the infrared absorbance in arbitrary units.

the deuterium lamp. Table 1 describes the band assignments of the main peaks that can be observed in the glycine and D-alanine spectra. A comparison of the IR spectra of glycine in a KBr pellet and a solid layer of glycine on a silicon disc is given in Fig. 6, to show their similarity.

An assumption used in the data processing is that the amino acid films are optically thin. We used the UV sensor to measure the amount of UV light from the deuterium lamp that was reflected from a silicon disc with and without a D-alanine coating. Silicon has an average reflectivity of $\sim 70\%$ (Edwards, 1985) for light in the wavelength range of 120 nm to 325 nm. This modest reflectivity was confirmed by measurements with the UV sensor, which additionally showed

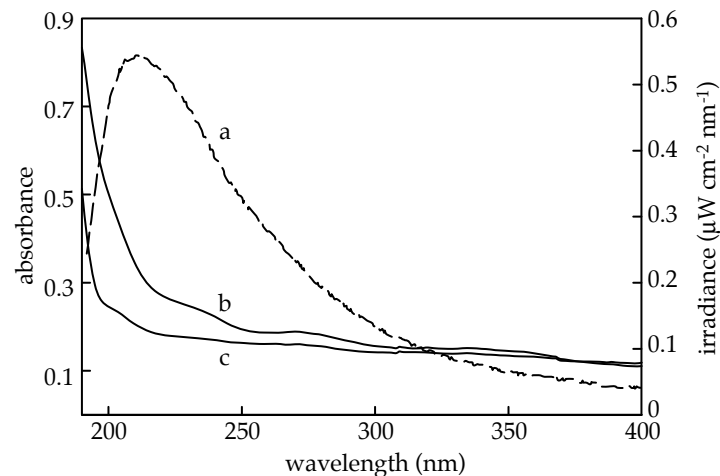


Fig. 7. (a) The spectrum of the deuterium lamp between 190 and 400 nm, recorded at the same distance from the lamp as the amino acid film, scaled to the right ordinate. The UV-visible absorption spectra of a ~ 300 nm layer of (b) solid glycine and (c) solid D-alanine on a silicon disc, in the range 190 to 400 nm, scaled to the left ordinate.

that the addition of a 250 ± 10 nm thick layer lowered the reflectivity by $\sim 10\%$ in the spectral window to which the sensor was responsive (245 through 265 nm, half-peak sensitivity, full-width). Absorption spectra of glycine and D-alanine (Fig. 7) at UV and visible wavelengths suggest that comparable amounts of light would be reflected back through the amino acids films at wavelengths other than those measured by the UV sensor. The thickness of the layers and the reflectivity of the silicon substrate also meant that an additional illumination flux of $\sim 65\%$ had to be considered from photons that pass through the layer and are then reflected by the disc back into the amino acid layer.

With the optically-thin assumption verified, first order reaction kinetics (Cottin *et al.*, 2003) were applied to calculate the half-life and the UV destruction cross section of the solid

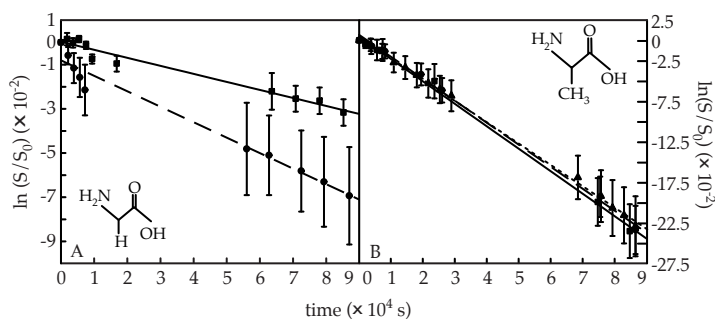


Fig. 8. The natural logarithm of the normalised integrated absorbance ($\ln(S/S_0)$) plotted against time, for the deuterium irradiation of (A) glycine (Table 4), and (B) D-alanine (Table 5).

glycine and D-alanine. The destruction rate is the slope of a linear fit through the natural logarithm of the normalised integrated absorbance plotted against time (Fig. 8). For these calculations the absorbance data of the peaks described in Table 1 are used. From the destruction rate the UV destruction cross section, σ , and the half-life are calculated (Cottin *et al.*, 2003).

In Table 2 and 3 the UV destruction cross sections and the half-lives are compiled for the hydrogen lamp irradiation of glycine and D-alanine. UV photodestruction of matrix isolated glycine has been measured previously by Ehrenfreund *et al.* (2001b) and Peeters *et al.* (2003). These data, however, cannot be directly compared to UV photodestruction of solid thin films. Tables 4 and 5 contain these values for the deuterium lamp irradiation of glycine and D-alanine. In our experiments all of the amino acid layers had thicknesses in the range of 160 to 400 nm. From our experiments it appears, as expected from an optically thin layer, that the layer thickness within this range does not influence the degradation cross section, and the half-life.

The uncertainty in the destruction cross section is dominated by two sources. First, the uncertainty of the hydrogen flow discharge lamp is estimated to be 25% by Cottin *et al.* (2003) and no appropriate independent sensors were available to confirm this number. Secondly, the calibration certificate of the UV sensor used to calibrate the deuterium UV lamp states an $\pm 10\%$ accuracy, and in use the deuterium lamp is stable to better than 1% of its output when measured over multiple

Table 2: glycine irradiated by the hydrogen flow lamp

experiment	σ (cm ² /molecule)	half-life (s)
1	$2.1 \pm 0.5 \times 10^{-19}$	$4.3 \pm 0.2 \times 10^3$
2	$1.6 \pm 0.4 \times 10^{-19}$	$5.9 \pm 0.3 \times 10^3$
3	$1.6 \pm 0.4 \times 10^{-19}$	$5.8 \pm 0.2 \times 10^3$
4	$3.8 \pm 1.0 \times 10^{-19}$	$2.5 \pm 0.2 \times 10^3$
5	$2.9 \pm 0.7 \times 10^{-19}$	$3.2 \pm 0.7 \times 10^3$
average	$2.4 \pm 1.5 \times 10^{-19}$	$4.4 \pm 0.6 \times 10^3$

Table 3: D-alanine irradiated by the hydrogen flow lamp

experiment	σ (cm ² /molecule)	half-life (s)
1	$2.9 \pm 0.7 \times 10^{-19}$	$3.2 \pm 0.2 \times 10^3$
2	$1.3 \pm 0.4 \times 10^{-19}$	$7.1 \pm 0.9 \times 10^3$
3	$2.1 \pm 0.7 \times 10^{-19}$	$4.3 \pm 0.9 \times 10^3$
4	$3.6 \pm 0.9 \times 10^{-19}$	$2.6 \pm 0.1 \times 10^3$
average	$2.5 \pm 1.4 \times 10^{-19}$	$4.3 \pm 1.3 \times 10^3$

Table 4: glycine irradiated by the deuterium discharge lamp

experiment	σ (cm ² /molecule)	half-life (s)
1	$5.7 \pm 1.1 \times 10^{-25}$	$1.5 \pm 0.2 \times 10^6$
2	$4.1 \pm 0.9 \times 10^{-25}$	$2.2 \pm 0.4 \times 10^6$
average	$4.9 \pm 1.4 \times 10^{-25}$	$1.8 \pm 0.4 \times 10^6$

Table 5: D-alanine irradiated by the deuterium discharge lamp

experiment	σ (cm ² /molecule)	half-life (s)
1	$3.1 \pm 1.0 \times 10^{-24}$	$2.8 \pm 0.8 \times 10^5$
2	$3.1 \pm 1.0 \times 10^{-24}$	$2.8 \pm 0.8 \times 10^5$
3	$2.9 \pm 0.6 \times 10^{-24}$	$3.0 \pm 0.3 \times 10^5$
average	$3.0 \pm 1.5 \times 10^{-24}$	$2.9 \pm 1.2 \times 10^5$

Table 6: half-lives of glycine and D-alanine in the laboratory set-up and extrapolated to Mars' equatorial surface irradiation at local noon.

compound	half-life in our lab set-up (s)	half-life on Mars (s)
glycine	$1.8 \pm 0.4 \times 10^6$	$8.0 \pm 1.8 \times 10^4$
D-alanine	$2.9 \pm 1.2 \times 10^5$	$1.2 \pm 0.5 \times 10^4$

days. The overall uncertainty in the measured output of the deuterium lamp is estimated to be $\pm 15\%$. Besides the uncertainties in the lamp flux, smaller uncertainties are taken into account reflecting the error in the linear fit that represents the destruction rate of the amino acid layers.

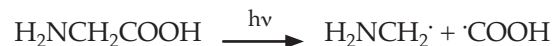
The half-lives calculated from the laboratory data for the deuterium lamp irradiation of both glycine and D-alanine were extrapolated to Mars' surface UV flux levels. Using data from a model for the martian atmosphere with a low dust-load (Patel *et al.*, 2002) an intensity of $930 \mu\text{W cm}^{-2}$ was calculated for the wavelength range of 190 nm to 325 nm. This UV flux was used to calculate the half-lives of glycine and D-alanine shown in Table 6.

4. DISCUSSION

Amino acids, the building blocks of proteins, are easily formed and can be well-characterized by different analytical methods. More than 70 different amino acids have been observed in meteorites (Botta and Bada, 2002). Many of these amino acids show isotopic excess confirming their extraterrestrial origin (Sephton, 2002, and references therein). We do not have any evidence for biogenic processes on Mars. If life as we know it developed in certain environments on Mars, amino acids may be present.

We have studied the survival of amino acids exposed to Mars-like UV conditions in the laboratory. In these experiments we found half-lives of $1.8 \pm 0.4 \times 10^6$ s and $2.9 \pm 1.2 \times 10^5$ s for glycine thin films and D-alanine thin films, respec-

tively, which correspond to half-lives of 22 ± 5 hours and 3 ± 1 hours for glycine and D-alanine, respectively, at Mars UV flux levels. The difference in measured destruction rate between glycine and D-alanine can be explained in terms of radical stabilisation. The destruction mechanism of glycine, suggested by Ehrenfreund *et al.* (2001b) starts with the separation of the carboxyl group:



Rearrangement of the proton on the $\text{H}_2\text{NCH}_2\cdot$ radical would lead to methylamine (CH_3NH_2) and CO_2 . The stability of this intermediate radical determines the rate of this process. Secondary and tertiary radicals appear to be more stable than primary radicals. The ethylamine radical ($\text{H}_2\text{NC}_2\text{H}_4\cdot$) made from D-alanine is therefore more stable and so D-alanine breaks down more rapidly than glycine.

From these results we attempted to obtain knowledge on how long amino acids could survive when embedded into the martian regolith. Our measured reaction rates can be used to calculate estimated decomposition rates for amino acids on Mars. Using first-order decomposition kinetics the concentration of amino acids at a given time can be calculated from Equation 1:

$$N_t = N_0 e^{-Jt} \quad (1)$$

where J is the destruction rate, a function of the destruction cross section and the flux. N_t is the concentration (number of

molecules) at time t , N_0 the initial concentration and t the time (s). From this relationship we can estimate the time it takes for an initial regolith load of 1 ppb of amino acids in the martian regolith to decrease to less than 1 part per trillion (ppt, $1 \text{ per } 10^{12}$). With an attenuation of the destruction rate by a factor of 10^9 , which is equivalent to the assumed regolith dilution ratio and caused by the shielding effect of the regolith, the level of amino acids would decrease from 1 ppb to 1 ppt in approximately 4×10^7 years for glycine and 5×10^6 years for D-alanine, in the absence of regolith mixing and additional amino acid inputs. This calculation represents the expected lower limit of the possible decrease in destruction rate due to dilution of amino acids in the regolith. An important indication of this result is that the decomposition rate is not determined by complexity of the compound. The relationship between decomposition and decrease in reaction efficiency due to regolith dilution effects by erosion are shown in Fig. 9. Continuous amino acid input to the regolith from meteoritic infall and weathering processes are not considered in Fig. 9. The actual concentration of organics in the martian regolith is expected to depend on the balance between the photodecomposition rate and the input rate of amino acids due to physical weathering and mixing occurring on the planet's surface. Physical weathering (processes that break down or fragment rocks and minerals) has many causes, including particle collisions, impact cratering, glacial processes, and volcanism. Currently, it appears that Mars is far less geologically active than it has been in the past and it is likely that the primary mechanism of physical weathering on Mars today is aeolian erosion caused by the collision of particles

moved by wind. Missions to Mars have returned evidence of the extent to which aeolian activity is currently occurring on Mars. Bridges *et al.* (1999) determined that approximately half of the rocks at the Mars Pathfinder site has been abraded by wind-borne particles. Although the Pathfinder site was formed by an ancient out-flow channel, aeolian resurfacing of the site has clearly occurred and is likely to be the dominant geological process occurring on the planet today. The rate of physical weathering determines the rate at which fresh surfaces are exposed to UV light. Once a surface is exposed, chemical weathering may proceed through UV induced oxidation process.

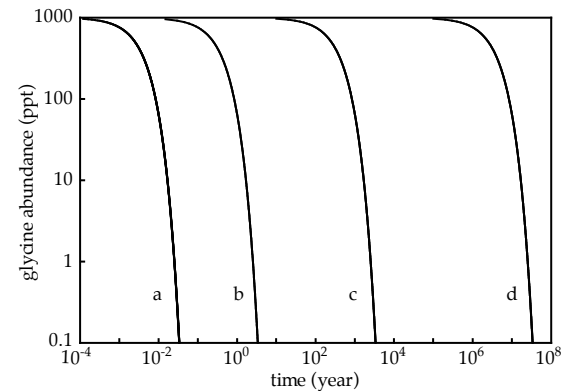


Fig 9. The concentration of glycine in the regolith as a function of time. The lines show the rates for different levels of destruction cross section attenuation due to dilution of the amino acid in the regolith. Levels of attenuation: (a) 1, (b) 10^2 , (c) 10^5 , (d) 10^9 .

Carr (1992) has estimated the average rate of deposition due to physical erosion on Mars to be 20 nm yr^{-1} , which corresponds to an approximate rate of $5 \times 10^{-5} \text{ kg m}^{-2} \text{ yr}^{-1}$. Assuming that surface rocks contain 1 ppb of amino acids, the erosional contribution to the regolith would be 50 picograms of amino acid $\text{m}^{-2} \text{ yr}^{-1}$. For accumulation of amino acids in the regolith to occur, input rates must exceed photodecomposition rates. Assuming a $2 \mu\text{m}$ penetration depth of UV photons into the regolith, this condition is met when attenuation of the measured destruction cross section is greater than 10^5 . In cases where the attenuation is below 10^5 , amino acids are removed more rapidly than the input rate.

It is reasonable to expect the decomposition rate of amino acids in the regolith on Mars to exceed the input rate, since the effective attenuation of the destruction cross section will likely be lower than the dilution ratio due to UV scattering by the regolith. There may be a further enhancement in the degradation rate resulting from catalytic regolith surfaces (Quinn and Zent, 1999).

There are two previously published laboratory studies that examined the photostability of amino acids in the martian surface material; in both cases only glycine was studied. Oró and Holzer (1979) demonstrated the UV decomposition of pure glycine in the presence of small amounts of O_2 gas in a dry nitrogen atmosphere. In their experiments 95 % of the glycine was recovered after 10^9 hours of illumination at Mars flux levels. No decomposition of glycine was observed in samples irradiated in dry nitrogen. Stoker and Bullock

(1997) measured the photodecomposition of glycine mixed in a palagonitic regolith in the presence of a simulated martian atmosphere and attributed their results to the effects of UV alone. Stoker and Bullock (1997) concluded that the presence of oxidising agents is not needed to explain the depleted level of organics in martian Viking regolith samples. This conclusion is at odds with the results of Oró and Holzer (1979). The decomposition rates reported in this paper are consistent with the results of Oró and Holzer (1979) for glycine decomposition in the presence of low levels of oxygen, indicating that radical induced decomposition mechanisms may have also played a role in our observed rates.

In our amino acid films, a limited amount of H_2O molecules may be incorporated in the amino acid thin films during deposition and/or irradiation. The irradiation of H_2O molecules can lead to the generation of OH^\cdot and other strongly oxidising radicals. The photochemical production of oxidizing radicals both in the near-surface atmosphere, and on exposed surface material, is thought to play a major role in the decomposition of organics on Mars (Zent and McKay, 1994). The background pressure in the simulation chamber during sample exposure to UV light was $< 10^{-5}$ mbar. In high vacuum systems the residual gas is predominately water and at 10^{-5} mbar the partial pressure of water corresponds to the approximately 1 part per million (ppm) of water vapour in the martian atmosphere. Therefore, the background gas phase water abundance in the chamber is consistent with Mars number densities and the uniformity of the IR spectra and the repeatability of the measured half-lives indicates that the water abundance in-

corporated into the samples is small, constant and not greater than expected Mars abundances.

This work is part of a comprehensive multi-year effort to describe the response of biologically important molecules to planetary environments, and in particular that of the martian surface. Studying the survival of endogenous or exogenous bio-relevant compounds involves multi-parameter simulations, of which the atmospheric interactions with the UV lighting found at Mars are of special interest and will be examined in future work.

5. CONCLUSIONS

We have constructed a system that allows *in situ* measurements of the destruction rates of amino acid in solid thin films exposed to UV radiation. These rates have been used to predict the decomposition rates of two amino acids, glycine and D-alanine, on the surface of Mars. We estimate that for a starting amino acid load of 1 ppb in the martian regolith, the amino acid concentration would decrease to less than 1 part per trillion (ppt) in approximately 4×10^7 years for glycine and 5×10^6 years for D-alanine. Additionally, for accumulation of amino acids from weathering processes to occur in the regolith, our measured destruction rate for pure glycine would have to be attenuated by a factor of 10^5 by regolith mixing. Given this attenuation factor combined with the additional rate increase that is expected due to radical generation in the regolith by UV, decomposition of amino acids is

expected to outstrip accumulation on the surface of Mars.

Attempts to detect organic compounds by the Viking landers were unsuccessful and indicated that the surface samples contained no detectable amount of native organic material. These *in situ* results along with our laboratory measurements indicate that levels of amino acids in the martian regolith are likely to be below the ppt level. Successful detection of organic compounds on Mars will require highly sensitive instrumentation such as the Mars Organic Analyzer (Skelley *et al.*, 2005). Instrumentation with high sensitivity to organics, coupled with measurements designed to understand oxidative mechanisms occurring in the regolith (Zent *et al.*, 2003), represent a promising strategy for understanding Mars carbon chemistry.

ACKNOWLEDGEMENTS

The authors wish to thank J. Romstedt for providing the AFM pictures. ILtK is supported by the BioScience Initiative of Leiden University, JG is supported by the SRON National Institute for Space Research, PE and ZP are supported by grant NWO-VI 016.023.003, RQ is supported by NASA Ames cooperative agreement NCC2-1408.

Chapter 4

The effects of martian near surface conditions on the photochemistry of amino acids

In order to understand the complex multi-parameter system of destruction of organic material on the surface of Mars, step-by-step laboratory simulations of processes occurring on the surface of Mars are necessary. This paper describes the measured effects of two parameters, a CO₂ atmosphere and low temperature, on the destruction rate of amino acids when irradiated with Mars-like ultraviolet light (UV). The results show that the presence of a 7 mbar CO₂ atmosphere does not affect the destruction rate of glycine and that cooling the sample to 210 K (average Mars temperature) lowers the destruction rate by a factor of 7. The decrease in the destruction rate of glycine by cooling the sample is thought to be predominantly caused by the slower reaction kinetics. When these results are scaled to martian illumination conditions, cold thin films of glycine are assumed to have half-lives of 250 hours under noontime peak illumination. It has been hypothesised that the absence of detectable native material in the martian regolith points to the presence of oxidising agents. Some of these agents might form via the interaction of UV with compounds in the atmosphere. Water, although a trace component of Mars' atmosphere, is suggested to be a significant source of oxidising species. However, gaseous CO₂ or adsorbed H₂O layers do not influence the photodestruction of amino acids significantly in the absence of reactive soil. Other mechanisms such as chemical processes in the martian regolith need to be effective for rapid organic destruction.

Inge Loes ten Kate, James R. C. Garry, Zan Peeters, Bernard H. Foing, Pascale Ehrenfreund
Planetary and Space Science; accepted 5 December 2005

1. INTRODUCTION

Mars is the target for future space missions with the search for traces of extinct or extant life as one of the main goals. Recent space missions have provided a wealth of information about the surface and atmospheric conditions on Mars (e.g. Squyres *et al.*, 2004a,b; Formisano *et al.*, 2004). The martian atmosphere is dominated by CO₂ (95 %). Other major gases in Mars' atmosphere are (percentage by moles) nitrogen (N₂, 2.7 %), argon (Ar, 1.6 %), oxygen (O₂, 0.13 %) and carbon monoxide (CO, 0.08 %). Water (H₂O) is a minor constituent (varying between 10 and 1000 parts per million, Encrenaz *et al.*, 2004a), as well as methane (CH₄, 5 parts per billion, Formisano *et al.*, 2004; Krasnopolsky *et al.*, 2004). The fractional abundance of O₃ in Mars' atmosphere, with a mixing ratio of 10⁻⁸, is directly related to the level of O₂, while the abundance of O₂ is regulated by catalytic cycles involving HO_x species. Hydrogen peroxide (H₂O₂) has been suggested as a possible oxidising agent of the martian surface. Photochemical models suggest that the mean column density of H₂O₂ should be in the range 10¹⁵ - 10¹⁶ cm⁻², and that H₂O₂ and H₂O abundances should be correlated. Encrenaz *et al.* (2004b) report a H₂O₂ atmospheric mixing ratio of 5 × 10⁻⁸ around the sub-solar point.

No organic matter was detected in martian regolith samples analysed by the two Viking landers (Biemann *et al.*, 1977). Given the current presumed rate of meteoritic infall, detectable amounts of organic matter should have accumulated

at the surface of Mars (Flynn and McKay, 1988). To account for this discrepancy, the effects of UV (ten Kate *et al.*, 2005), gaseous oxidants (Oró and Holzer, 1979) and surface catalysts (Quinn and Zent, 1999) on organic molecules have been examined in laboratory experiments. Of particular interest is the stability of simple amino acids, as they may be important biomarkers searched for by instruments on the payload of future missions to Mars.

When irradiated with Mars-like UV, 300 nm thick polycrystalline films of amino acids degrade with half-lives of around 2 × 10⁶ s (glycine) and 3 × 10⁵ s (D-alanine) (ten Kate *et al.*, 2005). However, this destruction was measured exclusively at room temperature and in vacuum (~10⁻⁶ mbar). In the current paper, we have examined the photostability of glycine samples at low temperature or in the presence of CO₂. These conditions are representative of the equatorial regions of Mars (~210 K, Kieffer *et al.*, 1992) with a low adsorbed water content (Möhlmann, 2002) and no condensed CO₂. Regolith mineralogy and chemistry are not taken into account in these experiments. The experiments and the simulation chamber used for these experiments are described in section 2, where also a description of the used UV source is given. In section 3, we report on the infra-red (IR) spectroscopy of the irradiated glycine samples and we tabulate the half-lives and UV destruction cross-sections measured in the reported experiments. The implications of the obtained results are explained in detail in section 4.

2. EQUIPMENT AND EXPERIMENTAL PROCEDURE

2.1 Equipment and experiments

Glycine (99.7 % purity, Merck) was deposited on silicon substrates, to form films with a thickness of 300 ± 50 nm, using a vacuum sublimation system, details of which are given in ten Kate *et al.* (2005). The films produced in this system have been shown to be optically thin (ten Kate *et al.*, 2005). Experiments have been performed in a modified version of the system as used by Peeters *et al.* (2003) (Fig. 1). The system consists of a small vacuum chamber equipped with several gas-inlet ports. A closed-cycle two-stage helium cryostat (Air products, Displex DE-202), which can be rotated while maintaining the vacuum, allows the temperature of the sample to be controlled to within 0.3 K in the range 20-300 K. In this system a Mars-like atmosphere, ~ 7 mbar CO_2 (Praxair, 99.996 %), was created at room temperature, representing a Mars-like daytime surface temperature in equatorial regions. Alternatively, samples were cooled down to 210 K under vacuum to simulate an average Mars surface temperature. The silicon substrate is mounted on the cryostat, allowing the vapour deposited amino acid sample layer to face either a UV source (see section 2.2) or the beam of a Fourier transform IR spectrometer (Excalibur FTS-4000, BioRad, 4000 to 500 cm^{-1} at 4 cm^{-1} resolution). Simultaneous cooling and using a 7 mbar atmosphere of CO_2 was not possible to achieve in our cryosystem, because CO_2 would selectively freeze on parts of the cryostat that are far colder (~ 40 K) than the 210 K at which the substrate window was maintained.

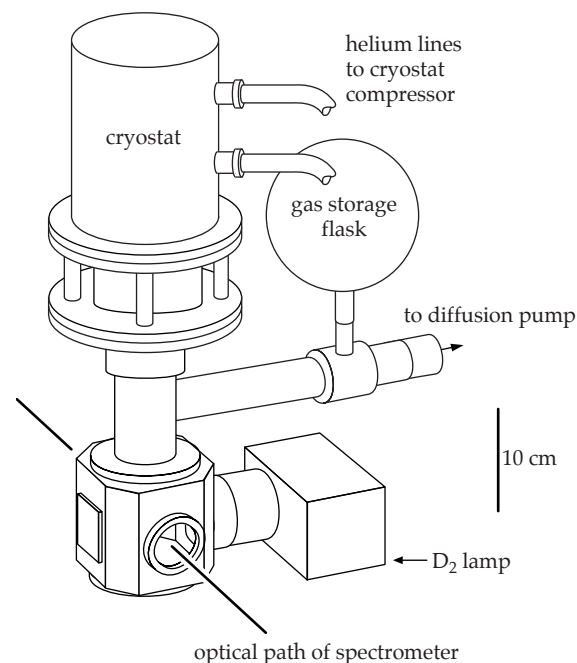


Fig. 1. The cryosystem used for the irradiation of amino acids.

2.2 UV source

The UV source is a deuterium discharge lamp (Heraeus-Noblelight, DX 202), which has been calibrated against a known UV standard (Bentham R48) using a monochromator equipped with a photomultiplier tube. The measured spectrum of the DX202 lamp is shown in Fig. 2 along with a curve

showing a representative noontime UV spectrum for Mars that was calculated for a low atmospheric dust-load by Patel *et al.* (2002). The integrated flux in the wavelength range 190-325 nm (on the amino acid layer) is 1.2×10^{14} photons $\text{cm}^{-2} \text{s}^{-1}$ in the current system. This is ~ 12 times lower than the integrated flux on Mars in the same wavelength range (1.4×10^{15} photons $\text{cm}^{-2} \text{s}^{-1}$).

As has been pointed out by Schuerger *et al.* (2003) a deuterium discharge light source is not an exact fit to the lighting spectrum found at Mars' surface. The deuterium emission

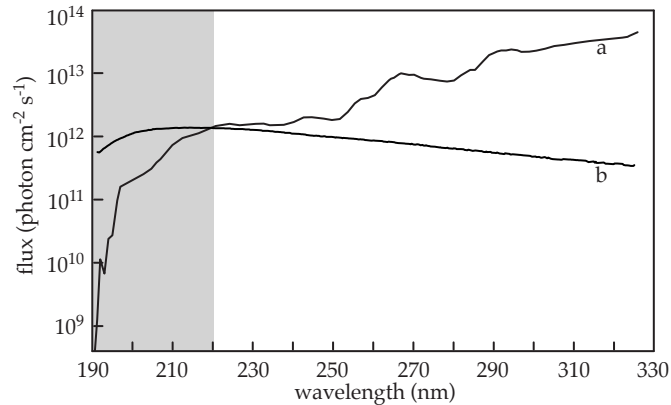


Fig. 2. The lighting spectrum (a) experienced by the equatorial noon-time surface of Mars at $L_S = 70^\circ$ and (b) of the deuterium lamp. The grey area marks the 190-220 nm range, which is used in the discussion.

spectrum peaks at around 200 nm, and is deficient in longer wavelengths compared to the UV spectrum at the martian surface. Thus, the work presented here places upper limits on the half-life of a sample under martian conditions.

3. RESULTS

Thin films of glycine deposited on silicon substrates have been irradiated with UV in vacuum ($\sim 10^{-7}$ mbar), in a CO_2 atmosphere (~ 7 mbar), and at a temperature of 210 K. Multiple experiments have been performed for each modified parameter to achieve high accuracy of the measurements. Fig. 3 shows the natural logarithm of the normalised integrated absorbance ($\ln(S/S_0)$) plotted against irradiation time for all experiments. The slope of the linear fit through $\ln(S/S_0)$ represents the destruction rate. Table 1 lists the temperature of the glycine samples, the average pressure in the system, and the corresponding average destruction rate of the different experiments. Also listed are the half-lives when extrapolated to a martian noontime equatorial UV flux of 1.4×10^{15} photons $\text{s}^{-1} \text{cm}^{-2}$. The destruction rates found in the vacuum-only experiments were in agreement with the values found by ten Kate *et al.* (2005), with a small shift within the error bars, due to the use of a different system.

The system can be heated under vacuum prior to the experiments so that water is desorbed from the stainless steel. The maximum amount of water accreted on the disc during 24 hour cooling at 210 K is in the order of 10^{16} molecules cm^{-2} .

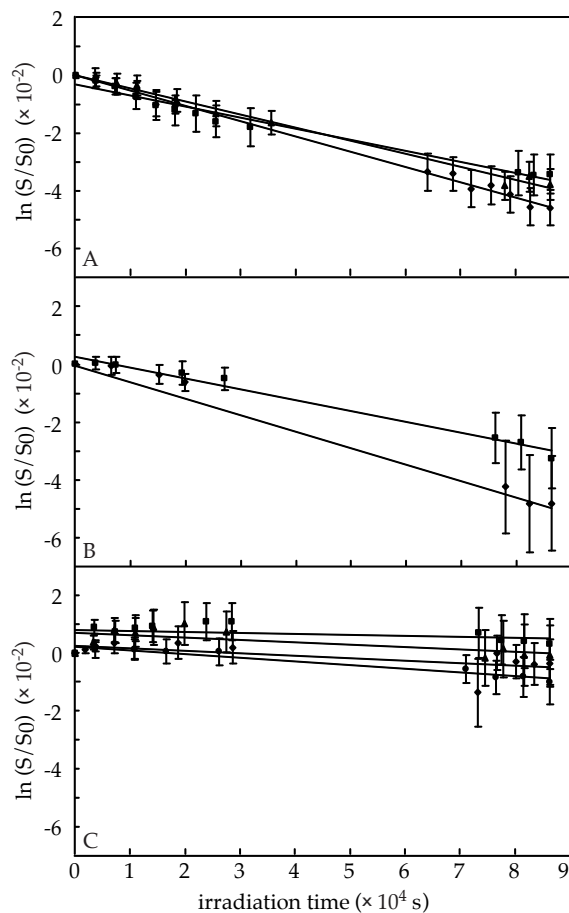


Fig. 3. The natural logarithm of the normalised integrated absorbance ($\ln(S/S_0)$) plotted against irradiation time, for the deuterium irradiation of glycine (A) in vacuum at 294 K, (B) in a 7 mbar CO_2 atmosphere at 294 K, and (C) in vacuum when cooled to 210 K. The different lines represent the destruction rates of the separate experiments that have been performed.

Table 1. Average destruction rates of thin films of glycine measured under different conditions in the laboratory when subjected to UV irradiation. Also listed are the extrapolated half-lives of glycine for a noontime equatorial flux on Mars.

tempe- rature (K)	number of repeated experiments	atmosphere (mbar)	destruction rate J (s^{-1})	Mars half-life (s)
294	3	$\sim 10^{-7}$	$4.5 \pm 2.3 \times 10^{-7}$	$1.3 \pm 0.8 \times 10^5$
294	4	~ 7 CO_2	$4.9 \pm 2.3 \times 10^{-7}$	$1.3 \pm 0.6 \times 10^5$
210	2	$\sim 10^{-7}$	$0.8 \pm 2.9 \times 10^{-7}$	$0.9 \pm 7.5 \times 10^6$

The amount of water and other contaminants in the CO_2 gas is in the order of 1 part per million (ppm). The background pressure in the system was in the order of 10^{-7} mbar.

4. DISCUSSION

The effects of low temperature or a CO_2 atmosphere on the photodestruction rate of amino acids have been examined. This has been done by irradiating 300 ± 50 nm thick

polycrystalline films of glycine deposited on silicon discs in the presence of a CO₂ atmosphere or when cooled to 210 K, corresponding to an average temperature on the surface of Mars. The results show no measurable effect of a CO₂ atmosphere on the destruction of glycine. However, when the samples are cooled to 210 K the destruction rate decreases by a factor of 7.

4.1 Effect of a CO₂ atmosphere

Thin films of glycine deposited onto silicon substrates have been irradiated with UV in a CO₂ atmosphere (~7 mbar). Adding a CO₂ atmosphere is assumed to have two effects, extinction of the UV flux reaching the glycine film and formation of O-radicals by photodissociation of CO₂. The extinction of UV can be divided into an absorption and a Rayleigh-scattering component, both with a corresponding cross-section (σ , cm²), σ_{abs} and σ_{scat} respectively. The wavelength range displayed in Fig. 2 can be divided into three regions, < 203 nm, 203-220 nm and > 220 nm. In the region > 220 nm the UV extinction is dominated by scattering with a very small cross-section $\sigma_{\text{scat}} < 10^{-25}$ cm² (upper limit of 10⁷ scattered or absorbed photons s⁻¹), and is therefore not further considered in this discussion. In the region 203-220 nm both scattering and absorption contribute equally to the UV extinction, while in the region 190-203 nm absorption is the dominant process (Karaiskou *et al.*, 2004 and Shemansky, 1972). Table 2 gives an overview of the solar noontime UV flux on the surface of Mars and the output of UV flux from the deuterium lamp, as well as the average absorption and scattering cross-sections

of CO₂, for the 190-203 and 203-220 nm intervals.

Above 167 nm dissociation of CO₂ occurs only through the reaction:



The upper limit of this reaction is 227 nm. Between 190 and 200 nm the CO-formation quantum yield (Φ_{CO}) is ~1, but above 200 nm this value decreases to 0.16 at 214 nm, and no photodissociation occurs above 227 nm (Okabe, 1978). The formation rate of O-radicals will therefore be dominated by UV in the wavelength range 190-200 nm. As can be seen from Table 2 the UV absorption of CO₂ between 190 and 200 nm is small, leading to an upper limit on the O-radical formation in the order of 10⁹ s⁻¹.

Table 2. Noontime solar UV flux at the surface of Mars, UV flux of the deuterium lamp and average absorption (σ_{abs}) and scattering (σ_{scat}) cross-sections of CO₂ for two wavelength ranges.

wavelength range (nm)	Mars flux ‡ (photon cm ⁻² s ⁻¹)	lamp flux § (photon cm ⁻² s ⁻¹)	σ_{abs} (cm ²)	σ_{scat} (cm ²)
190 – 203 *	4×10^{12}	1×10^{13}	3×10^{-23}	1×10^{-24}
203 – 220 †	1×10^{13}	2×10^{13}	7×10^{-25}	7×10^{-25}

* Shemansky (1972)

† Karaiskou *et al.* (2004)

‡ Patel *et al.* (2002)

§ measured from 200 nm and up, 190-200 nm adapted from the spectrum provided by Heraeus.

In summary, the total UV extinction in our experiments, through scattering and absorption by CO₂ over the full range of our lamp (190-325 nm), is in the order of 10⁹ photons s⁻¹. The formation rate of O-radicals by the photodissociation of CO₂ is ~10⁹ per second. These values are both a factor 10⁵ lower than the UV flux produced by the deuterium lamp, thus the destruction rate of glycine thin films is *expected* to be dominated by photodestruction by UV. This concurs with the experimental results, presented in Table 1, where we found no effect on the destruction rate of glycine, when a CO₂ atmosphere was added and noontime equatorial illumination on Mars was simulated.

4.2 Effect of cooling

Thin films of glycine deposited on silicon substrates have been irradiated with UV, when cooled to 210 K. This cooling resulted in a lower destruction rate of glycine, which is expected from reaction kinetics. At 210 K water is accreted onto the glycine film as has been shown by background water

accretion measurements, see section 3. Water accretion may influence the destruction rate; the reaction rate could either decrease due to UV absorption by the ice layer, or increase due to formation of for example OH-radicals.

The amount of water accreted on the sample during 24-hour cooling is in the order of 10¹⁶ molecules cm⁻², corresponding to a layer-thickness of ~5 H₂O molecules (~1.5 nm). Table 3 shows absorption coefficients of water (Thompson *et al.*, 1963) and the corresponding absorbance of the water layer on our samples at several wavelengths. These absorbances imply that in the wavelength range emitted by the deuterium lamp (190-325 nm) the absorption of UV photons by H₂O molecules hardly plays a role. The decrease in the destruction rate of the glycine film by cooling the sample, as measured in our experiments, is therefore thought to be predominantly caused by the slower reaction kinetics. A model of the upper martian surface from Möhlmann (2004) suggests an average of two monolayers at 200 K, adsorbed on the porous surface of martian soil. If only photodissociation of water adsorbed on amino acid layers is taken into account, the effect of these H₂O monolayers on the surface of Mars is negligible.

4.3 Water vapour

It has been postulated that the action of energetic UV photons on the water vapour present in the martian troposphere leads to the formation of OH-radicals, which influence the photochemistry of the soil (Hunten, 1979). Above 200 nm UV absorption by gaseous water is negligible, between 190 and

Table 3. Absorption coefficients of water and absorbance of a 1.5 nm thick water layer.

wavelength (nm)	absorption coefficient (cm ⁻¹)	absorbance
190	2 × 10 ⁻¹	3 × 10 ⁻⁸
200	3 × 10 ⁻³	5 × 10 ⁻¹⁰
250	1 × 10 ⁻⁴	2 × 10 ⁻¹¹

200 nm the absorption cross-section is smaller than 10^{-21} cm² (Chung *et al.*, 2001; Parkinson and Yoshino, 2003). The amount of residual water present as contamination in the CO₂ atmosphere in the chamber is in the order of 10^{-3} mbar, comparable to the average amount of gas phase H₂O in the martian atmosphere. The water vapour content in the atmosphere of Mars varies between 10 and 1000 ppm (Encrenaz *et al.*, 2004a). The amount of water in our system leads to a total absorption of 10^9 UV photons in the duration of the experiment. This is less than the total UV absorption and scattering by the CO₂ gas present in the system (see section 4.1). A control experiment has been performed in a different system (described in ten Kate *et al.*, 2005), in which a thin film of glycine was irradiated in a 10 mbar atmosphere, consisting of 50 % CO₂ and 50 % H₂O (data not shown here). The destruction rate found in this experiment was the same as the destruction rates of glycine thin films irradiated in vacuum. Photodestruction of H₂O into OH-radicals does not occur at wavelengths longer than 190 nm (Okabe, 1978), so is not expected to play a role in our experiments. On Mars, H₂O will be dissociated efficiently only in upper atmospheric layers, where UV irradiation is not substantially attenuated. The diffusion of radicals, formed by dissociation of water, to the surface, and their subsequent reactions are not well understood. UV irradiation of H₂O vapour close to the surface will not result in a significant amount of reactive species.

5. CONCLUSIONS

We measured the destruction rate of ~300 nm thick polycrystalline films of glycine deposited on silicon substrates, when irradiated with UV (190-325 nm) in vacuum ($\sim 10^{-7}$ mbar), in a CO₂ atmosphere (~ 7 mbar), and when cooled to 210 K. Regolith mineralogy and chemistry are not taken into account in these experiments. The results show that the presence of a 7 mbar CO₂ atmosphere does not affect the destruction rate of glycine by UV. The extinction of UV (with an extinction rate of 10^9 photons s⁻¹) and the formation of O-radicals (with a formation rate of 10^9 s⁻¹) are very small compared to the flux of the deuterium lamp. However, cooling the amino acid during irradiation reduces the destruction rate by a factor of 7. A thin layer of water (representative for martian conditions, see Möhlmann, 2002, 2004) accreted on the glycine film did not measurably influence the destruction rate. When the results on thin films of glycine by ten Kate *et al.* (2005) and the results of this work are scaled for martian noontime lighting conditions, glycine exposed to UV at temperatures between 210-295 K has a half-life of approximately 35-250 hours under continuous irradiation. Irradiation of 24 hours in our experiments corresponds to an irradiation time of ~2 hours on the surface of Mars at noontime. Only in the polar regions during their respective summers may sunlight shine on the surface for periods of > 24 hour, however with lower intensity than at the equator. The simple geometric relationship between latitude and surface intensity for a sphere allows one to scale the lifetime of glycine calculated for noon illumination conditions at the equator to other lati-

tudes. Our low temperature experiments performed at 210 K are more representative of mid and high latitude regions on Mars, and indicate that in those environments the destruction rate of amino acids may be reduced further. Furthermore the amount of water adsorbed on the surface has a regional, seasonal and diurnal dependence. Therefore the actual lifetime of exposed glycine on the cold surface of Mars will depend on several parameters. Using the model of amino acids embedded in martian regolith described by ten Kate *et al.* (2005), with a mixing ratio of glycine of 1 part per billion, we find a half-life of glycine of $\sim 10^8$ years.

Energetic UV photons are suggested to form OH-radicals from the water vapour present in the martian atmosphere (e.g. Nair *et al.*, 1994, Atreya and Gu, 1995). This dissociation takes place most efficiently in upper atmospheric layers, where UV irradiation is less attenuated. The OH-radicals formed in the atmosphere and other photochemical processes could play a role in the formation of oxidising agents in the regolith (Zent and McKay, 1994). However, OH-radical production on the martian surface can also occur through processes involving adsorbed H₂O, Fe(II)-ions and H₂O₂ (Southworth and Voelker, 2003). It has been suggested that the water abundance plays an important role in controlling reaction kinetics by triggering oxidative reactions involving photochemically produced dry acids that are adsorbed onto the soil (Quinn *et al.*, 2005c). Interaction of UV with Mars-analogue minerals in the presence of an oxygen atmosphere with a partial pressure comparable to that in the martian atmosphere showed the formation of oxygen radicals (O₂[·]) on the minerals that

likely destroy organic material (Yen *et al.*, 2000). The stability of the intrinsic organic component of martian soil analogues has recently been investigated by Garry *et al.* (2005). Those results support the idea that the key element in the destruction of organic material and micro-organisms is the interaction of accreted water with the soil in the presence of radiation.

In summary, we studied the behaviour of amino acids irradiated by 190 to 325 nm UV in a CO₂ atmosphere and when cooled to 210 K. Our results form a basis for the understanding of more complex processes occurring on the martian surface, in the presence of regolith and other reactive agents. Future research should involve a diurnal UV irradiation and temperature cycle, enabling to simulate the diurnal water frost deposition on the surface. Low temperatures may enhance the stability of amino acids in certain cold habitable environments, which may be important in the context of the origin of life.

ACKNOWLEDGEMENTS

ILtK is supported by the BioScience Initiative of Leiden University; JG is supported by SRON National Institute for Space Research, grant MG-058; PE and ZP are supported by grant NWO-VI 016.023.003. We acknowledge the support from ESA-ESTEC and SRON.

Chapter 5

Analysis and survival of amino acids in martian regolith analogues

We have investigated the native amino acid composition of two analogues of martian soil, JSC Mars-1 and Salten Skov. A Mars simulation chamber has been built and used to expose samples of these analogues to temperature and lighting conditions similar to those found at low-latitudes on the martian surface. The effects of the simulated conditions have been examined using high performance liquid chromatography (HPLC). Exposure to energetic ultraviolet (UV) light in vacuum appears to cause a modest increase in the concentration of certain amino acids within the materials, which is interpreted as resulting from the degradation of microorganisms. The influence of low temperatures shows that the accretion of condensed water on the soils leads to the destruction of amino acids, supporting the idea that reactive chemical processes involving H₂O are at work within the martian soil. We discuss the influence of UV radiation, low temperatures and gaseous CO₂ on the intrinsic amino acid composition of martian soil analogues and describe, with the help of a simple model, how these studies fit within the framework of life detection on Mars and the practical tasks of choosing and using martian regolith analogues in planetary research.

James R. C. Garry, Inge Loes ten Kate, Zita Martins, Per Nørnberg, Pascale Ehrenfreund
Meteoritics and Planetary Science; accepted 26 October 2005

1. INTRODUCTION

Mars' current atmospheric pressure is too low to allow pure liquid water to persist at its surface – liquid water will freeze and evaporate. Data from orbiters and rovers (Haskin *et al.*, 2005, Squyres *et al.*, 2004a,b) indicate that liquid water has been present in significant amounts on Mars in the past, possibly allowing biologically important reactions to occur (Squyres, 1984). The question of whether life arose on Mars has therefore been widely discussed in the planetary community, since the conditions in its early history may have resembled those of the early Earth by having a dense atmosphere and persistent liquid water at its surface (McKay, 1997). However, a combination of energetic UV radiation, the extreme dryness and the presumed oxidising nature of the soil make Mars' present surface an inhospitable place for terrestrial organisms. Organic matter carried by impacting meteorites appears to be affected by the same processes. The Viking Mars landers attempted to detect organic molecules in the upper surface three decades ago, but no evidence was found for organic matter that was not already present at low levels within the spacecraft's analysis equipment (Biemann *et al.*, 1977). However, the lower detection limit of the Pyrolysis Release experiment of Viking would not have detected bacterial communities numbering in the millions per gram (Klein, 1978). Thus, while many mechanisms have been proposed to explain the overall negative response of the Viking experiments, it is possible that organic matter may have present but at concentrations lower than could be detected by the equipment.

An international effort of Solar System exploration will lead to several space missions that will search for extinct or extant life on Mars during the next decade. In this context it is vital to obtain knowledge about the survival of organic material exposed to martian conditions. Laboratory simulations provide a convenient path to understanding chemical reactions on the martian surface and studies have shown that there are a number of processes, both photochemical and photolytic, that reproduce aspects of the biological results of Viking, a summary of which can be found in Klein (1978). It is known that pure amino acids can be destroyed by exposure to UV light with a spectrum similar to that found at the surface of Mars and the rate of degradation is high relative to geological timescales (ten Kate *et al.*, 2005; Stoker and Bullock, 1997). Unshielded glycine and D-alanine molecules have half-lives of the order of 10^4 to 10^5 s under noontime conditions at the martian equator (ten Kate *et al.*, 2005). More complex molecules are expected to be altered either by photolytic or photochemical pathways. Of particular interest is the role that water might play, either through the formation of gaseous oxidising agents in the atmosphere, or when chemisorbed into minerals or present as thin quasi-liquid films. Of particular interest is the role that water might play, either in the formation of gaseous oxidising agents in the atmosphere, or in similar oxidising reactions when chemisorbed into minerals or present as thin quasi-liquid films on mineral surfaces.

In this paper we report data on the native amino acid content of martian analogues using HPLC coupled with UV fluores-

cence detection. This technique is well-suited to the analysis of complex mixtures of organic matter and by using this method we have quantified the native amino acid content of the Mars-1 material from Johnson Space Center (JSC), and a Danish soil (Salten Skov), both of which are internationally used martian soil simulants. These materials were then exposed within a specially designed cryogen-cooled simulation chamber to conditions of temperature, UV lighting and pressure, that are similar to those on Mars. The composition and properties of the martian soil analogues are discussed in section 2 and the HPLC analyses are described in section 3. Our experimental simulations are outlined in section 4 with the results summarised in section 5. We then discuss the implications of these martian simulations in the context of future exploration efforts to detect organic molecules in the martian subsurface.

2. REGOLITH ANALOGUES

The two materials used in this study have different physical characteristics and mineralogy. It is not our intent to examine the broader view of how the degradation rate of organic matter varies with the general properties of regoliths such as grain size or mineralogy. Instead, by using materials that are available to the planetary science community, we provide information about these soil analogues that can be used for disciplines ranging from planetary protection to material compatibility tests, among others. Characteristics of each analogue are summarised briefly in the following sections.

2.1 JSC Mars-1

A martian soil analogue, hereafter referred to as Mars-1, is available to the research community from JSC. It is an ochre-coloured mixture of weathered volcanic ash collected from the Pu'u Nene cinder cone, located in the saddle between the Mauna Loa and Mauna Kea volcanoes on the island of Hawaii (Allen *et al.*, 1998). This soil approximates the composition, grain size, density, and magnetic properties of martian soil and has been used in a number of Mars-oriented research studies that examine physical (Sternovsky *et al.*, 2002) and biological processes (Kral *et al.*, 2004). The elemental abun-

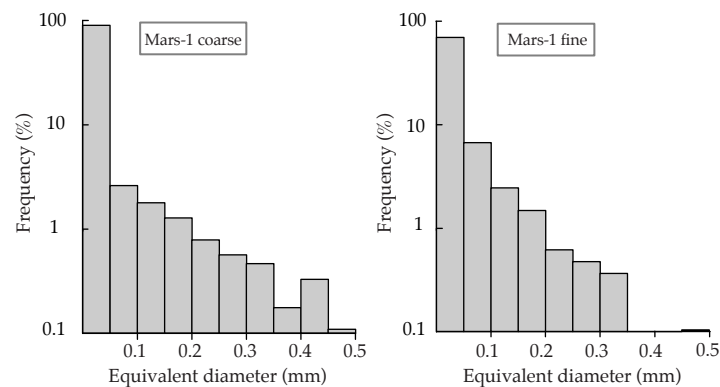


Fig. 1. The frequency distribution of grain diameters in two samples of the Mars-1 regolith.

dances of the Mars-1 material are broadly similar to that inferred from Viking surface studies although the degree to which its mineralogy is comparable to that of martian surface is not well known. Optical microscopic imaging of the powder shows irregular unweathered grains and computer analysis of these images, by the NIH Image software package, was used to find the distribution of grain cross-sections. From these data, an effective grain diameter distribution was calculated using the assumption that the grains were substantially spherical and the resulting data are shown in Fig. 1.

The broad range of grain sizes in the Mars-1 material causes a significant degree of self-sorting. This leads to a segregation of the material based on grain size. Additionally, it is possible that different mineralogies are present in the largest and smallest fractions of the material. Thus, two sub-samples were prepared from the bulk supply of Mars-1, one made up of the larger grains, and one predominantly containing the smaller grains. This separation was achieved by gentle shaking of approximately 500 g of the original material in a polyethylene bag and such action is intended to replicate the agitation that might occur in transit or in simple handling of the bulk material. No contamination-control documents were available for the two types of analogue used, and it is therefore possible that they contained organic material such as plasticisers, that had migrated from plastic scoops, bags, and similar handling tools. The extent to which such contamination might occur is limited, since the presented area of the regolith powders ($>100 \text{ m}^2$ per kg) is far larger than the internal area ($\sim 500 \text{ cm}^2$) of the smallest bag used in these experiments.

2.2 Salten Skov

This dark red Danish soil, named after its source in the central Jutland region, is rich in precipitates of iron oxides and is excavated from an area on the scale of several hundred m^2 . To date, this analogue has had limited use in martian simulation studies, with emphasis placed on its fine grain size and magnetic properties. A mineralogical study of this analogue has been made (Nørnberg *et al.*, 2004) but as yet the localised nature of the soil and its chemical nature are not well understood. The silt and clay size fraction ($< 63 \mu\text{m}$) used in this

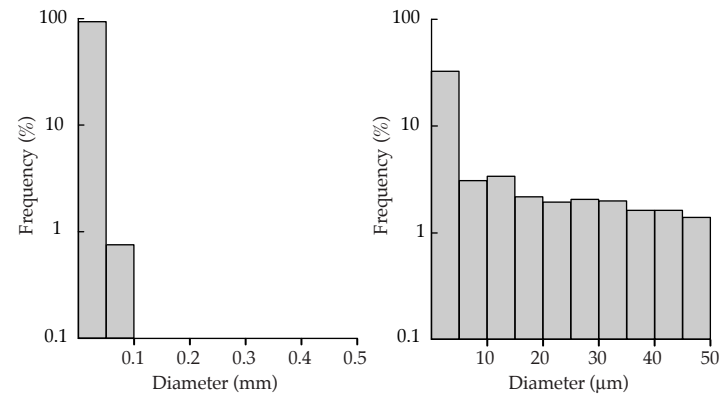


Fig. 2. Showing the grain size distributions of the Salten Skov material used.

experiment makes up 35.5 % of the particles smaller than 2 mm. This fraction was separated from the total sample by dry sieving. It has a free iron content of 35.8 % of which nearly 90 % is crystalline iron oxides (DCB/Oxalate extraction). Most of the grains with a diameter $< 63 \mu\text{m}$ consist of aggregates, which can be split into particles $\sim 2 \mu\text{m}$ in size. The particle size of the $< 63 \mu\text{m}$ fraction was determined by laser diffraction and the particle size distribution is seen in Fig. 2, which shows two charts of the same data. The leftmost chart uses the same scale as was used to plot the Mars-1 grain size data in Fig. 1, and illustrates the complete absence of particles with diameters larger than 0.2 mm. The second chart in Fig. 2 shows the same data as the left-most chart, but plotted over one tenth of the physical scale, showing that the Salten Skov material is composed predominantly of dust-size particles.

2.3 Control material

The extent to which cross-contamination of the samples occurred within the irradiation chamber was monitored by the use of a third material. This control sample was a quantity of finely crushed Pyrex. It was expected that accidental transport of grains during the use of the chamber's pumping equipment, or sublimation and recondensation of the amino acids when in vacuum, might be observed by the detection of novel compounds in the Pyrex at the end of the experiment.

3. EXPERIMENTS AND METHODS

3.1 Samples

All of the samples were separately ground into powder in a glove box purged with argon gas, and were stored in sterilised glass vials before being used in the experiments. An unused Pyrex test tube was crushed into powder and then heated to $500 \text{ }^\circ\text{C}$ for 3 hours for use as a reference blank, using the same process as for the samples.

3.2 Chemicals and reagents

All tips and Eppendorf tubes used in this work were sterilised. All tools, glassware and ceramics were sterilised by baking in aluminium foil at $500 \text{ }^\circ\text{C}$ for 3 hours. Amino acid standards were purchased from Sigma-Aldrich. AG[®] 50W-X8 resin was acquired from Bio-Rad. Sodium hydroxide and hydrochloric acid (37 %) were purchased from Boom and ammonium hydroxide (28-30 wt%) was obtained from Acros Organics. o-Phthaldialdehyde (OPA), N-acetyl-L-cysteine (NAC), sodium acetate trihydrate, sodium borate decahydrate as well as HPLC-grade water were bought from Sigma-Aldrich and methanol (absolute, HPLC-grade) was purchased from Biosolve Ltd.

3.3 Regolith simulation chamber

A stainless steel vessel was built that allowed up to seven sample cups to be cooled and simultaneously irradiated

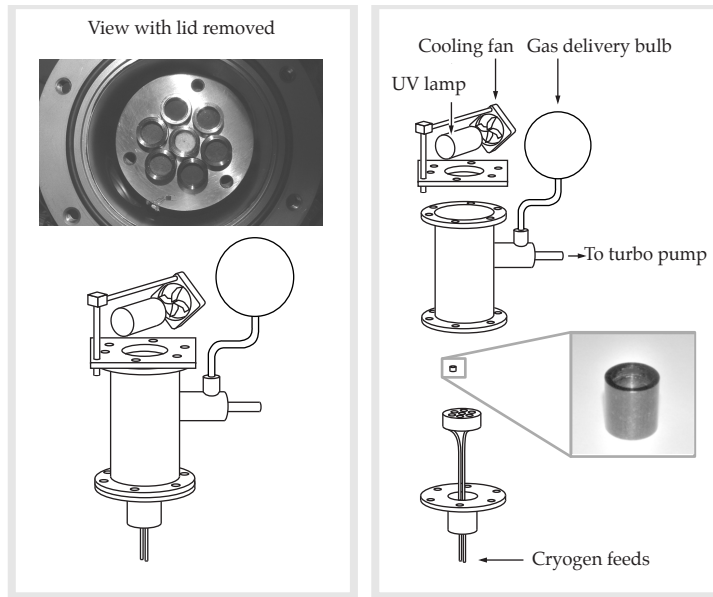


Fig. 3. The regolith exposure chamber, shown assembled in the lower left image and in its disassembled state in the right-hand image.

with UV light. The general form of the chamber is shown schematically in Fig. 3. A cylindrical block of brass held the seven stainless steel sample cups in six recesses around its perimeter with one recess in the centre. In this way all of the soil analogue samples had the same distance (~105 mm) from the discharge region of an external deuterium discharge lamp and thus received the same illumination intensity. The brass

block was soldered to a coiled copper pipe that exited the chamber via a flange. A Dewar vessel holding pressurised liquid nitrogen was connected to this copper pipe, and a solenoid valve was used to modulate the cryogen flow so as to control the temperature of the brass block. The solenoid valve was controlled by a digital thermal controller wired to a platinum thermometer fixed to the sample holder block.

A turbo pump was used to evacuate the chamber and was backed by a two-stage rotary pump. No special precautions were taken to prevent oil back-contamination, as the analysis performed on the samples is insensitive to the hydrocarbons present in pump lubricants.

3.4 Lighting system

The UV light was provided by a high stability deuterium discharge lamp (Heraeus Noblelight, DX202). This lamp was held above the chamber's window inside an air-cooled shroud. A UV sensor (Solartech, model 8.0) was used to measure the intensity of the lamp's output in a narrow wavelength range (246 to 264 nm) and provided data traceable to a NIST standard source with an accuracy of around 10 %. To gain information about the irradiance of the lamp outside of this spectral range a deuterium lamp (Bentham Instruments Ltd, model R48) with a known spectral profile was used to calibrate the response of a monochromator equipped with a photomultiplier tube (PMT), which gave an output precision of around 10 mV for values covering the PMT's full-scale output of 0 to 300 mV. This monochromator observed the

deuterium lamp's output at wavelengths from 200 to 360 nm and the resulting irradiance data were scaled to match the power measured by the narrowband UV sensor. The resulting spectral profile is shown in Fig. 4, and the total flux of the lamp in the target plane was calculated to be 10^{14} photons $\text{cm}^{-2} \text{s}^{-1}$. The thick grey line shows unconfirmed data from the lamp's manufacturer and is for guidance only as those wavelengths lie outside the monochromator grating's range. For comparison, the irradiance expected on the equatorial surface of Mars at local noon is shown as a solid line, as predicted by the model of Patel *et al.* (2002) for a low-dust atmosphere. If the lamp's output is integrated, 85 % of the energy delivered by the lamp falls in the wavelength range of 190 to 325

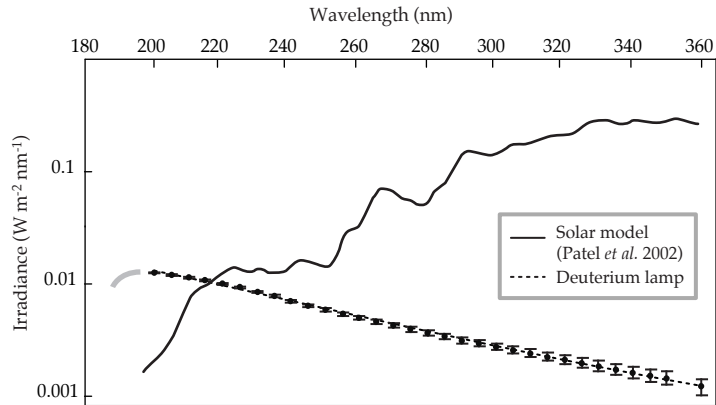


Fig. 4. The measured irradiance of the deuterium lamp in a plane 10 cm from the lamp's discharge point compared to the modelled irradiance at equatorial noon on Mars.

nm, yielding an areal power in that range of 1 W m^{-2} . This evaluation criterion allows a comparison to be made with the natural lighting found on Mars; for our experiments the lamp yields a total intensity in the range of 190 to 325 nm that is one tenth of the intensity at the martian equator at local noon. It is also expected that amino acid degradation results from the shorter, rather than the longer wavelength light in that range. If the diurnal lighting variation is accounted for, one day of martian illumination corresponds to 80 hours of lighting from the deuterium lamp.

3.5 Mars simulation experiments

Prior to the experiments the stainless steel sample cups and the spoons used for filling the cups with the powdered analogues were cleaned with acetone and then with a solution of ethanol and demineralised water. After air-drying, the cups and spoons were sterilised by being baked at $300 \text{ }^\circ\text{C}$ for 3 hours. Six sample cups were filled with the chosen regolith analogues and one with the same amount of crushed Pyrex, serving as a control sample. The soil-containing cups were placed in the recesses around the perimeter of the brass sample holder, with the Pyrex control positioned in the centre. The chamber was then evacuated to the operating pressure of around 1×10^{-5} mbar in the course of a few hours.

Four experiments were performed; in experiment I, samples were exposed for 24 hours to UV irradiation in vacuum ($\sim 1 \times 10^{-5}$ mbar). These conditions were similar to those employed by ten Kate *et al.* (2005) and thus provide an immediate com-

parison for the effect of embedding amino acids in a regolith. Secondly, an extended version of experiment I was performed, exposing fresh samples to 7 days of UV irradiation in vacuum ($\sim 1 \times 10^{-5}$ mbar) and was named experiment II. Both of these experiments were conducted at room temperature (RT). A third experiment, illuminating new samples of the same materials for 7 days at a low temperature (210 K) was performed in a 7 mbar CO₂ atmosphere and is referred to as experiment III. In this last experiment, the turbo pump was shut off from the chamber and a glass vessel of known volume holding CO₂ (Praxair, 99.996 % purity) at a known pressure was connected to the chamber. This last experiment was designed to permit water vapour to accrete at the surface of the samples. At the chosen temperature of 210 K water ice has a smaller partial pressure than the ambient gas in the chamber and the vestigial amount of water outgassing from the stainless steel of the chamber would accrete onto the sample holders. By cooling the samples and in doing so, coating them with a thin water film, the work described in ten Kate *et al.* (2006) could be extended, in which the photolytic UV destruction rates of cold amino acid films were measured. In that work cooling of the samples led to a reduction in the rate of photolysis (ten Kate *et al.*, 2006) for glycine and in section 5.2 the influence of water films on the degradation of organic matter adhered to real mineral surfaces will be examined.

The photolytic destruction of thin films of amino acids in vacuum has been described earlier by ten Kate *et al.* (2005) and so an additional experiment (IV) was conducted to verify that there were no unwanted influences arising from the use of the

irradiation chamber. A silicon disc was coated with a sub-micron layer of glycine and placed in the regolith illumination chamber. The disc was then illuminated with the UV lamp in vacuum. In contrast to the first three experiments, which used HPLC analysis, the amount of glycine on the silicon disc was measured with a Fourier transform infrared (FTIR) spectrometer (Excalibur FTS-4000, BioRad, range 4000 to 500 cm⁻¹, 4 cm⁻¹ resolution), in the manner described in ten Kate *et al.* (2005). Briefly, this consists of measuring the integrated area of specific regions in the infrared absorption spectrum of the silicon disc and its film both prior to and after irradiation in the regolith experiment chamber. Then, by assuming first-order reaction kinetics (Cottin *et al.*, 2003) the destruction rate of the amino acid can be calculated from a linear fit through plots of the natural logarithms of the normalised integrated areas from the spectrum both before and after irradiation.

3.6 HPLC analysis

Each material was analysed through use of an established procedure (Zhao and Bada, 1995; Botta *et al.*, 2002) for separating and analysing amino acids in meteorite samples. This procedure requires that each sample was flame sealed in a test tube with 1 ml of water and boiled for 24 hours at 100 °C in a heating block. One of two equal parts of the supernatants was then subjected to a 6 N HCl acid vapour hydrolysis for 3 hours, 150 °C. Both the hydrolysed and the non-hydrolysed extracts of the samples were desalted on a cation exchange resin. The amino acids eluted from the resin with 5 ml of ammonium hydroxide. They were derivatised for 1 minute or 15

minutes with OPA/NAC. The fluorescent OPA/NAC amino acid derivatives were separated by HPLC coupled with an UV fluorescence detector (Shimadzu, RF-10AXL). HPLC analysis was carried out in a C_{18} reverse phase (250×4.6 mm) Synergi 4μ Hydro-RP 80A column from Phenomenex®, with UV fluorescence occurring by excitation at a wavelength of 340 nm and emission at 450 nm. The conditions for amino acid separations for the mobile phase at 25 °C were as follows; the flow rate was set at 1 ml minute⁻¹, buffer A was 50 mM sodium acetate, containing 4 % methanol (v/v), and buffer B was methanol. The gradient used was 0 to 4 minutes, 0 % buffer B; 4 to 5 minutes, 0 to 20 % buffer B; 5 to 10 minutes, 20 % buffer B; 10 to 17 minutes, 20 to 30 % buffer B; 17 to 27 minutes, 30 to 50 % buffer B; 27 to 37 minutes, 60 % buffer B; 37 to 49 minutes, 60 % buffer B; 49 to 50 minutes, 60 to 0 % buffer B; 50 to 60 minutes, 0 % buffer B. Amino acids were identified by comparing their retention time with known standards. The amino acid abundances (part per billion by weight) in the soil samples were calculated by comparing the integrated peak area, corrected for the abundances in the blank Pyrex sample, with the integrated peak area of known amino acid standards.

4. RESULTS

4.1 Material characterisation

An investigation of the amino acid content in the two regolith analogues was made using HPLC. These materials were ana-

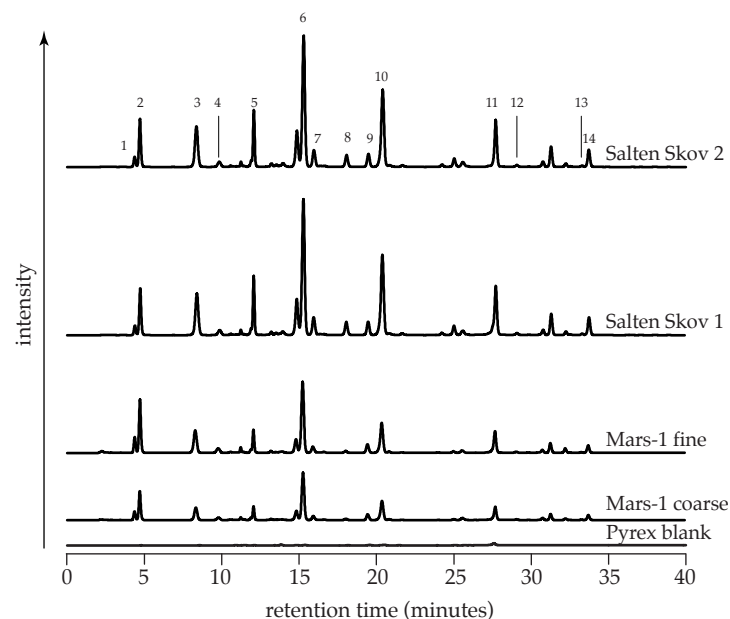


Fig. 5. The 0 to 40 minute region of the HPLC chromatograms for the un-irradiated materials. No peaks were detected outside this time period. OPA/NAC derivatisation (1 minute) of amino acids in the Mars-1 coarse material, Mars-1 fine grain sample, Salten Skov samples and blank are shown. The peaks were identified as follows: 1: D-aspartic acid; 2: L-aspartic acid; 3: L-glutamic acid; 4: D-glutamic acid; 5: D, L-serine; 6: glycine; 7: β -alanine; 8: γ -amino-n-butyric acid (γ -ABA); 9: D-alanine; 10: L-alanine; 11: L-valine; 12: D-valine; 13: D-leucine; 14: L-leucine. Other peaks are discounted, due to lack of signal, or ambiguous interpretation for the standards used.

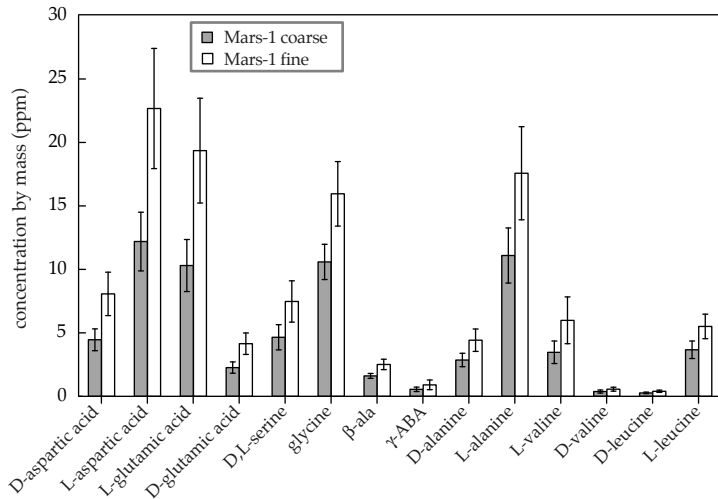


Fig. 6. Average absolute blank-corrected amino acid concentration in the unirradiated samples of coarse and fine-grained fractions of Mars-1.

lysed without any prior treatment, and were taken directly from the batches sent by their respective source institutes. Chromatograms for each of the materials used in this work are shown in Fig. 5.

The Mars-1 material was separated into two fractions, one having fine grains and one with coarser grains, as described earlier. Each of these fractions was sampled and analysed three times by HPLC using two different derivatisation periods. The average of the data from those three analyses are

shown as rectangular columns in Fig. 6 and the minimum and maximum values of the data are shown by the upper and lower ends of the capped vertical bars.

The concentration by weight of the detected amino acids differs between the Mars-1 coarse and fine samples. Crudely, for a given amino acid, the concentration in the fine sample of Mars-1 is around one third greater than the concentration of that compound in the coarse sample. The near-uniformity of this relationship suggests that the organic content of the fine and coarse samples is a function of grain area. By contrast,

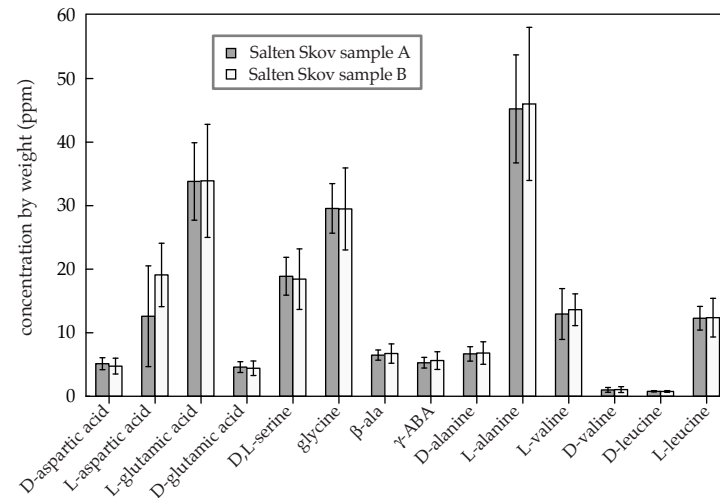


Fig. 7. Average absolute blank-corrected amino acid concentration in two samples of unirradiated Salten Skov material.

no variation could be seen in the Salten Skov material in two portions of the material taken from the top and bottom of the bulk. This is probably because the material used had already been sieved to yield a narrow grain size distribution and thus rendered homogenous, as is seen by the tightly clustered values for the mean concentration for each amino acid in Fig. 7. An identical processing sequence was used for this material as was used for the Mars-1 regolith and the rectangular columns in Fig. 7 show the average of all the data per sample. Again, the capped vertical bars indicate the span of the data.

The Salten Skov material does not have the same amino acid distribution as the Mars-1 analogue. Not only are the absolute concentrations of the detected amino acids higher by around a factor of 2 than in the Mars-1 regolith, but the Salten Skov material is richer in L-alanine, and deficient in L-glutamic acid, when compared to Mars-1. Despite their very different origins there are, however, common features in the amino acid make-up of the two soils that suggests that both Salten Skov and Mars-1 might have experienced a common contamination process, such as manual handling when they were collected. The ratio of L-valine/L-leucine in human sweat is around 2 (Hier *et al.*, 1946), in broad agreement with the ratio seen in both the Mars-1 and Salten Skov materials. If contamination from handling is neglected, amino acids may still arise in the Mars-1 soil as a result of abiotic processes in the production of fresh volcanic ash (Markhinin and Podkletnov, 1977) and the excavation site on Hawaii will in any case be exposed to aerosol-carried contaminants. The material excavated at Salten Skov has probably not experienced

Table 1: Showing the conditions and sample weights (mg) in each experiment.

Sample	Experiment type		
	I: 1 day UV, vacuum, ~300 K	II: 7 days UV, vacuum, ~300 K	III: 7 days UV, CO ₂ , 210 K
Pyrex blank	38.3	30.0	38.4
Mars-1 coarse	31.2, 31.3	30.3, 30.7	29.3, 30.2
Mars-1 fine	30.2, 29.8	30.1, 30.8	31.0, 33.2
Salten Skov A	35.5, 29.1	30.4, 33.1	29.6, 34.8

aeolian deposition, but will have had groundwater and readily soluble amino acids from bacterial metabolism and decay percolating through it.

4.2 MARS SIMULATIONS

Four different experiments were performed. In each experiment two samples of the Mars-1 material, and two samples of the Salten Skov soil were used to ensure higher accuracy. A Pyrex control sample was also exposed in the centre of the sample holder during each experiment. The weights of the samples were measured with a laboratory top-pan balance (Mettler AT200), and are shown in Table 1. Care was taken to ensure that the cups were not tilted or struck, so as to preserve the layer-like state of the powders within. The small quantities of material resulted in layers around 1 mm deep. For each experiment the same material was held in two diametrically opposed sample cups, hence two values are shown for each of the Mars-1 and Salten Skov weights in Table 1.

The conditions employed in the three experiments involving the irradiation of soils have been described in section 3.5. Before the data from those experiments are shown, the results from the fourth experiment are discussed. As described in section 3.5, a fourth test was performed to confirm that this particular experimental set-up could reproduce the degradation phenomena seen in earlier work using other equipment.

Table 2. Absolute blank-corrected amino acid average concentration and data scatter from HPLC measurements in experiment I.

Amino acid	Fine Mars-1		Coarse Mars-1		Salten Skov	
	ppb	span	ppb	span	ppb	span
D-aspartic acid	10375	1018	8939	1119	9521	1071
L-aspartic acid	24164	2262	20989	1502	35404	4482
L-glutamic acid	18499	1801	15963	1483	43769	4936
D-glutamic acid	5113	621	4390	761	6846	933
D,L-serine [†]	6931	1364	5930	897	23037	2518
glycine	20764	2171	18542	2577	44047	5470
β-ala	4685	393	4128	398	9997	1112
γ-ABA	1678	182	1373	200	6660	746
D-alanine	6469	750	5717	568	10332	1646
L-alanine	17368	2026	15351	2038	54002	6976
L-valine	3676	3326	3402	2804	16393	6371
D-valine	600	451	524	285	1269	973
D-leucine	587	61	536	34	1518	304
L-leucine	5198	593	4597	379	16294	2151

[†]Enantiomers could not be separated under the chromatographic conditions.

A thin film of glycine was prepared in the manner described by ten Kate *et al.* (2005), placed in the regolith irradiation chamber, and exposed to the UV lamp under a pressure of 10^{-6} mbar. The disc and its glycine coating were studied by FTIR prior to and after irradiation. From these data points the destruction rate for a thin film of glycine was found to be $2.6 \pm 5 \times 10^{-6}$ molecules s^{-1} , which is approximately a factor

Table 3. Absolute blank-corrected amino acid concentration and data scatter from HPLC measurements in experiment II.

Amino acid	Fine Mars-1		Coarse Mars-1		Salten Skov	
	ppb	span	ppb	span	ppb	span
D-aspartic acid	9947	1151	8315	710	7481	900
L-aspartic acid	27335	3056	22885	1921	38393	4442
L-glutamic acid	21299	2745	17770	1541	45993	5832
D-glutamic acid	4998	1219	4459	368	6108	1088
D,L-serine [†]	8777	1004	5757	3958	24920	2563
glycine	25140	1299	24024	1164	45284	4968
β-ala	5281	450	5320	428	10281	1279
γ-ABA	2240	302	1506	285	6193	940
D-alanine	6293	680	5699	531	9116	1064
L-alanine	20803	1502	18000	1112	56486	6817
L-valine	8007	4423	6142	3339	16655	14434
D-valine	336	228	376	177	915	485
D-leucine	436	66	397	87	959	144
L-leucine	5915	956	4784	786	17641	2763

[†]Enantiomers could not be separated under the chromatographic conditions.

of 2 larger than the figure calculated by ten Kate *et al.* (2005). This small difference can be attributed to the lack of data, as the fixed arrangement of the samples in the chamber did not allow in-situ measurements to be made of the film's IR transmission spectrum. In contrast, the equipment used by ten Kate *et al.* (2005) allowed a dozen or so transmission spectra to be recorded during the film's breakdown.

Table 4. Absolute blank-corrected amino acid concentration and data scatter from HPLC measurements in experiment III.

Amino acid	Fine Mars-1		Coarse Mars-1		Salten Skov	
	ppb	Span	ppb	Span	ppb	Span
D-aspartic acid	4345	784	6516	1621	5618	1057
L-aspartic acid	11552	2058	17583	4305	23828	4442
L-glutamic acid	9379	1614	14440	3552	31850	6001
D-glutamic acid	2175	445	3338	850	4403	1004
D,L-serine [†]	3644	479	5414	1390	15314	3516
glycine	7095	1265	10900	2749	20618	3682
β-ala	1751	307	2670	721	4744	884
γ-ABA	666	94	1699	436	3857	735
D-alanine	2392	425	3651	915	5617	1038
L-alanine	8104	1420	12383	3019	37181	7123
L-valine	6516	2460	7418	1435	19879	2540
D-valine	158	640	172	654	475	588
D-leucine	451	708	224	167	734	223
L-leucine	2245	1072	4000	964	12261	2262

[†]Enantiomers could not be separated under the chromatographic conditions.

In Tables 2, 3 and 4 the amino acid concentrations of the different analogues are shown for the first three experiments performed. The amino acid concentration by weight of each material, shown in the columns labelled 'ppb', is the average of data from the two samples of that analogue present in the chamber. The concentration shown for each of the three materials is an average of six HPLC measurements. The difference between the maximum and minimum values for the six concentration values for an amino acid in each material is tabulated in the columns headed 'Span'. Those values reflect the scatter in the concentration data and, given the complexity of the extraction and subsequent HPLC processes, should not be interpreted as an error in the sense of a random process occurring over many repeated identical trials.

Data for experiment I, consisting of exposure to UV light and vacuum at room temperature for one day are shown in Table 2. In Table 3, the data from experiment II, involving exposure to UV light and vacuum at room temperature for seven days are shown. Finally, in Table 4, the data from experiment III are listed, in which the samples were irradiated and cooled to 210 K in a CO₂ atmosphere.

For clarity, the shifts between the concentration of amino acids in the unirradiated samples and the concentrations in the soils in each of the three experiments (I, II, and III) are shown in Figs. 8 and 9 for the Mars-1 fine-grain analogue and the Salten Skov material respectively. The JSC Mars-1 coarse fraction data are not plotted, as they substantially follow the trends of the finer fraction.

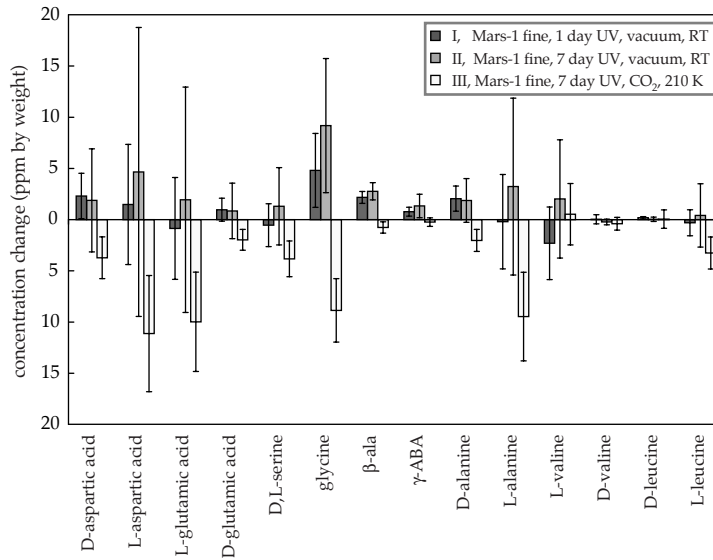


Fig. 8. The change in concentration in amino acids in the Mars-1 fine fraction resulting from experiments I, II, and III. An increase of certain amino acids can be observed after UV irradiation in vacuum at room temperature (RT). Enhanced destruction of D and L-aspartic acid, D and L-serine, L-glutamic, glycine, and L-alanine was observed in an experiment at 210 K and in a CO₂ atmosphere.

5. DISCUSSION

The data shown in Figs. 8 and 9 appear to show three trends. Firstly, there is an apparent increase in the concentrations of certain amino acids as a result of exposure to vacuum and UV

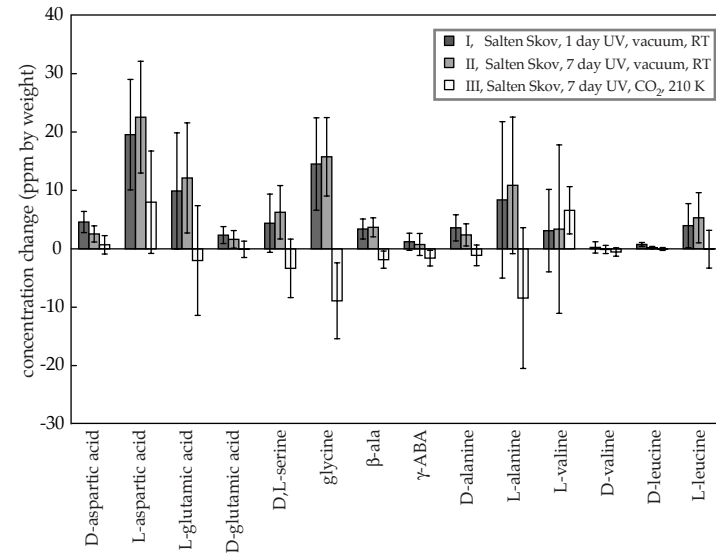


Fig. 9. The change in concentration in amino acids in the Salten Skov material resulting from experiments I, II, and III. An increase of certain amino acids was measured after UV irradiation in vacuum at room temperature. Enhanced destruction of glycine and L-alanine was observed in an experiment at 210 K and in a CO₂ atmosphere.

light. For the Salten Skov material the largest relative increase is seen for L-aspartic acid, which more than doubles in concentration when compared to its unirradiated concentration. The Mars-1 fine fraction displays broadly similar but smaller relative changes, with L-leucine doubling in concentration,

and the remainder rising in concentration by a lesser amount upon exposure to vacuum and UV light. No obvious sources of contamination were identified, and the same procedures were followed for analysis of pre-irradiated and post-irradiated samples, which ordinarily yielded values that were repeatable to a few ppm (Fig. 6). Secondly, the concentrations of the detected amino acids in the regolith samples do not change significantly when the UV exposure duration is changed from 1 day to 7 days, indicating that the process causing the rise in amino acid concentrations is rapid. Thirdly, in experiment III the concentrations of the measured amino acids after irradiation were uniformly lower than the concentrations of the amino acids recorded at the end of experiment II. This change is most pronounced in the Mars-1 data, which show a reduction in the amino acid concentration to levels, broadly, below that of the unirradiated samples. Experiments by ten Kate *et al.* (2006) demonstrate that cooling pure films of amino acids to 210 K slows down their rate of degradation by a factor of 7 or so, when they are exposed to a UV source. The lamp used in that work is the same model as used in the fourth experiment presented here, and it is therefore apparent that photolytic degradation cannot explain the absolute reduction in amino acid concentration that is seen in experiment III. A related experiment by ten Kate *et al.* (2006) shows that an ambient 7 mbar atmosphere of CO₂ at room temperature, makes no measurable change to the UV-induced degradation rate of a thin amino acid film. That study argues that no significant quantities of reactive species are generated within the gas around the samples, as the degradation rate is essentially unchanged from that seen for amino acids in a hard vacuum.

It is important to note that in experiment III only the sample holder was cooled, not the whole chamber. Therefore the gas within the chamber would have been substantially warmer than the 210 K of the brass sample holder and the soils. The difference between that study and the illumination of a soil is that in experiment III the organic matter is intimately connected to irregular mineral grains, which will scatter and absorb infalling UV light, rather than reflecting it. It is likely then that processes driven by UV photons, such as the mobilisation of electrons at a surface and the subsequent formation of trapped radicals, will proceed more effectively on UV absorbing mineral surfaces coated with water, than on a weakly absorbing or reflecting surface.

The apparent increase in amino acid concentrations as a result of exposure to vacuum and UV is worthy of extended discussion. Neither the Mars-1 nor the Salten Skov samples were cleaned in any manner. Thus it is likely that these materials contained organic contaminants from atmospheric aerosols, microbes from a variety of species, and bulk organic matter from the original excavation sites. Analysis of the JSC Mars-1 soil by Mendez *et al.* (2005) and Allen *et al.* (2000) showed the presence of fungi and culturable and non-culturable bacteria within it and it is possible that the Salten Skov material could also be host to bacterial or fungal spores. It is very likely that some of the apparent formation of amino acids, such as L-glutamic, L-aspartic, L-alanine, and so on, indicates the degradation of cell walls and the lysis of living bacteria or bacterial spores present in the regoliths. Certainly, these amino acids are present in the cell wall proteins of common

bacilli such as *E. coli*. (Howe *et al.*, 1965). To test the degradation hypothesis would require work perhaps involving some form of genetic or biomarker tracing. A similar rise is seen in the amino acid concentrations of the Mars-1 and Salten Skov material despite their different amino acid make-up in their unirradiated state. Therefore it might be argued that such a common change is the result of a common biological process, such as spore degradation.

5.1 Model of amino acid degradation within a regolith

The regolith analogues used in this work were exposed to the UV light generated by a deuterium lamp. No UV light with an intensity greater than $0.1 \mu\text{W cm}^{-2}$ in the range of 245 to 265 nm penetrated shallow (~1 mm thick) layers of Mars-1 or the Salten Skov material when illuminated with a UV intensity of $500 \mu\text{W cm}^{-2}$ from a xenon solar simulator. Thus, photolytic processes will only occur at the exposed surface of the regolith samples. If the powders are treated as spherical grains that are optimally packed, then the actual grain area that the radiation may strike is larger than the geometric cross-section of the sample cups. If the grains are assumed to be perfect absorbers, then only direct light from the lamp and radiation scattered from the sample cup walls can strike the regolith. If a vessel of radius R holds a powder of well-packed spheres with radius r , then only the upper hemispheres of the grains at the surface can be irradiated. Thus light penetrates only a distance r into the powder. The powdered sample has a known mass, m , and a bulk density ρ_{bulk} , and so the thickness, d , of the sample is given by equation 1.

$$d = \frac{m}{\rho_{\text{bulk}}\pi R^2} \quad (1)$$

The sample holders have a cylindrical geometry, and so total area of the sample varies linearly with sample thickness. Thus, the ratio, A , of the irradiated area at the surface to the total shadowed area is given by equation 2.

$$A = \frac{r}{\left(\frac{m}{\rho_{\text{bulk}}\pi R^2}\right)} \quad (2)$$

It will be assumed that all of the samples used have modal grain sizes of ~100 micron, as the difference between the coarse and fine Mars-1 materials appears to lie in the inclusion of large grains in the 'coarse' sample rather than the exclusion of finer material. The weights of the materials used in each experiment were listed in Table 1 and a nominal average bulk density, ρ_{bulk} of 900 kg m^{-3} will be assumed. The bulk density of Mars-1 can lie between 870 and 1070 kg m^{-3} (Allen *et al.*, 1998). For the vessel ($R = 5 \text{ mm}$) used to hold the powders, the fractional area, A , of a sample that receives direct radiation is of the order of 25 % of the total surface area in the sample. Thus, if the regolith and any incumbent organic contamination with a photolytic characteristic lifetime of τ are exposed to a photolytically degrading process, then the concentration, C , of that organic matter remaining after time t is simply

$$C = C_{(t=0)} \left[(1-A) + Ae^{-\frac{t}{\tau}} \right] \quad (3)$$

The photolytic degradation rates of glycine and D-alanine are known from earlier experiments (ten Kate *et al.*, 2005) and so only these compounds will be discussed. D-alanine, with its half-life of 3 hours under martian equatorial noon-time conditions, should have been completely removed from the upper A fraction of the analogues used in this work during one day. In that time the overall concentration glycine would have only been reduced by around 13 %. Further irradiation for 6 days would not change the total amount of D-alanine in the regolith, as it will have been depleted from the region accessible to UV, whereas the overall concentration of glycine would fall to ~75 % of the original concentration. Given the accuracy and precision of the HPLC technique used, it is possible that this change would have been detected. The absence of a lowering of the amino acid concentrations in experiment II, suggests that either the grains stabilised surficial organic compounds against photolysis, or that the production of amino acids by the postulated breakdown of cell walls surpassed their photolytic removal.

5.2 Candidate photochemical processes

Several compounds and processes have been suggested as potential oxidising agents that are presumed to operate at the martian surface (Banin, 2005; Zent and McKay, 1994). It is worth examining some of these to assess whether the removal of amino acids in experiment III can be explained through the action of a reactive compound. For example, through photolysis water can form OH· radicals, which then can dimerise to hydrogen peroxide (H₂O₂) although other paths to its pro-

duction are possible. The low thermal stability of H₂O₂ makes this a good candidate for the oxidation of matter at low temperatures and on Mars it may be stable at significant depths within a regolith column (Bullock *et al.*, 1994). The expected martian equilibrium surface adsorbed concentrations for H₂O₂ are of the order of 250 nmoles cm⁻³, based on a production rate of around 5×10^{10} cm⁻² s⁻¹ (Bullock *et al.*, 1994). The formation of H₂O₂ is ultimately dependent on the concentration of water vapour in the atmosphere, and so it is possible to scale the production rate on Mars to the conditions present in the regolith illumination chamber. The chamber could be evacuated to a low pressure with the turbo pump. When the chamber was valved-off from the pump's inlet, the pressure in the chamber rose over the course of a day to an equilibrium value of around 10⁻² mbar. The source of this vapour is presumed to be water vapour outgassing from the regolith and from the chamber walls. This last source is expected in stainless steel vacuum systems that have been opened to ambient air. The partial pressure of water in Mars' atmosphere at the surface is believed to be around 10⁻³ mbar, and so a crude estimate for the production rate of H₂O₂ in the chamber from water photolysis can be made by comparing the optical path length of the chamber to the effective column height of Mars' atmosphere. By doing so, a formation rate of ~10⁶ cm⁻² s⁻¹ is found, which results in a fractional areal coverage rate of one part in 10⁸ per day for each regolith sample in the chamber. Changes in the amino acid concentrations over the course of one day would be undetectable with the HPLC method described in this work.

Water may also play a less direct role in forming oxidising agents. It has been shown that the interaction of oxygen with UV irradiation (Oró and Holzer, 1979) leads to the degradation of amino acids, but oxygen is a minor constituent of the martian atmosphere. The presence of water frosts on mineral surfaces is pertinent, as the exposure of thin water frosts on iron-bearing minerals to UV has been shown to cause the release of oxygen upon warming (Huguenin *et al.*, 1979), arising from the formation of a condensed oxidising agent at the mineral surface. Later experiments with feldspar by Yen *et al.* (2000) demonstrate that superoxide radicals such as O_2^- are formed through the combination of cold mineral surfaces ($-30\text{ }^\circ\text{C}$), Mars-like UV lighting, free oxygen, and low concentrations of water. The quantum efficiency for this process has been estimated by Yen *et al.* (2000) as being 10^{-6} radicals photon^{-1} , who also predict a production rate of $10^7\text{ cm}^{-2}\text{ s}^{-1}$. It is appropriate to ask if these UV-generated radicals are therefore responsible for the degradation seen in experiment III. Our experiments with cooled mineral surfaces under UV irradiation were performed in an ambient gas with a mixing ratio of oxygen no greater than 50 ppm by volume according to the manufacturer's datasheets, this is a concentration around 20 times smaller than in the martian troposphere. Thus, scaling for the lower illumination levels and oxygen content in the regolith chamber, approximately 10^4 radicals $\text{cm}^{-2}\text{ s}^{-1}$ would be expected to form on the surfaces of the regolith samples studied in this work. In the course of one day O_2^- radicals may have an areal coverage of 1 part in 10^{10} of the exposed regolith. The above calculations are based on the amount of gaseous oxygen in the CO_2 atmosphere of experiment III and

neglect the potential for oxygen to be formed from the decomposition of adsorbed water by photolysis at the cold mineral surfaces of experiment III. It is therefore still possible that the amino acid degradation seen in experiment III is driven by oxidative attack from O_2^- radicals and perhaps other photochemical species, formed within the adsorbed water layers bound to the surfaces of the soil grains that are illuminated by energetic UV.

Water can also play a role as a mediating agent for the mobilisation of acids generated through nitrogen and sulphur oxidation (Quinn *et al.*, 2005d). In the work presented here neither of those compounds was present in the gas-phase at levels above a few ppb in any of the experiments and so dry-acid deposition by aerosols is not expected. However, water adsorbed at the surface of a mineral can leach soluble species from the rock, leading to a situation in which Fe(II) ions generate $\text{OH}\cdot$ ions via the photo-Fenton reaction of H_2O_2 with UV. This process is well studied on Earth (Southworth and Voelker, 2003) and in martian scenarios (Benner *et al.*, 2000, Möhlmann, 2005). Thus, a plausible pathway for the formation of a vigorous reactive species is present in experiment III, involving the presence of water adsorbed onto mineral surfaces. In experiment III the samples were cooled to 210 K in the presence of water with a partial pressure of around 10^{-2} mbar, around an order of magnitude higher than the partial pressure of water in the near-surface atmosphere of Mars (Schorghofer and Aharonson, 2004). A theoretical model presented by Möhlmann (2004) indicates that a few monolayers of water would be ubiquitous on exposed martian surfaces,

with the total thickness fixed by the partial pressure of water. We therefore suggest that the samples within experiment III were coated with a quasi-liquid water layer, permitting the generation of the OH· radicals to occur within that adsorbed water. The exact chemical path for its formation is not decidable from our data, and several candidate pathways are available aside from those indicated in section 5.2, such as the photo-Fenton reaction on iron-bearing minerals (Möhlmann, 2004).

5.3 Comparison to the martian environment

The martian surface experiences lighting spectra and material transport processes that are difficult to emulate in a laboratory. To first order, we assume that the spectrum of the light can be modelled with a fixed profile. In the apparatus used to illuminate the samples the lamp produces an integrated power in the wavelength range of 190 to 325 nm that is around one tenth of the intensity expected to occur in that band at noon in the equatorial regions of Mars. Furthermore, the surface of Mars is not a static environment and the action of wind, saltating grains, and sporadic meteorite impact, all act to till the regolith over different timescales. Thus the uppermost UV-exposed regolith grains will be progressively mixed into the ground. If a grain is removed from the surface by some form of gardening in a time that is shorter than the organic matter's photolytic lifetime, then there will be no sharp boundary between the UV-cleansed upper surface and deeper layers.

A further relevant point concerns the use of constant temper-

atures for periods greater than one day, of ~300 K in experiments I and II, and 210 K in experiment III. These conditions do not accurately reflect the equatorial diurnal temperature cycle seen on Mars, as the warming and cooling cycle experienced by the martian surface throughout a full day is not simulated. This is an important factor as the reactivity of chemical species formed either through photochemical or photolytic pathways on the martian surface will be influenced by the ambient temperature. The longevity of such species (H₂O₂, etc.) will also depend on the surface temperature and their abundance will be influenced by the porosity of the regolith. It is possible that a balance will be struck between the rate at which a species may decompose during the day, and the rate at which they may condense during the night. We do not mimic other processes occurring on Mars, such as burial by dust at sundown, that could lead to the preservation of oxidising agents formed through interaction with water.

6. CONCLUSION

We have performed analyses of two martian regolith simulants and have quantified their amino acid content. In doing so we have obtained data that are useful to biological, chemical, and physical studies of analogues for martian surface materials. If biological processes occurred on Mars in the past, they may have been exposed to climatic conditions different from those currently seen on that planet. The chemical signatures from these processes, and the materials brought by meteorites throughout Mars' history, are subject to a number of

destructive processes that operate at different timescales and in the presence of different materials. We have studied the effect of an important process, UV radiation, on two soil analogues. Exposure of these materials to conditions of vacuum and energetic UV appears to generate higher concentrations of amino acids within the materials. This process is rapid and repeatable in all the samples used, with exposures of one day yielding results similar to those arising from seven days of irradiation. It should be noted that seven days of irradiation in the laboratory is equivalent to the light received during 2 full days on Mars. It is postulated that this in-situ formation results from the degradation of extant biota within the soils, and the fingerprint of amino acids present is suggestive of the degradation of cell walls, as indicated in section 5.

With the method used, photolysis of the amino acids present in the soils, or generated through cell destruction was not detected. The shallow samples permit a significant fraction (of order 30 %) of the material to be irradiated, a value comparable to the precision of the HPLC process employed. Separately, we have demonstrated that a pure amino acid film can be degraded within the experimental chamber when the sample is lit by the UV lamp used in the experiments described here. The degradation rate from that measurement is in line with expectations from earlier work (ten Kate *et al.*, 2005) and therefore photolytic degradation should occur in the regolith samples exposed to UV, but other factors dominate the changes seen in the amino acid concentrations.

Cooling of the regolith samples to 210 K and simultaneous

exposure to an atmosphere of carbon dioxide leads to the removal of amino acids when compared to unirradiated samples. It is probable that adsorbed water on the mineral surfaces is key to the generation of reactive species on the grains, and the subsequent degradation of the amino acid content within the soil, as is discussed by Quinn (2005d) and Zent and McKay (1994). While the details of this process are not visible from this work, it is worth noting that the amino acid degradation caused by cooling in the presence of background water is comparable in magnitude to the degradation expected by photolysis in the same period, see section 5.1.

If the apparent formation of amino acids in regolith simulants is taken at face value, there are implications for the use of these and other analogues in future. The diverse nature of the planetary research community means that a single material cannot reasonably represent the wide range of physical and chemical properties that are pertinent to martian science. A specific and timely concern is the nature of analogues that are appropriate for forthcoming missions that will engage in biological studies of in-situ and returned martian samples. For example, it is conceivable that materials used in simulations of a sample-return mission would, for purposes of verifying the curation and dispersal procedures, be subject to the same planetary protection regulations as a real sample (Rummel, 2001). As a part of such a process, qualification samples with no detectable organic content would be needed. While the physical properties (such as grain size distribution and so on) of an analogue can be controlled relatively easily, it is difficult to conceive of a process that would remove extant biota and

their corpses from a regolith analogue without changing the mineralogy of the material. Techniques employed in spacecraft sterilisation processes such as heat-sterilisation, irradiation with ionising particles and quanta, and exposure to oxidising gasses and plasmas, are unable to remove significant quantities of organic matter from a material. Thus, it would be desirable to establish a database of analogues for planetary regoliths, which are separately designed for chemical, biological, and engineering studies. We have demonstrated that an analogue, such as Mars-1, designed to be a spectral and physical match to a nominal average martian soil is inappropriate for a life-science study in its raw state.

ACKNOWLEDGEMENTS

JRCG is supported by grant MG058 from the SRON National Institute for Space Research, ILtK is supported by the BioScience Initiative of Leiden University, ZM is supported by Fundação para a Ciência e a Tecnologia (scholarship SFRH/BD/10518/2002), PE is supported by grant NWO-VI 016.023.003. We thank Zan Peeters for his help with the HPLC analyses and the clarity of this manuscript was improved by constructive comments from A. J. Jull, and the reviewers M. Sephton and C. McKay. Oliver Botta is thanked for his insight into HPLC processing.

Chapter 6

The behaviour of halophilic archaea under martian conditions

Mars is thought to have had liquid water at its surface for geologically long periods. The progressive desiccation of the surface would have led to an increase in the salt content of remaining bodies of water. If life had developed on Mars, then some of the mechanisms evolved in terrestrial halophilic bacteria to cope with high salt content may have been similar to those existing in martian organisms. We have exposed samples of the halophilic *Natronorubrum* sp. strain HG-1 (*Nr.* strain HG-1) to conditions of ultraviolet radiation (UV) similar to those of the present-day martian environment. Furthermore, the effects of low temperature and low pressure on *Nr.* strain HG-1 have been investigated. The results, obtained by monitoring growth curves, indicate that the present UV radiation at the surface of Mars is a significant hazard for this organism. Exposure of the cells to high vacuum inactivates ~50 % of the cells. Freezing to -20 °C and -80 °C kills ~80 % of the cells. When desiccated and embedded in a salt crust, cells are somewhat more resistant to UV radiation than when suspended in an aqueous solution. The cell inactivation by UV is wavelength dependent. Exposure to UV-A (> 300 nm) has no measurable effect on the cell viability. Comparing the inactivating effects of UV-B (250-300 nm) to UV-C (195-250 nm) indicates that UV-C is the most lethal to *Nr.* strain HG-1. Exposure to UV-B for a duration equivalent to ~80 hours of noontime equatorial illumination on the surface of Mars, inactivated the capability to proliferate of more than 95 % of the cells. It can be concluded that *Nr.* strain HG-1 would not be a good model organism to survive on the surface of Mars.

Inge Loes ten Kate, Florian Selch, James Garry, Kees van Sluis, Dimitri Sorokin, Gerard Muyzer, Helga Stan-Lotter, Mark van Loosdrecht, Pascale Ehrenfreund
in preparation

1. INTRODUCTION

Mars is the subject of numerous investigations concerning its planetary properties and the search for life by remote-sensing spacecraft and in-situ rovers (Rummel and Billings, 2004). Sample-return missions are being considered, and are likely to be included in a future round of missions that are expected to accommodate sophisticated (bio)chemically-oriented payloads. An important objective of those missions is to establish the presence and state of organic matter in the near-surface regolith of Mars. Almost thirty years ago the two Viking landers found no evidence (Biemann *et al.*, 1977; Klein, 1978) for the presence of native carbon-containing compounds in samples taken from two locations¹. Given the meteoritic infall of organic matter that is expected at Mars (Flynn and McKay, 1990), the absence of organic material suggests that the martian near-surface harbours one or more chemically aggressive processes that degrade organic compounds. Laboratory experiments have been conducted to identify these processes (Oró and Holzer, 1979; Huguenin *et al.*, 1979; Stoker and Bullock, 1997; Yen *et al.*, 2000; ten Kate *et al.*, 2005; Garry *et al.*, 2005). It is therefore possible that molecular indications of a past martian biosphere will have been degraded or altered on Mars. Several possibilities can be envisaged.

1) Life has evolved on Mars but is now extinct due to the changed environmental conditions. Therefore robotic missions should look for compounds associated with life. If terrestrial geology and biology are taken as a guide, then isotope ratios and perhaps chirality measurements would

be critical to unambiguously identify a biogenic origin of detected compounds. Indirect methods such as investigating biochemical remnants in geologic deposits, used on Earth (e.g. Russell, 1996; Hu Ming-An *et al.*, 1995) could be applied as well. However, this is a more complex method open to misinterpretation.

2) Life is still present on Mars but only in isolated niche areas. Some degree of adaptation would have been needed for the organisms to endure the changing climate of Mars. However, conditions in certain areas, such as those located deep in the crust, may have changed relatively little in the period during which the martian surface desiccated. The degree of environmental stress on an organism will therefore be a function of its location.

3) Life has never been present on Mars. All organic matter found in the martian environment is generated by purely abiotic processes, which may include meteoritic infall, chemical synthesis in volcanic processes and similar reactions.

In general, the conditions on the martian surface are hostile to terrestrial life. The main hazards are thought to be the lack of liquid water in the near-surface and the energetic UV radiation present in the sunlight. These conditions, combined with ionic reactions on or within mineral surfaces, may lead to aggressive oxidative agents (Yen *et al.*, 2000; Quinn, 2005d). On Earth, however, organisms exist that are able to adapt to extreme conditions and are therefore referred to as 'extremophiles'.

¹ Chryse Planitia and Utopia Planitia, landing sites of the Viking 1 and 2 landers, respectively.

Salt tolerant organisms, belonging to the domain of Archaea, evolved early in Earth's history (Oren, 2002). A class of these organisms is termed 'Halophiles', as they not only tolerate but also thrive in environments with salt concentrations up to ten times higher than that of present ocean water. Geological formations millions of years old still contain viable halophilic archaea and bacteria (e.g. the Permian-Triassic era, 290–206 Ma, Stan-Lotter *et al.*, 1999; McGenity *et al.*, 2000). In general, organisms can respond to environmental stress by the use of one or more protective mechanisms. Halophilic archaea appear to employ several protective mechanisms to provide tolerance to highly saline environments. It is possible that the diversity of such strategies is the result of multiple adaptations in ancient times. A possible connection between the origin of life on Earth and the ability of microorganisms to grow at high salt concentrations has been described by Dundas (1998).

Litchfield (1998) concluded that "the ability of halophilic archaea to survive within low-water activity environments such as 'evaporites' and their requirement for elevated salt concentrations make them likely candidates for life on Mars." Indeed, the ability of some halophilic Archaea to tolerate UV exposure and osmotic stress, is exemplified by their resistance to hard vacuum and unfiltered solar radiation during spaceflight (Mancinelli *et al.*, 1998).

Advances in the understanding of terrestrial biochemistry allows the evaluation of other life systems, either theoretically or practically, giving a better insight into how robust non-

terrestrial life might be. In this light we have examined the response of the halophilic archaeon *Nr.* strain HG-1 to various Mars-like conditions. The rationale for using this species is the similarity of its natural growing environment to that of a martian setting as postulated from the results of the Mars Exploration Rovers (e.g., Squyres *et al.*, 2004 a,b). In this study we describe the effects of several environmental conditions on the survival of *Nr.* strain HG-1. The organism has been exposed to radiation in three different wavelength ranges, has been cooled to low temperatures, and was exposed to high vacuum. We have investigated the *Nr.* strain HG-1 both in suspension and after desiccation, which leads to dried cells, because *Nr.* strain HG-1 does not form spores. In section 2 details of the *Nr.* strain HG-1 are given along with its growth characteristics and the desiccation method used for the experiments. Experimental procedures concerning irradiation, cooling, and vacuum storage are discussed in section 3. Section 4 summarises the results of the behaviour of *Nr.* strain HG-1 to extreme conditions. In section 5 the implications of those results for future planetary exploration are discussed.

2. MATERIALS AND METHODS

2.1 Strain and culture conditions

The archaeal strain *Natronorubrum* sp. strain HG-1 (*Nr.* strain HG-1) used in our studies has been isolated and described by Sorokin *et al.* (2005). It is an Euryarchaeon of the class Halobacteria and belongs to the order of Halobacteriales, in the

family of Halobacteriaceae. The cells are polymorphic rods with a diameter of 0.5-1 μm and a major axis length of 1.5-5 μm , which transform into irregular coccoids during stationary growth phase. 10 ml *Nr.* strain HG-1 cultures were grown in an agitated aqueous medium at 45 °C within closed 50 ml flasks. The growth medium included 240 g l⁻¹ NaCl, 2 g l⁻¹ K₂HPO₄, and 0.5 g l⁻¹ (NH₄)₂SO₄, and the pH was adjusted to a value of 7.3 before the solution was sterilised by heating for 20 minutes at 120 °C. After sterilisation, the medium was supplemented with 2mM MgCl₂, 10 mM sodium acetate, 0.05 g l⁻¹ yeast extract, and 1 ml l⁻¹ of trace elements solution (Pfenig and Lippert, 1966).

2.2 Growth curves

Cells used for experiments were harvested in the exponential growth phase and their initial concentration was estimated by optical counting. After treatment, cultures of 10⁷ cells ml⁻¹ were incubated for up to 5 days. The concentration of cells within samples was estimated by optical counting, using a microscope, during the exponential growth phase. In this stage the number of dead or dying cells is assumed to be negligible in comparison to the number of living cells. Plating on solid medium could not be used, because *Nr. strain HG-1* does not form colonies on agar plates. At intervals of roughly 12 hours, the absorption spectra of the samples were measured over the 200-900 nm wavelength range using a UV-Vis diode-array spectrophotometer (Hewlett Packard, model 8453). Growth was monitored by plotting the absorbance at a wavelength of 600 nm (OD₆₀₀) as a function of incubation

time. For each treated cell sample a new culture was prepared and incubated. Optical density, however, could only be detected at cell concentrations greater than 10⁷ cells ml⁻¹. The number of living cells after treatment determines the time interval needed for a culture to reach a detectable optical density. From this delay in time the number of surviving cells can be calculated (see section 4.2).

2.3 Light sources

Two light sources have been used in our studies, a xenon solar simulator (ScienceTech, model 100150XUV, generating radiation between 200-2500 nm) and a deuterium discharge lamp (Heraeus-Noblelight, model DX 202, 190-400 nm). The xenon lamp is equipped with an AirMass 0 filter to remove strong xenon features that do not resemble the unfiltered solar spectrum. Intensity of the light was measured for both lamps in the UV and visible regions, using a Solartech UV-C sensor (model 8.0) and an Extech light meter (model EA30). The Solartech sensor measures irradiance over a Gaussian-shaped sensitivity profile centred on 250 nm, with a half-peak full-width value of 20 nm. The EA30 sensor is a broadband optical sensor and was used to ensure that the xenon lamp's output was stable over the experiment run.

Using the Solartech sensor, the intensity (in W m⁻²) of both the xenon and the deuterium lamp in the wavelength range 245-265 nm was measured. From these values the irradiance of both spectra for our illumination scenarios could be derived.

Fig. 1 shows the spectrum from 190-400 nm of a generic xenon lamp of the same construction and type as the xenon lamp used in this work. Additionally, the spectrum of the deuterium

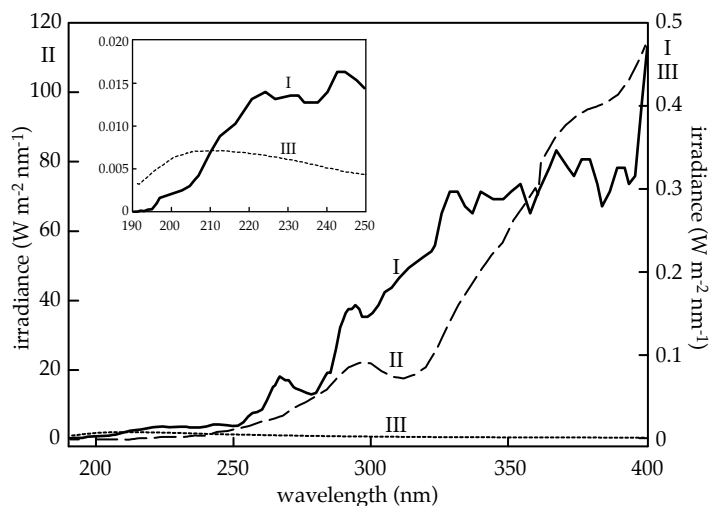


Fig 1. (I) The predicted noontime equatorial UV spectrum at the surface of Mars in the presence of a non-dusty atmosphere (continuous line) (Patel *et al.* 2002), with its irradiance plotted on the right ordinate. (II) The spectrum of the xenon lamp (dashed line), with its irradiance plotted on the left ordinate. (III) The spectrum of the deuterium lamp (dotted line), with its irradiance plotted on the right ordinate. The inset box shows the UV spectrum at the surface of Mars (I) and the spectrum of the deuterium lamp (III) from 190-250 nm.

rium lamp and the noontime illumination spectrum expected at equatorial regions on Mars, for a non-dusty atmosphere, as modelled by Patel *et al.* (2002) are shown.

When comparing the three spectra in this wavelength range, the xenon lamp gives an acceptable representation of the solar spectrum on Mars, although 250 times more intense. The deuterium lamp generates light with a spectrum that, when compared to the solar or xenon spectra, is enhanced in the shorter wavelengths (190-250 nm) and has a maximum output around 210 nm. At this wavelength the irradiance of the deuterium lamp is comparable to the solar irradiance at Mars. The inset box in Fig. 1 shows that, in the 190-250 nm range, the intensity of the deuterium lamp is of the same order as the solar intensity on Mars, and, as such, approximately 250 times lower than the intensity of the xenon lamp. The difference in UV output between the xenon and the deuterium lamp enables us to discriminate between the longer (250-300 nm) and shorter (195-250 nm) wavelength range of the UV spectrum.

3. EXPERIMENTAL PROCEDURES

The effect of various treatments has been examined using two types of cell samples, in liquid suspension and in desiccated state.

- 1) Cell suspensions have been irradiated using the xenon discharge lamp.
- 2) Desiccated cells have been irradiated using either a

xenon or a deuterium discharge lamp.

- 3) Desiccated cell samples have been placed in vacuum at room temperature, and, separately, have been exposed to low temperatures.

3.1 Irradiation of cell suspensions

Cell suspensions of 10^8 cells ml^{-1} were irradiated in sterile Petri dishes with the xenon lamp, while being constantly stirred. 1 ml samples were taken for analysis after defined periods of irradiation (30, 60, 120, 300, and 600 seconds). All samples, including a non-irradiated control, were diluted with 9 ml of growth medium, resulting in a concentration of 10^7 cells ml^{-1} . 10 ml Cultures were then incubated and growth curves were measured as described.

3.2 Irradiation of desiccated cells

Desiccated samples were prepared by heating 1 ml of cell suspension, containing 10^8 cells ml^{-1} , in Petri dishes for 1 h at 50 °C. These desiccated samples were exposed to three different types of irradiation. Firstly, desiccated samples were irradiated with the xenon lamp at the same intensity as the cell suspensions in section 3.2. To be able to discriminate between the effect of UV and visible light, the second set of desiccated samples was covered with a borosilicate glass plate during irradiation with the xenon lamp, thus filtering out light with wavelengths shortward of 300 nm. Both the first and second irradiation process took place for durations of 30, 60, 120, 300, and 600 s. The third set of desiccated samples was irradiated

with the deuterium lamp for 21 h to measure the effect of UV only. The long exposure time was needed because the lamp's low intensity was expected to lead to a weak damaging effect on the cells. After irradiation, the dried cell samples were resuspended by adding 9 ml medium and 1 ml sterile water, resulting in a concentration of 10^7 cells ml^{-1} , equal to the concentration of the cells irradiated in suspension. The sample cultures were then incubated and growth curves were measured as previously described.

3.3 Desiccated cells in vacuum and in a cold environment

Three batches of desiccated samples were prepared as described in the previous subsection. The samples were separately exposed to one of three different environments: (1) -20 °C for 1 h, (2) -80 °C for 21 h, and (3) high vacuum (1.4×10^{-4} mbar) for 15 h. After freezing and exposure to vacuum, the samples were resuspended and incubated as described.

4. RESULTS

We have measured the response of the archaea *Nr.* strain HG-1 to UV and visible radiation, both in suspension and in a desiccated state. Furthermore, the response of desiccated cells to hard vacuum and low temperatures has been investigated. In support of these experiments, growth curves have been measured, from which the growth rate at 45 °C could be derived.

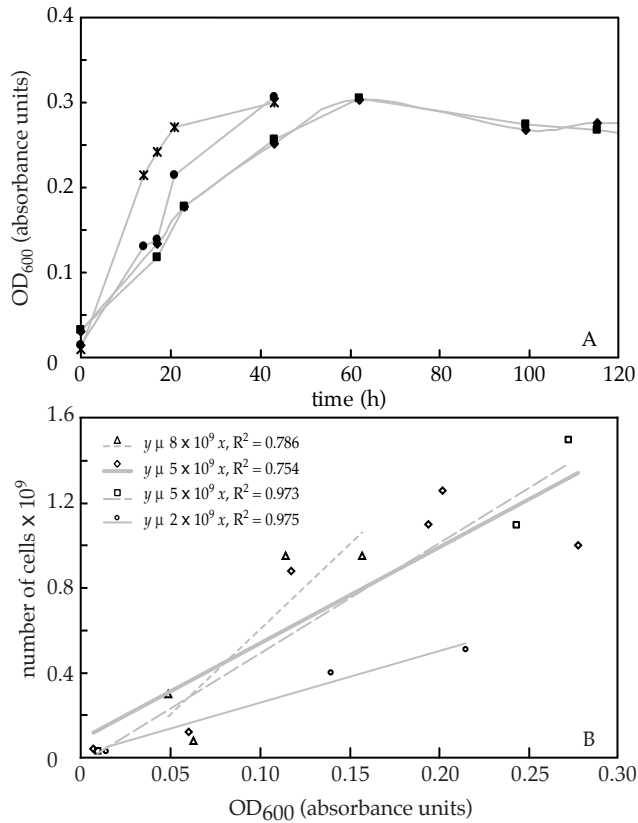


Fig 2. (A) Growth curves of *Nr.* strain HG-1 measured as OD₆₀₀ versus incubation time. (B) Number of cells as functions of OD₆₀₀. The concentration is obtained by cell counting. The deviation in the data is caused by normal biological variation.

4.1 Growth curves

Several independent control cultures were been grown to obtain a reliable value of the growth rate at 45 °C. The optical density of the sample was followed by measuring the OD₆₀₀ (absorbance at 600 nm). Fig. 2A shows growth curves of four representative *Nr.* strain HG-1 cultures, plotting the OD₆₀₀ as a function of incubation time. The relation of the OD₆₀₀ to the number of cells ml⁻¹ counted by microscopy for the same set of four cultures is given in Fig. 2B, leading to an average concentration per OD of $5 \pm 2 \times 10^9$ cells ml⁻¹ OD⁻¹. This number has been used to convert OD₆₀₀ values into cell concentrations.

The concentration (cells ml⁻¹) in a culture after a certain incubation time t can be expressed by the following relation:

$$\frac{dC}{dt} = \mu C \quad \text{Eq. 1}$$

Here, C is the concentration (cells ml⁻¹) as function of the incubation time t (h), and μ the growth rate (h⁻¹). Eq. 1 applies only to the exponential growth phase of a culture. It does neither account for the lag phase, where the cell has to adapt to the medium and start growing, nor for the stationary growth phase, where an equilibrium between growth and death is reached due to the limiting amount of nutrients.

Using the average concentration $5 \pm 2 \times 10^9$ cells ml⁻¹ OD⁻¹, the available data yield an average growth rate of 0.12 ± 0.01 hr⁻¹. This is approximately three times faster than the rate reported

by Sorokin *et al.* (2005), a difference most probably caused by the different incubation temperature. Sorokin *et al.* (2005) incubated their cultures at 30 °C, in contrast to our incubation temperature of 45 °C.

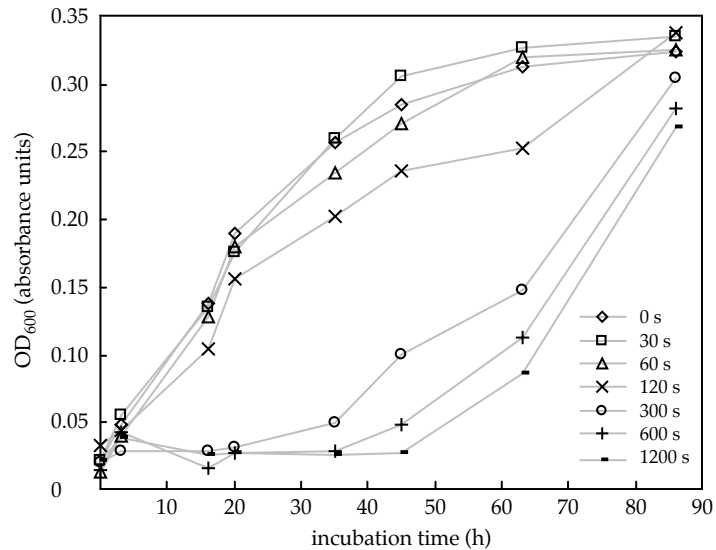


Fig. 3. Growth curves after different doses of irradiation with a xenon discharge lamp. The different curves correspond to different irradiation durations as described in the figure inset. The solid lines are a guide to the eye to show the trend of the growth, the markers represent the data points.

4.2 Irradiation of cell suspensions

Cell suspensions have been irradiated with UV and visible light from a xenon source. In the first and second experiment an amount (10ml) of the liquid cell suspension was irradiated. After exposure durations of 30, 60, 120, 300, and 600 seconds, 1 ml samples were taken out for analysis, using incubation and OD₆₀₀ measurements. In the third experiment an extra sample was taken after an irradiation time of 1200 s. The results presented in Fig. 3 show the effects of the different irradiation intervals on the growth rate of the sample cultures.

From the growth curves shown in Fig. 3, the incubation time at which an OD₆₀₀ of 0.15 was reached, $t_{0.15}$, can be calculated. The OD₆₀₀ value of 0.15 was used, because it is around the point where maximum growth is expected and is sufficiently high above the detection limit of the optical density meter for that stage to be clearly detectable.

Integration of Eq. 1, leads to

$$C_{0.15} = C_{tr} e^{\mu t_{0.15}} \quad \text{Eq. 2}$$

Here, $C_{0.15}$ is the concentration of 7.5×10^8 cells ml⁻¹, corresponding to an OD₆₀₀ of 0.15, $t_{0.15}$ is the incubation time at which this concentration is reached, μ is the growth rate of 0.12 generations h⁻¹, and C_{tr} is the initial concentration of viable cells *after* treatment (irradiation, vacuum, or cold). The number of cells still able to proliferate after radiation exposure is expressed by the ratio of C_{tr} to C_{untr} where C_{untr} is the concentration of the sample *before* treatment. Table 1 shows

Table 1. $t_{0.15}$ and C_{tr}/C_{untr} corresponding to different irradiation time steps, for irradiation with the xenon lamp. The $t_{0.15}$ and C_{tr}/C_{untr} values are averages of three experiments, with their standard deviations. The 1200 s irradiation has only been performed once.

irradiation time (s)	$t_{0.15}$ (h)	C_{tr} / C_{untr}
0	19.4 ± 2.0	1.9 ± 0.8
30	21.3 ± 2.2	1.5 ± 0.4
60	21.2 ± 2.0	1.4 ± 0.5
120	26.7 ± 2.7	0.79 ± 0.3
300	58.4 ± 1.2	0.018 ± 0.007
600	60.4 ± 3.4	0.017 ± 0.01
1200	70.8	0.0019

$t_{0.15}$ and the C_{tr}/C_{untr} ratio as function of irradiation time. The results in Table 1 and in Fig. 3 show a delay in reaching the growth phase caused by progressive inactivation or death of a fraction of the cells.

4.3 Irradiation of desiccated cells

Desiccated cells embedded in a ~1 mm thick salt crust have been irradiated with UV and visible light from the xenon lamp. Subsequent experiments were performed with much of the UV (200-300 nm) filtered out. In both cases samples were irradiated for 30, 60, 120, 300 and 600 s. The trends in Fig. 4A (irradiation with the full xenon spectrum, with a wavelength range > 200 nm) can be compared with the data in Fig. 4B (results from the filtered xenon spectrum, with a wavelength

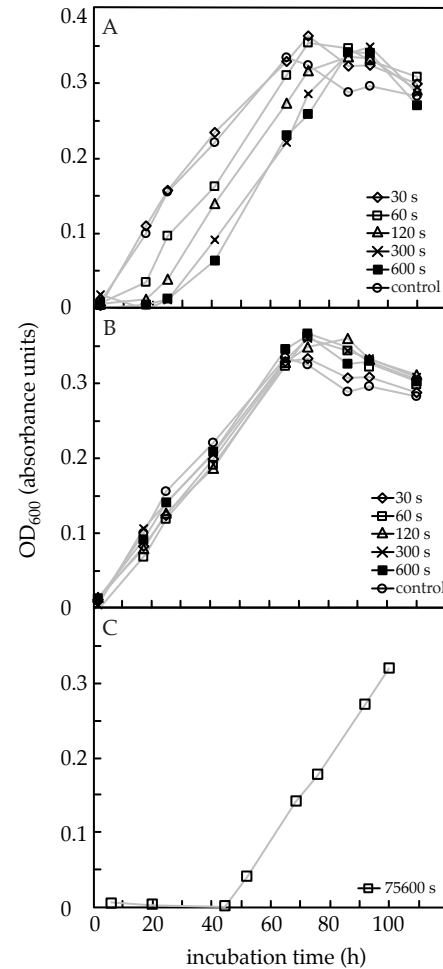


Fig. 4. The growth curves of resuspended irradiated desiccated samples, (A) after irradiation with the full xenon spectrum (> 200 nm), (B) after irradiation with the filtered xenon spectrum (> 300 nm), and (C) after irradiation with the deuterium lamp (190-400 nm). The keys show the irradiation times for the different conditions.

Table 2. $t_{0.15}$ and C_{tr}/C_{untr} corresponding to different irradiation times, for three different irradiation scenarios.

irradiation time (s)	> 200 nm		> 300 nm		190-400 nm	
	$t_{0.15}$ (h)	C_{tr}/C_{untr}	$t_{0.15}$ (h)	C_{tr}/C_{untr}	$t_{0.15}$ (h)	C_{tr}/C_{untr}
0	27.2	1.1	27.2	1.1	27.2	1.1
30	26.8	1.2	30.4	0.78		
60	36.9	0.36	32.5	0.61		
120	44.0	0.15	30.8	0.74		
300	50.6	0.07	28.6	0.97		
600	52.8	0.053	29.6	0.86		
75600					70.9	0.0061

range > 300 nm). Using the method described in section 4.2, the incubation time needed to reach an OD_{600} of 0.15 and the C_{tr}/C_{untr} ratio, representing the fraction of proliferating cells, were calculated. These values are given in Table 2 as function of irradiation time. The C_{tr}/C_{untr} ratio decreases after irradiation with > 200 nm light, indicating that a smaller fraction of cells has survived irradiation. This is in contrast to the C_{tr}/C_{untr} ratio after irradiation with > 300 nm light, which does not change and is independent of the irradiation duration, within the expected error. The results in Table 2 show that visible light has a negligible effect on survival and that the 200-300 nm range of the xenon spectrum causes much more lethal damage to the cells.

Fig. 4C shows the effect of 21-hour irradiation with UV only, using the deuterium lamp. The $t_{0.15}$ and C_{tr}/C_{untr} values can

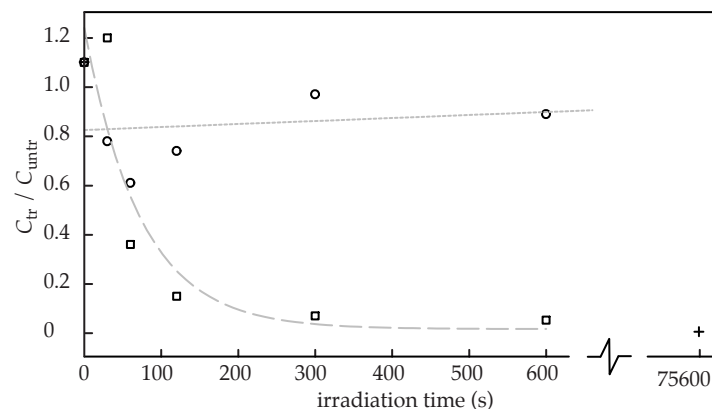


Fig. 5. Relative concentration of viable cells after irradiation (C_{tr} / C_{untr}) corresponding to different times of irradiation with (a) longward of 200 nm light (open squares), (b) longward of 300 nm light (open circles), and (c) 190-400 nm light, enhanced between 190-250 nm (plus signs). The trends (dotted for > 200 nm, dashed for > 300 nm) are plotted as a guide for the eye.

be found in the last column of Table 2. Irradiation by the deuterium lamp was for a period ~125 times longer than the irradiation by the xenon lamp (10 min.). Since the deuterium lamp is ~250 times weaker than the xenon lamp, as described in section 2.3, one would expect that the effect of the deuterium lamp would be approximately half the effect caused by the xenon lamp. However, the data in Table 2, plotted in Fig. 5 show that the effect of light from the deuterium lamp is ~10 times stronger than the effect of light from the xenon lamp, comparing the C_{tr}/C_{untr} ratios. This enhancement is probably

Table 3. $t_{0.15}$ and C_{tr}/C_{untr} after subjection to $-20\text{ }^{\circ}\text{C}$, $-80\text{ }^{\circ}\text{C}$, and hard vacuum (1.4×10^{-4} mbar). All collected data are given.

condition			$t_{0.15}$	C_{tr}/C_{untr}
temperature ($^{\circ}\text{C}$)	pressure (mbar)	time ¹ (h)	(h)	
+20	1.0×10^3	24	27.2	1.1
			24.5	1.6
+20	1.4×10^{-4}	15	32.0	0.6
			34.2	0.5
-20	1.0×10^3	1	45.0	0.1
-80	1.0×10^3	21	38.8	0.3
			42.0	0.2

¹ Time is the duration the samples have been exposed to the conditions given in the table. These samples have not been irradiated.

caused by the different spectral profiles of the UV and xenon lamps; the UV lamp generates light with a spectrum skewed toward short, more energetic, UV, while the xenon lamp produces light with a longer-wavelength bias.

4.4 Desiccated cells in vacuum and a cold environment

Two desiccated samples were placed in a $-80\text{ }^{\circ}\text{C}$ environment for 21 h, one sample was kept at $-20\text{ }^{\circ}\text{C}$ for one hour, and two samples were exposed in a vacuum system, at room temperature, to a pressure of 1.4×10^{-4} mbar for 15 h. These conditions have been applied without irradiation. Table 3 shows the effects of the different conditions on *Nr.* strain HG-1 (see section 4.2). The effects of cooling and exposure to

vacuum are small compared to the effects of 5 and 10 minutes irradiation with the xenon lamp and 21 h with the deuterium lamp. However, exposing the samples to vacuum inactivates $\sim 50\%$ of the cells. Freezing causes inactivation of 70-90 % of the cells, an effect that seems to be independent of the storage temperature.

5. DISCUSSION

We do not know at present whether there is, or has been, any biological activity on Mars. Similarly, there are no compelling reasons to expect that the mechanisms evolved by terrestrial organisms to cope with stressful changes in their environment would be similar to those employed by any hypothetical martian biota. However, given the constraints imposed by biochemistry, there are relatively few steps available to an organism facing the loss of a vital fluid such as water.

It is widely thought that Mars may have shared many of the properties of the Earth in its past. Relict fluvial valleys and the presence of surface concretions resulting from aqueous alteration, point to the presence of bodies of water existing at some time under a warmer and denser martian atmosphere. Because the details of the terrestrial setting in which early life developed on Earth are not known, it is only possible to make a most speculative link to a hypothetical martian origin for life.

During crystallisation and desiccation caused by drought,

cells are often trapped within salt crystals in pockets of brine, where they can remain viable for very long time (Norton and Grant, 1988; McGenity *et al.*, 2000). Most halophilic microorganisms contain pigments that can protect them against damage by high radiation intensities (Oren, 2002). It has been suggested that brines may have existed on the surface of Mars in the past (Rothschild, 1990), which leads to the assumption that microorganisms similar to halophilic Archaea on Earth could have been present on Mars as well (Litchfield, 1998). If they still would be present in a desiccated state on the martian surface, their pigments could protect them against damage by the current high UV intensities at the surface.

In this work we have subjected *Natronorubrum* sp. strain HG-1 (*Nr.* strain HG-1) to various conditions, simulating several aspects of the current conditions on Mars. Sorokin *et al.* (2005) showed the presence of a pigment very similar to haloarchaeal bacterioruberins. Bacterioruberin pigments have several functions, including protection against DNA damage by high intensity UV and visible light and exposure to H₂O₂, and reinforcement of the cell membrane (Oren, 2002). The presence of this pigment in *Nr.* strain HG-1 and the ability of the species to adapt to desiccation make *Nr.* strain HG-1 an interesting candidate to survive on the surface of Mars.

Comparing the results from irradiation of cell suspensions and of desiccated cell samples, both irradiated with a xenon lamp (> 200 nm), shows that desiccated cells are more resistant to irradiation. This suggests that the damage generated through UV exposure is more critical for non-desiccated cells.

Nicholson *et al.* (2000) suggest UV-generated reactive oxygen species in the cell cytoplasm to act as damaging agents to cell DNA and other cellular components. UV interaction with water leads to the formation rate of damaging radicals. Low water-content cells, such as desiccated *Nr.* strain HG-1 samples, have little available water with which UV photons can interact. By contrast, cells in aqueous suspension would acquire higher levels of damaging radicals, a trend visualised by the data shown in Fig. 5. The results of our experiments show that desiccation itself has no measurable effect on the growth of *Nr.* strain HG-1 after resuspension. Placing desiccated cell samples in hard vacuum inactivates only ~50 % of the cells. Freezing desiccated cell samples inactivates around 80 % of the cells. These amounts of inactivation, however, are smaller than the inactivation caused by long duration UV irradiation, where only a few percent of an initial population survives. No conclusions can be drawn from these experiments about the protective of the pigment that is present in *Nr.* strain HG-1 to cell protection or recovery from UV-generated cell damage.

To be able to discriminate between higher and lower wavelength ranges in the UV spectrum, the irradiation results of the deuterium lamp are compared with those of the xenon lamp. The UV spectrum of the deuterium lamp is dominated by light in the short wavelength range (195-250 nm) when compared to the xenon lamp (see Fig. 1). Table 1 shows that irradiation with shorter wavelength light (195-250 nm) is more effective in inactivating the cells.

Scaling the results obtained from irradiation experiments with the xenon lamp to martian conditions, where the xenon lamp is ~250 times stronger than the illumination on the martian surface, would imply that approximately 5 % of a population *Nr.* strain HG-1 would survive ~80 hours continuous noontime irradiation, at a temperature of ~ 300 K. Although 80 hours continuous noontime irradiation will not occur, it seems still valid to conclude that *Nr.* strain HG-1 is not likely to survive the conditions at the surface. In desiccated state no water is available to the cells and no recovery process can take place during night time. Accumulation of shorter intervals of irradiation may therefore be as lethal as long continuous exposure. Furthermore, noontime equatorial temperatures are not always around 300 K, but may very well be colder. The results in Table 3 show that freezing also affects the viability of *Nr.* strain HG-1. Irradiation of *Nr.* strain HG-1 in colder environments than 300 K, for example during winter time or at polar regions, will have a higher inactivating effect on the cells than irradiation at higher temperatures.

From the reported experiments it can be concluded that the strain *Nr.* strain HG-1 would not be a good candidate organism to survive on the surface of Mars, even when embedded in salt crystals. On the other hand, the inability of *Nr.* strain HG-1 to survive these Mars-like conditions, makes it also an unlikely candidate to survive a trip from Earth to Mars on a spacecraft surface, as temperatures are even lower and UV radiation is even more energetic than the conditions on Mars. Halophiles, like *Nr.* strain HG-1, thriving in extreme environments on Earth, will not be able to survive unshielded on the

surface of Mars even in a salt crust. It cannot be excluded that they can survive when embedded in the soil or buried underneath rocks, but further experiments are required to distinguish how soil activity (Garry *et al.*, 2005) will effect the halophiles.

ACKNOWLEDGEMENTS

The authors thank Zan Peeters for his useful contribution to the clarity of this article. ILtK is supported by the BioScience Initiative of Leiden University, JG is supported by the SRON National Institute for Space Research, and PE is supported by grant NWO-VI 016.023.003.

Chapter 7

Nederlandse samenvatting

In dit proefschrift staan de resultaten beschreven van onderzoek naar de reacties van bepaalde aminozuren en micro-organismen op condities die op het oppervlak van Mars heersen. Dit hoofdstuk geeft een beschrijving van de planeet Mars alsmede van de geschiedenis van het Marsonderzoek. Het derde deel van dit hoofdstuk is gewijd aan het onderzoek dat in dit proefschrift is beschreven.

1 DE GESCHIEDENIS VAN HET MARSONDERZOEK

Sinds mensenheugenis kijkt de mens naar de sterren en planeten aan de nachtelijke hemel. Eén van de meest fundamentele vragen die men zich daarbij stelde en stelt, is: „Is er leven buiten de aarde?” Mars, de volgende planeet in ons zonnestelsel, heeft altijd een grote rol gespeeld in het beantwoorden van deze vraag. Ons zonnestelsel bestaat uit 10 planeten, ongeveer 100 manen bij deze planeten, en een groot aantal kleinere objecten zoals kometen en asteroïden. De planeten kunnen grofweg worden onderverdeeld in rotsachtige aardse planeten Mercurius, Venus, aarde, Mars, en reusachtige gasplaneten Jupiter, Saturnus, Uranus, Neptunus. Deze planeten draaien om de zon in een min of meer circulaire baan. Daarnaast zijn er Pluto en de pas ontdekte tiende planeet (tijdelijke naam: 2003UB313). Deze twee planeten bestaan uit een combinatie van rotsen en ijs en bewegen zich in een zeer elliptische baan om de zon. Van de vier aardachtige planeten is Mars de planeet die het meest op de aarde lijkt en aan welke de grootste kans op het eventueel herbergen van leven (vroeger of nu) wordt toegedicht.

In 1892 en 1902 publiceerde Camille Flammarion het boek “La Planète Mars” (in twee delen), waarin hij de tot dan uitgevoerde waarnemingen van Mars bundelde en commentarieerde. Hij veronderstelde onder meer dat de kleur aan Mars werd veroorzaakt door begroeiing en hij speculeerde over kanalen, gebouwd door een ontwikkelde beschaving. Dit idee is waarschijnlijk gebaseerd op waarnemingen van Mars door Giovanni Schiaparelli in 1877. Schiaparelli zag patronen van rechte lijnen die hij ‘canali’ noemde. Hierbij doelde hij op verbindingen in het algemeen, en niet zozeer op kunstmatig aangelegde kanalen. Zo werd het echter wel vertaald in het Engels (canals i.p.v. channels), wat leidde tot groot aantal nieuwe onderzoeken gericht op Mars. Schiaparelli’s waarnemingen inspireerden ook Percival Lowell, die onmiddellijk zijn eigen observatorium liet bouwen. Hij publiceerde tekeningen die honderden rechte lijnen (‘kanalen’) en hun kruispunten lieten zien (‘oases’ genoemd door Lowell), en volgens hem gebouwd door een vroegere beschaving. Lowell beschouwde de lichte vlekken op het oppervlak van Mars werden door als woestijnen en de donkere als begroeiing, die werd bevoeid door smeltwater dat van de polen door de kanalen stroomde. In 2002 werd een verklaring gepubliceerd voor de vermeende kanalen van Lowell. Lowell heeft waarschijnlijk het diafragma van zijn telescoop zo vernauwd dat hij een oftalmoscoop¹ creëerde waarmee hij de reflectie van de aderen in zijn oogbol geprojecteerd zag op het beeld van Mars. Desondanks hielden een aantal van zijn overige theorieën lange tijd stand. In ‘Physics of the Planet Mars’, een overzicht van het Marsonderzoek tot de jaren ’50 van de twintigste eeuw, schreef Gérard de Vaucouleurs op

¹ oogspiegel (Van Dale), instrument om de binnenkant van het oog te bekijken.

basis van waarnemingen van Lowell dat Mars een atmosfeer had van stikstof, met een atmosferische druk van 85 mbar (ongeveer een tiende van de luchtdruk op aarde); dat het er koud was maar met een te verdragen temperatuur, dat er verschillende seizoenen waren die waarschijnlijk veroorzaakt werden door begroeiing en dat de poolkappen gevormd werden door waterijs.

In 1960 luidde de toenmalige Sovjet Unie een nieuw tijdperk in het Marsonderzoek in met een poging tot het sturen van een sonde naar Mars, de Mars 1960A. Helaas mislukte deze missie evenals zijn 5 opvolgers, zodat de Amerikaanse missie Mariner 4 in 1965 de eerste werd die Mars bereikte (zie tabel 2, hoofdstuk 1). Mariner 4 naderde Mars tot op ongeveer 9900 km hoogte en maakte foto's van ongeveer 1% van het oppervlak, die een gekraterd maanachtig uiterlijk vertoonde. Uit metingen werden een atmosferische druk van 4 tot 7 mbar (vergelijk aarde: 1014 mbar) en een dagtemperatuur van rond de -100 °C afgeleid, evenals de afwezigheid van een magnetisch veld. Mariner 6 en 7, gelanceerd in 1969, naderden Mars tot op ca 3400 km en legden 20 % van het oppervlak vast, waarmee ze onder andere lieten zien dat het oppervlak van Mars juist heel anders is dan dat van de maan, met veel minder kraters en meer vlakke gebieden. Bovendien lieten ze zien dat de zuidpoolkap voornamelijk bestond kooldioxide ijs (CO₂-ijs), in tegenstelling tot wat de Vaucouleurs een paar jaar eerder nog gepubliceerd had.

In 1971 stuurde de Sovjet Unie twee missies naar Mars, beide bestaande uit een satelliet en een lander, Mars 2 en 3. Ondanks het mislukken van beide landingen waren deze

missies toch succesvol door de hoeveelheid gegevens van de satellieten. Deze missies leidden tot de ontdekking van onder meer bergen (vulkanen) tot zeker 22 km hoog, water in de atmosfeer, zij het 5000 keer minder dan de hoeveelheid water in de aardse atmosfeer, en stofdeeltjes die door stofstormen tot zeker 7 km hoogte in de atmosfeer werden opgewerveld. Ook maten ze een oppervlaktetemperatuur van 160 tot 290 K (-113 tot +17 °C). Mariner 9 (1971) was de eerste missie die in een baan om Mars gebracht kon worden. Hierdoor werd het mogelijk zeer gedetailleerde foto's van de vulkanen, van Valles Marineris, de poolkappen en beide manen van Mars, Phobos en Deimos, te maken. Mariner 9 deed bovendien ook atmosferisch onderzoek en nam de tot nu toe langst-durende stofstorm waar, die de hele planeet bedekte. Nog meer gegevens over het oppervlak en de atmosfeer werden verzameld door de gedeeltelijk gelukke Sovjet missies Mars 5 en Mars 6 (1975). Het eerste tijdperk in Marsonderzoek vanuit de ruimte werd afgesloten door de Amerikaanse Viking missie, de onafhankelijk van elkaar gelanceerde Viking 1 en Viking 2.

Viking 1 en 2 bestonden beide uit een satelliet en een landingsmodule. De landingsmodule van Viking 1 landde in juli 1976 en die van Viking 2 in september van hetzelfde jaar. De belangrijkste doelen van de missie waren om zeer gedetailleerde foto's te maken van het Marsoppervlak, die duidelijkheid moesten geven over de bodem en de atmosfeer van Mars, en het zoeken naar 'tekens van leven'. Zowel de satellieten als de landers hadden een pakket instrumenten aan boord, waarvan die voor biologisch en moleculair onder-

zoek de meest in het oog springende instrumenten waren. Van deze vier instrumenten was er één die de mogelijke aanwezigheid van bacteriën aantoonde aan de hand van stoffen die gevonden werden bij de analyse van Marsgrond. Omdat de overige drie instrumenten echter geen tekenen van leven vonden, is dit resultaat uiteindelijk uitgelegd als veroorzaakt door stoffen in de bodem (zie hoofdstuk 2 voor een gedetailleerde beschrijving van instrumenten en resultaten). De Viking 1 lander heeft na het beëindigen van de experimenten uiteindelijk nog tot 1983 als weerstation gefungeerd.

Na de Viking missie duurde het meer dan 10 jaar voordat er weer een missie richting Mars gestuurd werd. De Sovjet Unie lanceerde in 1988 de Phobos missie, eveneens twee na elkaar gelanceerde satelliet-lander combinaties. Phobos 1 ging al verloren op weg naar Mars. Phobos 2, met twee landers aan boord, heeft Mars wel bereikt, maar ging verloren door communicatieproblemen vlak voordat de landers losgekoppeld zouden worden. Sinds 1990 zijn er dertien missies naar Mars gelanceerd, waarvan er 6 mislukten om uiteenlopende redenen. De meest opvallende was de Amerikaanse Climate Orbiter, waarbij in de besturingssoftware internationale eenheden (meters) en Engelse eenheden (inches) door elkaar waren gebruikt. De overige 7 missies leverden daarentegen wel spectaculaire gegevens op. De in 1996 gelanceerde Mars Global Surveyor (MGS) ontdekte onder andere relatief (geologische gezien, d.w.z. rond de 10.000 jaar) jonge 'gullies', geulen in onder andere canyonwanden (zie Fig. 5, hoofdstuk 1), en andere karakteristieken in het landschap die kunnen wijzen op de mogelijke aanwezigheid van vloeibaar water

op het oppervlak. De eerste volledig succesvolle landing na Viking 1 en 2, was de Mars Pathfinder, die in 1997 landde en bedoeld was om te testen hoe instrumenten het best naar en op het Mars oppervlak getransporteerd konden worden. Deze missie bestond uit een vaste lander met het karretje Sojourner dat vanaf de aarde bestuurd werd. Samen maakten lander en voertuig meer dan 17.000 foto's en deden 15 geologische en chemische experimenten om de samenstelling van de bodem en de rotsen te bepalen. Sojourner vond onder andere silicaatrijke rotsen en ronde en uitgeslepen rotsen, wat zou kunnen wijzen op vloeibaar water in het verleden. De samenstelling van de bodem bleek te lijken op die van de plaatsen waar Viking 1 en 2 waren geland. Naast het geologische onderzoek deed Pathfinder metingen aan wervelwinden en aan waterijswolken, die 's ochtends in de atmosfeer voorkomen en verdampen zodra de temperatuur oploopt. De eventuele aanwezigheid van water werd nog eens benadrukt door de resultaten van de 2001 Mars Odyssey, die grote hoeveelheden waterstof aantoonde net onder het oppervlak, die kunnen wijzen op waterijs.

In 2004 brak er een drukke tijd aan in het Marsonderzoek. Eind 2003 was de Europese satelliet Mars Express reeds gearriveerd in een baan om Mars, samen met de Beagle 2 lander, die de landing helaas niet overleefde. In januari en februari 2004 landden de twee Amerikaanse Mars Exploration Rovers, Spirit en Opportunity. Mars Express had zeven instrumenten bij zich, en detecteerde onder meer sporen van methaan in de atmosfeer, vond meer aanwijzingen voor de aanwezigheid van water en maakte zeer gedetailleerde stereofoto's van het

oppervlak. Ook Spirit en Opportunity waren uitgerust met een instrumentenpakket, waaronder een camera, een microscoop en instrumenten waarmee stukjes rots konden worden afgeslepen voor analyse. De rovers hebben gedetailleerde analyses gemaakt van de samenstelling van de bodem en van rotsen. Verder hebben zij aanwijzingen gevonden die wijzen op de aanwezigheid van water (zie sectie 2, dit hoofdstuk). De missies van zowel Mars Express als de Mars Exploration Rovers zijn verlengd tot in ieder geval eind 2006, een uitbreiding van de levensduur van bijna 2 jaar voor de rovers en een jaar voor Mars Express. Inmiddels is er in augustus 2005 weer een satelliet richting Mars gelanceerd, de Mars Reconnaissance Orbiter, die verder zal zoeken naar water en onder meer het klimaat op Mars en stof en water in de atmosfeer zal bestuderen.

2. ALGEMENE WETENSWAARDIGHEDEN OVER MARS

Mars is de 4^e planeet in ons zonnestelsel gezien vanaf de zon (zie fig 1 hoofdstuk 1) en de 7^e in grootte, ongeveer half zo groot als de aarde. Omdat de baan van Mars om de zon veel ellipsvormiger is dan die van de aarde, zijn er grote temperatuurverschillen tussen het perihelium (het punt waar Mars het dichtst bij de zon staat) en het apohelium (waar de afstand tussen Mars en de zon het grootst is). In Tabel 1 zijn een aantal karakteristieke kenmerken van Mars en de aarde weergegeven.

Geologisch gezien is Mars opgebouwd uit een gedeeltelijk vaste en gedeeltelijk vloeibare kern met een diameter van

Tabel 1. Karakteristieken van Mars. Deze gegevens zijn afkomstig van <http://nssdc.gsfc.nasa.gov/planetary/factsheet/marsfact.html>

Karakteristieken	Mars	aarde
Straal	3397 km	6378 km
Massa	0.64×10^{24} kg	5.97×10^{24} kg
Valversnelling	3.71 m s^{-2}	9.80 m s^{-2}
Gemiddelde dichtheid	3933 kg m^{-3}	5515 kg m^{-3}
Gemiddelde afstand tot de zon	227.9 miljoen km of 1.52 AE	149.6 miljoen km of 1 AE (astronomische eenheid)
Ellipticiteit van baan om de zon	0.09	0.02
Inclinatie	1.85	0.00
Omlooptijd om de zon	686.98 dagen	365.26 dagen
Rotatietijd om eigen as	24 uur 37 min	23 uur 56 min
Oppervlakte-temperatuur	140 - 300 K (-133 °C - +25 °C) gem.: 210 K (-63 °C)	184 - 330 K (-89 °C - -57 °C) gem.: 288 K (15 °C)
Samenstelling van de atmosfeer	95.3 % CO ₂ , 2.7 % N ₂ , 1.6 % Ar, 0.15 % O ₂ , 0.08 % CO, 0.03 % H ₂ O	78.1 % N ₂ , 20.9 % O ₂ , 0.9 % Ar, en sporen van CO ₂ , CH ₄ , Ne, He, Kr, H
Atmosferische druk	gemiddeld 6.36 mbar (4-9 mbar)	gemiddeld op zeeniveau 1014 mbar
Natuurlijke satellieten	Phobos (straal ~11 km, afstand ~7700 km) Deimos (straal ~6 km, afstand ~22000 km)	Maan (straal ~3500 km, afstand ~400000 km)

ongeveer 1700 km, omgeven door een gesmolten stenen mantel en een dunne korst. Omdat de dikte van de mantel en de korst van Mars alleen bepaald zijn via indirecte metingen bestaan er uiteenlopende schattingen en modellen over hun verhoudingen (tussen de 1500 en 2100 km voor de mantel en 9 en 130 km voor de korst). Mars heeft in vergelijking met de overige aardse planeten een relatief lage dichtheid (ongeveer 4000 kg m^{-3} , tegenover ongeveer 5400 kg m^{-3} van Mercurius, ongeveer 5200 kg m^{-3} van Venus en ongeveer 5500 kg m^{-3} van de aarde), wat erop kan wijzen dat de planeet voor een relatief groot deel bestaat uit elementen lichter dan ijzer en nikkel, waaruit de aarde voornamelijk is opgebouwd, zoals bijvoorbeeld zwavel. Er zijn echter meerdere combinaties van elementen en van de verhouding tussen de hele kern en het vaste en vloeibare deel mogelijk, die de dichtheid van de planeet kunnen verklaren. Wat de mineralogische samenstelling betreft lijkt Mars op de aarde.

De korst van de aarde bestaat uit losse platen die als het ware drijven op het vloeibare gedeelte van de mantel (de lithosfeer) en de beweging van deze platen (plaattektoniek) zorgt onder andere voor vulkanisme en aardbevingen en hierdoor voor vernieuwing van de aardkorst. Daarnaast is plaattektoniek verantwoordelijk voor de circulatie van CO_2 in de atmosfeer, wat bijdraagt aan het broeikaseffect. Dit broeikaseffect is op aarde een van de belangrijkste voorwaarden voor het (blijven) bestaan van leven. Mars koelde door zijn kleinere afmetingen veel sneller af dan de aarde, waardoor de lithosfeer veel dikker werd. Dit had tot resultaat dat de tektonische activiteit op Mars al 3 tot 4 miljard jaar geleden tot stilstand kwam.

Het oppervlak van Mars verschilt hemelsbreed van dat van de aarde. Het noordelijk halfrond van Mars, bestaand uit relatief jong laagland, verschilt heel erg van het zuidelijk halfrond, dat gekenmerkt wordt door oude gekraterde hoogvlakten, een verschil dat benadrukt wordt door het abrupte hoogteverschil van 2 tot 4 km waarmee de halfronden van elkaar gescheiden worden. Daarnaast heeft het oppervlak van Mars nog een aantal opvallende kenmerken, waaronder de vulkaan Olympus Mons (met 24 km de hoogste berg in ons zonnestelsel), Tharsis (een 4000 km lange bult, die 10 km boven de rest van het omliggende oppervlak uittorent), Valles Marineris, (een canyonsysteem met dieptes tussen de 2 en 7 km), en Hellas Planitia (een 6 km diepe inslagkrater met een doorsnede van 2000 km).

Mars herbergt de grootste vulkanen in ons zonnestelsel. Deze vulkanen blijven zo enorm door het ontbreken van plaattektoniek. Nieuwe data van Mars Express lijken te wijzen op "recente" vulkanische activiteit met een cyclus van zo'n 2 miljoen jaar.

Ook erosie speelt op Mars een rol. Verschillende processen doen zich op het oppervlak voor, zoals verweering, landverschuiving en erosie door wind en stofstormen.

Beide polen van de planeet zijn bedekt met ijskappen die variëren met de seizoenen. Zowel de noord- als de zuidpool wordt in de winter bedekt door een laag CO_2 -ijs. Daaronder verschilt de samenstelling van de polen. De noordpoolkap bestaat in de zomer vrijwel volledig uit waterijs, waar de zuidpoolkap bestaat uit bevroren mengsel van stof, water en CO_2 . Meer aanwijzingen voor de aanwezigheid van water

op het oppervlak zijn gevonden tijdens recente Marsmissies. Zowel Spirit als Opportunity hebben mineralen gevonden, zoals hematiet en jarosiet, die op aarde gevormd worden in de aanwezigheid van water. Ook vonden ze kleine rondgeslepen bolletjes en groeven in rotsen. Deze vormen sterke aanwijzingen voor de aanwezigheid van vloeibaar water op het oppervlak van Mars in vroegere tijden.

Mars is omgeven door een ijle atmosfeer. Deze atmosfeer is zeer verschillend van die van de aarde (zie tabel 1). Het grootste deel (95 %) bestaat uit CO₂ en de luchtdruk is slechts 7 mbar, minder dan 1 % van de aardse atmosferische druk. Dit wordt veroorzaakt door de lage zwaartekracht, die niet sterk genoeg is om de atmosfeer vast te houden.

3. CONTEXT VAN HET ONDERZOEK

De zoektocht naar leven op Mars wordt op verschillende manieren uitgevoerd; door middel van onderzoek met satellieten en landers, maar ook met behulp van simulaties en experimenten in laboratoria. Eén van de takken van onderzoek kijkt naar de aanwezigheid van organische moleculen, die op aarde als bouwstenen fungeren van levende cellen. Circa 140 moleculen zijn gedetecteerd in de ruimte. Onlangs is ook het eerste aminozuur, glycine, aangetoond in de ruimte, in zogenaamde 'hot molecular clouds'. Daarnaast zijn 70 verschillende aminozuren en een heel scala aan andere organische moleculen aangetoond op het enige harde bewijs uit de ruimte dat we hebben, meteorieten. Grotere organische mol-

eculen, zoals PAKs (polycyclische aromatische koolwaterstoffen) en kerogenen (amorfe netwerken), zijn aangetoond op interplanetaire stofdeeltjes en meteorieten. Vermoedelijk komen ze ook voor in de vrije ruimte (het interstellair medium). PAKs en kerogenen worden niet snel afgebroken door de UV straling die aanwezig is in de ruimte. Daardoor kunnen ze lange tijd overleven en door middel van inslagen intact op het oppervlak van een planeet terecht komen. Aangezien er ook aminozuren in meteorieten op aarde zijn aangetroffen zouden deze eveneens op het oppervlak van Mars terecht kunnen zijn gekomen.

Een andere richting van onderzoek richt zich op het zoeken naar vormen van leven, in extreme omgevingen op aarde, bijvoorbeeld op Antarctica, in 'hot springs' (heet water bronnen) in Yellow Stone Park, en in 'hydrothermal vents', geisers op de oceaانبodem. Hieruit blijkt dat microscopisch leven heel goed in staat is zich aan te passen aan vrijwel elke omgeving op aarde, waardoor het vermoeden ontstaat dat ook op Mars leven op bacterieniveau mogelijk is. Tot op heden zijn er op Mars geen aanwijzingen gevonden voor de aanwezigheid van organisch materiaal, leven of de overblijfselen daarvan, hoewel er in het verleden omstandigheden zouden kunnen zijn geweest waarin leven zou kunnen zijn ontstaan. De Vikingmissie (1976) was echter de enige missie tot op heden die gericht was op het zoeken naar leven.

Verschuillende hypothesen zijn geopperd om de afwezigheid van organisch materiaal op Mars zoals gemeten door Viking te verklaren. Afgezien van de meest voor de hand liggende

verklaring dat de instrumenten van Viking niet gevoelig genoeg waren, bestaat ook de mogelijkheid dat organisch materiaal is afgebroken door de oppervlakte condities, maar zich wel kan bevinden op plaatsen waar tot op heden niet gezocht is, onder rotsen of onder het oppervlak. Een cruciale vraag is welke rol (eventueel) aanwezig water hierin speelt.

4. HET ONDERZOEK

Het onderzoek beschreven in dit proefschrift heeft zich gericht op de stabiliteit en de afbraaksnelheid van organisch materiaal op het oppervlak van Mars. Hierin spelen UV straling, de atmosfeer en temperatuur een rol. Het effect van deze condities is zowel apart als in combinatie onderzocht. In de hoofdstukken 3 en 4 zijn de effecten van straling-, atmosferische en temperatuurcondities op onbeschermd dunne laagjes van diverse aminozuren bestudeerd. Vervolgens zijn in hoofdstuk 5 de effecten van deze condities op aminozuren in grondmonsters bestudeerd, die qua samenstelling lijken op de bodem van Mars. Hoofdstuk 6 is gewijd aan halofiele archaea, micro-organismen die in hoge zoutconcentraties leven, en de effecten van UV en zichtbaar licht in de samenstelling zoals deze gemodelleerd is voor het oppervlak van Mars op de overleving van deze organismen.

4.1 Aminozuren

Het effect van UV licht in het golflengtegebied dat het oppervlak van Mars bereikt, namelijk boven de 190 nm, is ge-

meten op onbeschermd aminozuren. Om het spectrum van zonlicht dat het Marsoppervlak bereikt zo goed mogelijk na te bootsen, is een deuterium lamp gebruikt. De emissie van deze lamp in het gebied tussen 190 en 300 nm komt goed overeen met het spectrum van de zon op het Marsoppervlak. De aminozuren die gebruikt zijn in deze experimenten, glycine en D-alanine, worden geleverd als kristallen. Omdat effecten van UV straling op kristallen moeilijk te meten zijn, zijn dunne laagjes (ongeveer 200 nm) gemaakt. Dit is gedaan door de aminozuren te sublimeren die vervolgens neersloegen op silicium schijfjes. Deze sublimatie werd uitgevoerd in een speciale tank onder vacuüm (in de orde van 10^{-5} mbar), waarbij de groei van de laagjes tijdens de sublimatie met behulp van een laser werd gevolgd (zie Fig. 2, hoofdstuk 3). Met deze met aminozuren bedekte schijfjes zijn drie verschillende soorten experimenten uitgevoerd die hieronder kort worden beschreven.

UV & vacuüm op kamertemperatuur

In de eerste serie experimenten werden de samples blootgesteld aan de UV straling, terwijl ze zich onder vacuüm bevonden. Na korte intervallen van UV bestraling werden infrarood spectra opgenomen (zie Fig. 5, hoofdstuk 3). De infrarood absorptiekenmerken in de spectra verdwijnen naarmate er langer bestraald wordt. Hieruit kan de afbraaksnelheid van de aminozuren berekend worden.

UV & CO₂ op kamertemperatuur

Op Mars heerst echter geen vacuüm, maar is er een atmosfeer van ongeveer 7 mbar voornamelijk bestaand uit CO₂. De

tweede serie experimenten werd daarom uitgevoerd terwijl de opstelling gevuld was met ongeveer 7 mbar CO₂. De effecten werden op dezelfde manier gemeten.

UV & vacuüm op 210 K

De volgende conditie op het oppervlak van Mars die nagebootst werd, was de temperatuur. De gemiddelde temperatuur op het oppervlak van Mars is ongeveer 210 K (-60 °C). Om de afbraak van aminozuren onder invloed van UV te meten bij die temperatuur, werd een nieuwe opstelling gebruikt. Deze was vergelijkbaar met de eerste, met als toevoeging dat de samples afgekoeld konden worden (zie Fig. 1, hoofdstuk 4). Op deze manier kon gemeten worden of de aminozuren onder afgekoelde omstandigheden anders op UV licht zouden reageren dan op kamertemperatuur.

Resultaten

De eerste serie experimenten ('alleen-UV') is uitgevoerd met dunne laagjes glycine en D-alanine, de volgende experimenten zijn uitgevoerd met alleen glycine. Glycine, het meest eenvoudige aminozuur, komt voor op meteorieten en als losse moleculen in 'hot molecular cores' in de ruimte, en is goed gekarakteriseerd, wat vergelijking met andere onderzoeken mogelijk maakte. De afbraaksnelheid van de aminozuren is gemeten, waaruit vervolgens de halveringstijd en levensduur kan worden berekend. In tabel 2 zijn resultaten van de experimenten op glycine weergegeven per conditie. Omdat de gebruikte UV lamp een lagere intensiteit heeft dan de UV straling van de zon op het oppervlak van Mars, is ook de levensduur in dat geval uitgerekend. In de tweede kolom

Tabel 2. Halveringstijd van glycine bij bestraling door UV in vacuüm op kamertemperatuur, in vacuüm op 210 K en in een CO₂ atmosfeer op kamertemperatuur.

Conditie	Halveringstijd in het lab (s)	Halveringstijd bij Mars UV intensiteit	
		(s)	(uur)
UV in vacuüm	$1.5 \pm 0.8 \times 10^6$	$1.3 \pm 0.8 \times 10^5$	36 ± 22
UV in CO ₂	$1.5 \pm 1.4 \times 10^6$	$1.3 \pm 0.6 \times 10^5$	36 ± 17
UV op 210 K in vacuüm	$0.8 \pm 4.2 \times 10^7$	$0.9 \pm 7.5 \times 10^6$	250 ± 2083

staan deze waarden.

Bij een gemeten halveringstijd van 36 uur en een beginconcentratie van 1 microgram aminozuren per gram bodem-materiaal, is in 4×10^7 (40 miljoen) jaar, de hoeveelheid afgenomen tot 1 op 10^9 . Dit is de detectielimiet van de apparatuur op de volgende Marsmissies in 2009 en 2011, die op Mars het oppervlak zullen onderzoeken op het voorkomen van aminozuren.

4.2 Aminozuren in grondmonsters

De volgende fase in het onderzoek betrof aminozuren die zich in grondmonsters bevonden. Twee verschillende typen aardse grondmonsters zijn gebruikt, die wat samenstelling betreft lijken op de samenstelling van de bodem op Mars. Het ene monster, JSC Mars-1, is afkomstig van het gebied tussen de Mauna Loa en Mauna Kea vulkanen op Hawaii, en lijkt wat samenstelling, korrelgrootte, dichtheid en magnetische eigenschappen op Marsgrond. Wat chemische samenstelling

betreft lijkt het monster op de grondanalyses die de Vikings hebben gedaan, over de mineralogische overeenkomst is echter niet veel bekend. JSC Mars-1 is in verschillende Marsgerelateerde studies gebruikt. Salten Skov, het tweede grondmonster, is afkomstig uit de omgeving van Salten Skov, Midden Jutland, Denemarken, en bevat een grote hoeveelheid ijzeroxide. Salten Skov heeft vooral qua korrelgrootte (zeer fijn) en magnetische eigenschappen overeenkomsten met de grond op Mars. Over de chemische samenstelling van de JSC en Salten Skov grondmonsters is maar beperkte kennis aanwezig. Ondanks deze onbekende factoren zijn betere analoge monsters niet beschikbaar, omdat ook de exacte samenstelling van Marsgrond niet bekend is. Deze twee grondsoorten zijn direct als uitgangsmateriaal gebruikt in de experimenten, zonder enige reinigende of steriliserende behandeling vooraf. Het JSC Mars-1 monster kon onderverdeeld worden in een deel grote en een deel kleine korrels, die elk afzonderlijk als proefmonster dienden en beide met behulp van een vijzel tot korrels van poedergrootte werden gemalen om een grotere gelijkensis met Mars te verkrijgen. In totaal zijn er zo drie grondmonsters gebruikt, Salten Skov, Mars-1 grof en Mars-1 fijn. Als vierde is er een controle monster aan toegevoegd dat bestond uit zeer fijn gemalen Pyrex (hittebestendig glas), dat voor het begin van de experimenten wél gesteriliseerd was (ontdgaan van alle bacteriën en aminozuren door 3 uur lang verhitten op 500 °C). Vooraf is van alle bodemonsters een extract gemaakt, dat op aminozuren geanalyseerd is met behulp van HPLC². In dit geval is er gekeken naar de hoeveelheden en soorten aminozuren in de grondmonsters.

Drie experimenten zijn uitgevoerd. In het eerste experiment werden de monsters op kamertemperatuur in vacuüm gedurende 24 uur bestraald met UV. Het tweede experiment was een herhaling van het eerste met een bestralingstijd van een week. In het derde werden de monsters wederom een week bestraald, deze keer in een CO₂ atmosfeer van 7 mbar en afgekoeld tot 210 K. Na elke behandeling werd door middel van extractie en HPLC analyses de hoeveelheid aminozuren bepaald en vergeleken met de hoeveelheid in de originele monsters. Voor deze experimenten is een opstelling gebouwd (zie Fig. 3, hoofdstuk 5), die vacuüm gepompt kon worden en gevuld met gasen zoals CO₂. Als testexperiment is een siliciumschijfje met een dun laagje glycine bestraald met UV, waarna de afbraak werd vergeleken met experimenten uit sectie 4.2 (dit hoofdstuk), die zijn uitgevoerd in een andere opstelling. De resultaten komen overeen, waaruit kan worden afgeleid dat de hoeveelheid UV die de grondmonsters bereikt te vergelijken is met de hoeveelheid UV die de plaatjes bestraalde in de eerste experimenten.

Na bestraling met UV onder vacuüm bleek de hoeveelheid aminozuren in de monsters te zijn toegenomen. De bestralingsduur (24 uur en 7 dagen) had geen invloed op de resultaten. Dit zou erop kunnen wijzen dat de toename van de aminozuren al in het begin van het bestralen plaatsvond. Misschien is deze toename veroorzaakt door fotolyse van bacteriën die zich in de monsters bevonden. Afbraak van aminozuren door UV werd in deze experimenten niet waargenomen. Wanneer de resultaten van de bestraling van koude monsters (210 K) in CO₂ worden vergeleken met die van de

² HPLC - High Performance Liquid Chromatography - een techniek waarmee de verschillende componenten van vloeistoffen worden gescheiden, om de samenstelling van de vloeistof te achterhalen.

monsters bestraald op kamertemperatuur in vacuüm, zien we een afname van de hoeveelheid aminozuren. Bij vergelijking met de originele monsters blijkt de hoeveelheid ook licht te zijn afgenomen. Deze afbraak zou veroorzaakt kunnen zijn doordat het beetje water dat zich in de opstelling bevond, vastgevroren is op de monsters en op die manier reactieve stoffen vormden, die de aminozuren afbraken. Details van de processen die in deze experimenten een rol speelden konden echter niet bekeken worden.

4.3 Halofielen

De derde fase in het onderzoek, was de analyse van de effecten van de marsachtige condities op levende organismen. Het hiervoor gebruikte organisme is het halofiele archaeon *Natronorubrum* sp. strain HG-1 (*Nr.* strain HG-1). Dit is een zogeheten “zoutminnend” (halofiel) micro-organisme, dat alleen kan groeien bij hoge zoutconcentraties. Verder zou dit organisme bestand zijn tegen een bepaalde mate van uitdrogen, en zou zo langere periodes van droogte, bijvoorbeeld in aardse zoutmeren, kunnen overleven. Ook bevat het een pigment dat het DNA beschermt tegen onder andere beschadiging door UV straling en waterstofperoxide, waarvan gedacht wordt dat het voorkomt op het oppervlak van Mars. Gezien de droogte op het oppervlak van Mars én de mogelijke aanwezigheid van zouten op het oppervlak, zou dit type micro-organisme een model kunnen zijn voor de overleving van bacteriën op bepaalde plaatsen waar water is geweest. In deze studie is gekeken naar het effect van UV (190-400 nm) en zichtbaar (400-700 nm) licht op *Nr.* strain HG-1 in suspensie

in groeimeidium en in ingedroogde toestand. Gebruikt zijn de reeds beschreven deuterium UV lamp en een xenonlamp met filter, die een redelijk nauwkeurige weergave geeft van het spectrum van de zon op Mars. De xenonlamp straalt licht uit met een golflengte van 200 tot 1500 nm. In het UV deel van het spectrum zendt de xenonlamp voornamelijk licht uit in het langere golflengtegebied (250-300 nm), waar de deuteriumlamp licht uitzendt aan de korte kant (195-250 nm). Door het effect van de twee lampen te vergelijken, kan bekeken worden welke golflengtes het fataalst zijn voor dit type bacterie. Hiernaast is gekeken naar het effect van bevriezing en van vacuüm op de cellen. Effecten van de verschillende condities zijn gemeten als de mate van reproduceerbaarheid van de cellen nadat ze aan deze condities zijn blootgesteld. Uit de resultaten blijkt dat ingedroogde *Nr.* strain HG-1 cellen resistenter zijn tegen UV bestraling dan wanneer *Nr.* strain HG-1 cellen zich in suspensie bevinden. Licht boven de 300 nm heeft geen invloed op de reproduceerbaarheid van de cellen. Vergelijking van de resultaten van bestraling met de deuterium- en de xenonlamp suggereert dat lagere golflengtes UV licht een groter effect hebben op de reproduceerbaarheid van *Nr.* strain HG-1. Bevriezing heeft een groter effect op de reproduceerbaarheid dan vacuüm, met respectievelijk 30 % en 50 % overlevende cellen.

5. CONCLUSIE

In het onderzoek beschreven in dit proefschrift is gekeken naar het effect van UV straling op twee aminozuren, onder

verschillende omstandigheden. Bovendien is het effect van UV, lage druk en bevriezing op een archaeon, die wat eigenschappen betreft model zou kunnen staan voor eventuele micro-organismen op Mars. Uit de resultaten van de onderzoeken hier beschreven zou geconcludeerd kunnen worden dat de omstandigheden op het oppervlak van Mars niet geschikt zijn voor leven. Aan de andere kant blijkt uit de aanwezigheid van organismen op de meest uiteenlopende plaatsen op aarde dat de aanwezigheid van leven nooit geheel uitgesloten kan worden.

Dit proefschrift beschrijft slechts een zeer klein deel van alle mogelijke processen die zich voordoen en voor zouden kunnen doen op het oppervlak van Mars. Behalve meer laboratoriumonderzoek en modelering, zijn ook metingen ter plaatsen noodzakelijk om een beter beeld te krijgen van de planeet Mars.

Reference list

- Acuña M. H., Connerney J. E. P., Ness N. F., Lin R. P., Mitchell D., Carlson C. W., McFadden J., Anderson K. A., Rème H., Mazelle C., Vignes D., Wasilewski P., and Cloutier P. 1999. Global distribution of crustal magnetization discovered by the Mars Global Surveyor MAG/ER experiment. *Science* 284:790-793.
- Acuña M. H., Connerney J. E. P., Wasilewski P., Lin R. P., Mitchell D., Anderson K. A., Carlson C. W., McFadden J., Rème H., Mazelle C., Vignes D., Bauer S. J., Cloutier P., and Ness N. F. 2001. Magnetic field of Mars: Summary of results from the aerobraking and mapping orbits. *Journal of Geophysical Research-Planets* 106(E10):23403-23418.
- Allen C. C., Morris R. V., Jager K. M., Golden D. C., Lindstrom D. J., Lindstrom M. M., and Lockwood J. P. 1998. Martian regolith simulant JSC-Mars1. (abstract #1690). 29th Lunar and Planetary Science Conference. CD-ROM
- Allen C. C., Griffin C., Steele A., Wainwright N., and Stansbery E. 2000. Microbial life in martian regolith simulant JSC-Mars1 (abstract #1287). 31st Lunar and Planetary Science Conference. CD-ROM
- Atreya S. K. and Gu Z. G. 1995. The photochemistry and stability of the atmosphere of Mars. *Advances in Space Research* 16(6):57-68.
- Banerdt W. B., Golombek M. P., and Tanaka K. L. 1992. Stress and tectonics on Mars. In *Mars*, edited by Kieffer H. H., Jakosky B. M., Snyder C. W., and Matthews M. S. Tuscon: University of Arizona Press. pp. 249-297.
- Banin A. 1988. The soils of Mars. Proceedings, Lunar and Planetary Inst., Workshop on Mars Sample Return Science. pp. 35-36.
- Banin A. 2005. The enigma of the martian soil. *Science* 309:888-890.
- Barrat J. A., Gillet Ph., Lesourd M., Blichert-Toft J., and Popeau G. R. 1999. The Tatahouine diogenite: Mineralogical and chemical effects of sixty-three years of terrestrial residence. *Meteoritics and Planetary Science* 34:91-97.
- Becker L., Bada J. L., Winans R. E., and Bunch T. E. 1994. Fullerenes in Allende meteorite. *Nature* 372:507-507.
- Becker L., Popp B., Rust T., and Bada J. L. 1999. The origin of organic matter in the martian meteorite ALH84001. *Earth And Planetary Science Letters* 167:71-79.
- Benner S. A., Devine K. G., Matveeva L. N., and Powell D. H. 2000. The missing organic molecules on Mars. *Proceedings of the National Academy of Science* 97:2425-2430.
- Bianchi R. and Flamini E. 1977. Permafrost on Mars. *Societa Astronomica Italiana, Memorie* 48:807-820.
- Bibring J-P., Langevin Y., Poulet F., Gendrin A., Gondet B., Berthé M., Soufflot A., Drossart P., Combes M., Bellucci G., Moroz V., Mangold N., Schmitt B. and the OMEGA team. 2004. Perennial water ice identified in the south polar cap of Mars. *Nature* 428:627-630.

Reference list

- Biemann K., Oró J., Toulmin P. III, Orgel L. E., Nier A. O., Anderson D. M., Simmonds P. G., Flory D., Diaz A. V., Rushneck D. R., Biller J. E., and Lafleur A. L. 1977. The search for organic substances and inorganic volatile compounds in the surface of Mars. *Journal of Geophysical Research* 82:4641-4658.
- Biemann K. and Lavoie J. M. 1979. Some final conclusion and supporting experiments related to the search for organic compounds on the surface of Mars. *Journal of Geophysical Research* 84:8385-8390.
- Bland P. A. and Smith T. B. 2000. Meteorite accumulations on Mars. *Icarus* 144:21-26.
- Botta O. and Bada J. L. 2002. Extraterrestrial organic compounds in meteorites. *Surveys in Geophysics* 23:411-467.
- Botta O., Glavin D. P., Kminek G., and Bada J. L. 2002 Relative amino acid concentrations as a signature for parent body processes of carbonaceous chondrites. *Origins of Life and Evolution of the Biosphere* 32:143-163.
- Boynton W. V., Feldman W. C., Squyres S. W., Prettyman T. H., Brückner J., Evans L. G., Reedy R. C., Starr R., Arnold J. R., Drake D. M., Englert P. A. J., Metzger A. E., Mitrofanov I., Trombka J. I., d'Uston C., Wänke H., Gasnault O., Hamara D. K., Janes D. M., Marcialis R. L., Maurice S., Mikheeva I., Taylor G. J., Tokar R., and Shinohara C. 2002. Distribution of hydrogen in the near surface of Mars: Evidence for subsurface ice deposits. *Science* 297:81-85.
- Bridges N. T., Greeley R., Haldemann A. F. C., Herkenhoff K. E., Kraft M., Parker T. J., and Ward A. W. 1999. Ventifacts at the Pathfinder landing site. *Journal of Geophysical Research* 104(E4):8595-8615.
- Bullock M. A., Stoker C. R., McKay C. P., and Zent A. P. 1994. A coupled soil-atmosphere model of H₂O₂ on Mars. *Icarus* 107:142-154.
- Byrne S. and Ingersoll A. P. 2003. A sublimation model for martian south polar ice features. *Science* 299:1051-1053.
- Cao X. and Fischer G. 1999. New infrared spectra and the tautomeric studies of purine and α L-alanine with an innovative sampling technique. *Spectrochimica Acta Part A* 55:2329-2342.
- Cao X. and Fischer G. 2000. Infrared spectra of monomeric L-alanine and L-alanine-N-d₃ zwitterions isolated in a KBr matrix. *Chemical Physics* 255:195-204.
- Carr M. H. 1992. Post-Noachian erosion rates: implications for Mars climate change. Proceedings, 23rd Lunar and Planetary Science Conference. pp. 205-206.
- Chapman C. R., Pollack J. B., and Sagan C. 1969. An analysis of Mariner-4 cratering statistics. *Astronomical Journal* 74(8):1039-1051.
- Chappelow J. E. and Sharpton V. L. 2005. Influence of atmospheric variations on Mars's record of small craters. *Icarus* 178:40-55.
- Christensen P. R. 2003. Formation of recent martian gullies through melting of extensive water-rich snow deposits. *Nature* 422:45-48.
- Chung C.-Y., Chew E. P., Cheng B.-M., Bahoub M., and Leeb Y.-P.

2001. Temperature dependence of absorption cross-section of H₂O, HOD, and D₂O in the spectral region 140–193 nm. *Nuclear Instruments and Methods in Physics Research A* 467–468:1572–1576.
- Chyba C. F., Thomas P. J., Brookshaw L., and Sagan C. 1990. Cometary delivery of organic-molecules to the early Earth. *Science* 249: 366-373.
- Chyba C. F. and Sagan C. 1992. Endogenous production, exogenous delivery and impact-shock synthesis of organic molecules: An inventory for the origins of life. *Nature* 355:125-132.
- Clancy R. T., Sandor B. J., and Moriarty-Schieven G. H. 2004. A measurement of the 362 GHz absorption line of Mars atmospheric H₂O₂. *Icarus* 168(1):116-121.
- Connerney J. E. P., Acuña M. H., Wasilewski P. J., Kletetschka G., Ness N. F., Rème H., Lin R. P., and Mitchell D. L. 2001. The global magnetic field of Mars and implications for crustal evolution. *Geophysical Research Letters* 28(21):4015-4018.
- Connerney J. E. P., Acuña M. H., Ness N. F., Kletetschka G., Mitchell D. L., Lin R. P., and Rème H. 2005. Tectonic implications of Mars crustal magnetism. *Proceedings of the National Academy of Sciences* 102(42):14970-14975.
- Cooper G. W. and Cronin J. R. 1995. Linear and cyclic aliphatic carboxamides of the Murchison meteorite - hydrolyzable derivatives of amino acids and other carboxylic acids. *Geochimica et Cosmochimica Acta* 59(5):1003-1015.
- Cottin H., Moore M. H., and Bénilan Y. 2003. Photodestruction of relevant interstellar molecules in ice mixtures. *Astrophysical Journal* 590(2):874-881.
- Cronin J. R., Pizzarello S., and Frye J. S. 1987. ¹³C NMR-spectroscopy of the insoluble carbon of carbonaceous chondrites. *Geochimica et Cosmochimica Acta* 51(2):299-303.
- Cronin J. R., Pizzarello S., and Cruikshank D. P. 1988. In *Meteorites and the early solar system*. Tucson: University of Arizona Press. pp. 819-857.
- Cronin J. R. and Chang S. 1993 In *The chemistry of life's origin*. Dordrecht: Kluwer Academic Publishers. pp. 209-258.
- Cronin J. R. and Pizzarello S. 1997. Enantiomeric excesses in meteoritic amino acids. *Science* 275(5302):951-955.
- Crovisier J. 2004. The molecular complexity of comets. In *Astrobiology: Future perspectives*, edited by Ehrenfreund P., Irvine W., Owen T., Becker L., Blank J., Brucato J., Colangeli L., Derenne S., Dutrey A., Despois D., Lazcano A. and Robert F. Dordrecht: Kluwer Academic Publishers.
- Cruikshank D. P., Roush T. L., Bartholomew M. J., Geballe T. R., Pendleton Y. J., White S. M., Bell J. F., Davies J. K., Owen T. C., de Bergh C., Tholen D. J., Bernstein M. P., Brown R. H., Tryka K. A., and Dalle Ore C. M. 1980. The composition of Centaur 5145 Pholus. *Icarus* 135(2):389-407.

Reference list

- Dundas I. 1998. Was the environment for primordial life hypersaline? *Extremophiles* 2:375-377.
- Edwards D. F. 1985. *Handbook of optical constants of solids-I*, edited by Palik E. D. Orlando: Academic Press. pp. 547.
- Ehrenfreund P. and Charnley S. B. 2000. Organic molecules in the interstellar medium, comets, and meteorites: a voyage from dark clouds to the early Earth. *Annual Review of Astronomy and Astrophysics* 38:427-83.
- Ehrenfreund P., Bernstein M. P., Dworkin J. P., Sandford S. A., and Allamandola L. J. 2001b. The photostability of amino acids in space. *Astrophysical Journal* 550:L95-L99.
- Ehrenfreund P., Glavin D., Botta O., Cooper G. W. G., and Bada J. B. 2001a. Extraterrestrial amino acids in Orgueil and Ivuna: Tracing the parent body of CI type carbonaceous chondrites. *Proceedings of the National Academy of Sciences* 98(5):2138-2141.
- Ehrenfreund P., Irvine W., Becker L., Blank J., Brucato J. R., Colangeli L., Derenne S., Despois D., Dutrey A., Fraaije H., Lazcano A., Owen T., and Robert F. 2002. Astrophysical and astrochemical insights into the origin of life. *Reports on Progress in Physics* 65:1427-1487.
- Encrenaz Th., Bézard B., Greathouse T. K., Richter M. J., Lacy J. H., Atreya S. K., Wong A. S., Lebonnois S., Lefèvre F. and Forget F. 2004b. Hydrogen peroxide on Mars: evidence for spatial and seasonal variations. *Icarus* 170(2):424-429.
- Encrenaz Th., Lellouch E., Atreya S. K., and Wong A. S. 2004a. Detectability of minor constituents in the martian atmosphere by infrared and submillimeter spectroscopy. *Planetary and Space Science* 52:1023-1037.
- Feldman W. C., Boynton W. V., Tokar R. L., Prettyman T. H., Gasnault O., Squyres S. W., Elphic R. C., Lawrence D. J., Lawson S. L., Maurice S., McKinney G. W., Moore K. R., and Reedy R. C. 2002. Global distribution of neutrons from Mars: results from Mars Odyssey. *Science* 297:75-78.
- Feldman W. C., Prettyman T. H., Boynton W. V., Murphy J. R., Squyres S., Karunatillake S., Maurice S., Tokar R. L., McKinney G. W., Hamara D. K., Kelly N., and Kerry K. 2003. CO₂ frost cap thickness on Mars during northern winter and spring. *Journal of Geophysical Research* 108(E9).
- Flynn G. J. and McKay D. S. 1988. Meteorites on Mars. Proceedings, Lunar and Planetary Inst., Workshop on Mars Sample Return Science. pp 77-78.
- Flynn G. and McKay D. S. 1990. An assessment of the Meteoritic Contribution to the martian Soil. *Journal of Geophysical Research* 95: 14497-14509.
- Flynn G. J. 1996. The delivery of organic matter from asteroids and comets to the early surface of Mars. *Earth, Moon and Planets* 72:469-474.

- Formisano V., Atreya S., Encrenaz T., Ignatiev N., and Giuranna M. 2004. Detection of methane in the atmosphere of Mars. *Science* 306: 1758-1761.
- Gardinier A., Derenne S., Robert F., Behar F., Largeau C., and Maquet J. 2000. Solid state CP/MAS C-13 NMR of the insoluble organic matter of the Orgueil and Murchison meteorites: Quantitative study. *Earth and Planetary Science Letters* 184 (1):9-21.
- Garry J. R. C., ten Kate I. L., Martins Z., Nørnberg P., and Ehrenfreund P. 2005. Analysis and survival of amino acids in martian regolith analogs. *Meteoritics & Planetary Science* Accepted 26 October 2005.
- Glavin D. P., Schubert M., Botta O., Kminek G., and Bada J. L. 2001. Detecting pyrolysis products from bacteria on Mars. *Earth and Planetary Science Letters* 185:1-5.
- Golden D. C., Ming D. W., Schwandt C. S., Morris R. V., Yang S. V., and Lofgren G. E. 2000. An experimental study on kinetically-driven precipitation of calcium-magnesium-iron carbonates from solution: Implications for the low-temperature formation of carbonates in martian meteorite Allan Hills 84001. *Meteoritics and Planetary Science* 35:457-465.
- Golombek M. P. 1997. The Mars Pathfinder Mission. *Journal of Geophysical Research* 102:3953-3965.
- Greenberg J. M. 1998. Making a comet nucleus. *Astronomy & Astrophysics* 330 (1): 375-380.
- Haskin. L. A., Wang A., Joliff B. L., McSween H. Y., Clark B. C., DesMarais D. J., McLennan S. M., Tosca N. J., Hurowitz J. A., Farmer J. D., Yen A. S., Squyres S. W., Arvidson R. E., Klingelhöfer G., Schröder C., de Souza P. A., Ming D. W., Gellert R., Zipfel J., Brückner J., Bell J. F., Herkenhoff K. E., Christensen P. R., Ruff S., Blaney D., Gorevan S., Cabrol N. A., Crumpler L., Grant J., and Soderblom L. 2005. Water alteration of rocks and soils on Mars at the Spirit rover site in Gusev crater. *Nature* 436:66-69.
- Hayes J. M. 1967. Organic constituents of meteorites - a review. *Geochimica et Cosmochimica Acta* 31(9):1395-1440.
- Heldmann J. and Mellon M. 2004. Observations of martian gullies and constraints on potential formation mechanisms. *Icarus* 168:285-304.
- Henning Th. and Salama F. 1998. Carbon - Carbon in the Universe. *Science* 282(5397):2204-2210.
- Herbst E. 1995. Chemistry in the interstellar-medium. *Annual Review of Physical Chemistry* 46:27-53.
- Herr K. C., Horn D., McAfee J. M., and Pimente G. C. 1970. Martian topography from Mariner 6 and 7 infrared spectra. *Astronomical Journal* 75(8):883-894.
- Hier S. W., Cornbleet T., and Bergeim O. 1946. The amino acids of human sweat. *Journal of Biological Chemistry* 166(1):327-333.

Reference list

- Hiroi T., Pieters C. M., Zolensky M. E., and Lipshutz M. E. 1993. Evidence of thermal metamorphism on the C-asteroid, G-asteroid, B-asteroid, and F-asteroid. *Science* 261(5124):1016-1018.
- Horowitz N. H., Hobby G. L., and Hubbard G. S. 1977. Viking on Mars - carbon assimilation experiments. *Transactions-American Geophysical Union* 58(8):829-829.
- Howe J. M., Featherstone W. R., Stadelman W. J., and Banwartz G. J. 1965. Amino acid composition of certain bacterial cell-wall proteins. *Applied Microbiology* 13 (5):650-652.
- Hu Ming-An, Disnar J. R., and Sureau J.-F. Organic geochemical indicators of biological sulphate reduction in early diagenetic Zn-Pb mineralization: the Bois-Madame deposit (Gard, France). 1995. *Applied Geochemistry* 10:419-435.
- Huguenin R. L., Miller K. J., and Harwood W. S. 1979. Frost-weathering on Mars: Exponential evidence for peroxide formation. *Journal of Molecular Evolution* 14:103-132.
- Huguenin R. L. 1982. Chemical-weathering and the Viking biology experiments on Mars. *Journal of Geophysical Research* 87(NB12):69-82.
- Hunten D. 1979. Possible oxidant sources in the atmosphere and surface of Mars. *Journal of Molecular Evolution* 14:71-78.
- Ihs A., Liedberg B., Uvdal K., Törnkvist C., Bodö P., and Lundström I. 1990. Infrared and photoelectron spectroscopy of amino acids on copper: glycine, L-alanine and β -alanine. *Journal of Colloid and Interface Science* 140(1):192-206.
- Irvine W. M. 1998. Extraterrestrial organic matter: A review. *Origins Of Life And Evolution Of The Biosphere* 28(4-6):365-383.
- Jull A. J. T., Courtney C., Jeffrey D. A., and Beck J. W. 1998. Isotopic evidence for a terrestrial source of organic compounds found in martian meteorites Allen Hills 84001 and Elephant Moraine 79001. *Science* 279:366-374.
- Karaiskou A., Vallance C., Papadakis V., Vardavas I. M., and Rakitzis T. P. 2004. Absolute absorption cross-section measurements of CO₂ in the ultraviolet from 200 to 206 nm at 295 and 373 K. *Chemical Physics Letters* 400:30-34.
- Kieffer H. H., Jakosky B. M., and Snyder C. M. 1992. The planet Mars: from antiquity to present. In *Mars*, edited by Kieffer H. H., Jakosky B. M., Snyder C. W., Matthews M. S. Tuscon: University of Arizona Press. pp. 1-33.
- Kirkland B. L., Lynch F. L., Rahnis M. A., Folk R. L., Molineux I. J., and McLean R. J. C. 1999. Alternative origins for nanobacteria-like objects in calcite. *Geology* 27:347-350.
- Kissel J. and Krueger F. R. 1987. The organic-component in dust from comet Halley as measured by the Puma mass-spectrometer on board Vega-1. *Nature* 326(6115):755-760.
- Klein H. P. 1978. The Viking biological experiments on Mars. *Icarus* 34:666-674.

- Klein H. P. 1979. The Viking biological investigation: general aspects. *Journal of Geophysical Research* 82:4677-4680.
- Klein H. P., Horowitz N. H., and Biemann K. 1992. In *Mars*, edited by Kieffer H. H., Jakosky B. M., Snyder C. W., Matthews M. S. Tuscon: University of Arizona Press. pp. 1221-1233.
- Klingelhöfer G., Morris R. V., Bernhardt B., Schröder C., Rodionov D. S., de Souza P. A. Jr., Yen A., Gellert R., Evlanov E. N., Zubkov B., Foh J., Bonnes U., Kankleit E., Gütlich P., Ming D. W., Renz F., Wdowiak T., Squyres S. W., and Arvidson R. E. 2004. Jarosite and hematite at Meridiani Planum from Opportunity's Mössbauer spectrometer. *Science* 306:1740-1745.
- Knoll A. H., Carr M., Clark B., Des Marais D. J., Farmer J. D., Fischer W. W., Grotzinger J. P., McLennan S. M., Malin M., Schröder C., Squyres S., Tosca N. J., and Wdowiak T. 2005. An astrobiological perspective on Meridiani Planum. *Earth and Planetary Science Letters* 240:179-189.
- Kral T. A., Bakkum C. R., and McKay C. P. 2004. Growth of methanogens on a Mars soil stimulant. *Origins of Life and Evolution of the Biosphere* 34:615-626.
- Krasnopolsky V. A., Maillard J. P., and Owen T. C. 2004. Detection of methane in the martian atmosphere: Evidence for life? *Icarus* 172: 537-547.
- Krishnamurthy R. V., Epstein S., Cronin J. R., Pizzarello S., and Yuen G. U. 1992. Isotopic and molecular analyses of hydrocarbons and monocarboxylic acids of the Murchison meteorite. *Geochimica et Cosmochimica Acta* 56(11):4045-4058.
- Kuiper. 1955. On the martian surface features. *Publications Of The Astronomical Society Of The Pacific* 67(398):271.
- Lenardic A., Nimmo F., and Moresi L. 2004. Growth of the hemispheric dichotomy and the cessation of plate tectonics on Mars. *Journal of Geophysical Research* 109:10.1029/2003JE002172.
- Levin G. V. and Straat P. A. 1977. Recent results from Viking labeled release experiment on Mars. *Transactions-American Geophysical Union* 58(8):829-829.
- Levin G. V. and Straat P. A. 1981. A search for a non-biological explanation of the viking labeled release life detection experiment. *Icarus* 45(2):494-516.
- Litchfield C. 1998. Survival strategies for microorganisms in hypersaline environments and their relevance to life on Mars. *Meteoritics and Planetary Science* 33:813-819.
- Longhi J., Knittle E., Holloway J. R., and Wäncke H. 1992. The bulk composition, mineralogy and internal structure of Mars. In *Mars*, edited by Kieffer H. H., Jakosky B. M., Snyder C. W., Matthews M. S. Tuscon: University of Arizona Press. pp. 184-208
- Luu J., Jewitt D., and Cloutis E. 1994. Near-infrared spectroscopy of primitive solar-system objects. *Icarus* 109(1):133-144.

Reference list

- Malin M. C. and Edgett K. S. 2000. Evidence for recent groundwater seepage and surface runoff on Mars. *Science* 288:2330-2335.
- Mancinelli R.L., White M.R., and Rothschild L. J. 1998. Biopan-survival I: exposure of the osmophiles *synechococcus* sp. (Nageli) and *haloarcua* sp. to the space environment, *Advances in Space Research* 22(3):327-334.
- Markhinin E. K. and Podkletnov N. E. 1977. The phenomenon of formation of prebiological compounds in volcanic processes. *Origins of Life and Evolution of the Biosphere* 8(3):225-35.
- Marov M. Ya. and Petrov G. I. 1973. Investigations of Mars from Soviet automatic stations Mars-2 and 3. *Icarus* 19(2):163-179.
- McDonald G. D., Thompson W. R., Heinrich M., Khare B. N., and Sagan C. 1994. Chemical investigation of Titan and Triton tholins. *Icarus* 108:137-145.
- McGenity T. J., Gemmell R. T., Grant W. D., and Stan-Lotter H. 2000. Origins of halophilic microorganisms in ancient salt deposits. *Environmental Microbiology* 2(3):243-250.
- McKay D. S., Gibson E. K. Jr., Thomas-Keprta K. L., Vali H., Romanek C. S., Clemett S. J., Chilliier X. D. F., Maechling C. R., and Zare R. N. 1996. Search for past life on Mars: Possible relic biogenic activity in martian meteorite ALH84001. *Science* 273:924-930.
- McKay C. P. 1997. The search for life on Mars. *Origins of Life and Evolution of the Biosphere* 27:263-289.
- Mendez C., Garza E., Gulati P., Morris P. A., and Allen C. C. 2005. Isolation and identification of microorganisms in JSC Mars-1 simulant soil. (abstract #2360). 36th Lunar and Planetary Science Conference. CD-ROM
- Millar T. J. 2004. Organic molecules in the instellar medium. In *Astrobiology: Future perspectives*, edited by Ehrenfreund P, Irvine W., Owen T., Becker L., Blank J., Brucato J., Colangeli L., Derenne S., Dutrey A., Despois D., Lazcano A. and Robert F. Dordrecht: Kluwer Academic Publishers.
- Mitrofanov I., Anfimov D., Kozyrev A., Litvak M., Sanin A., Tre'tyakov V., Krylov A., Shvetsov V., Boynton W., Shinohara C., Hamara D., and Saunders R. S. 2002. Maps of subsurface hydrogen from the High Energy Neutron Detector, Mars Odyssey. *Science* 297: 78-81.
- Möhlmann, D. 2002. Adsorption water in mid- and low-latitude martian soil. In: *ESA SP-518 Proc. Second European Workshop on Exo-/Astro-Biology Graz*, 1st ed., edited by H. Sawaya-Lacoste. Noordwijk: European Space Agency. pp. 169-172.
- Möhlmann D. 2004. Water in the upper martian surface at mid- and low-latitudes: presence, state, and consequences. *Icarus* 168:318-323.
- Möhlmann, D. 2005. The importance of adsorption water in the upper martian surface. (abstract #1120). 36th Lunar and Planetary Science Conference. CD-ROM
- Mustard J. F., Poulet F., Gendrin A., Bibring J.-P., Langevin Y.,

- Gondet B., Mangold N., Bellucci G., and Altieri F. 2005. Olivine and pyroxene diversity in the crust of Mars. *Science* 307:1594-1597.
- Nair H. M., Allen M., Anbar A. D., Yung Y. L. and Clancy R. T. 1994. A photochemical model of the martian atmosphere. *Icarus* 111:124-150.
- Naraoka H., Shimoyama A., Komiya M., Yamamoto H., and Harada K. 1988. Hydrocarbons in the Yamato-791198 carbonaceous chondrite from Antarctica. *Chemistry Letters* 5: 831-834.
- Neukum G., Jaumann R., Hoffmann H., Hauber E., Head J. W., Basilevsky A. T., Ivanov B. A., Werner S. C., van Gasselt S., Murray J. B., McCord T. and The HRSC Co-Investigator Team. 2004. Recent and episodic volcanic and glacial activity on Mars revealed by the High Resolution Stereo Camera. *Nature* 432:971-979.
- Nicholson W. L., Munakata N., Horneck G., Melosh H. J., and Setlow P. 2000. Resistance of *Bacillus* Endospores to Extreme Terrestrial and Extraterrestrial Environments. *Microbiology and Molecular Biology Reviews* 64(3):548-572.
- Nørnberg P., Schwertmann U., Stabjek H., Andersen T., and Gunnlaugsson H.P. 2004. Mineralogy of a burned soil compared with four anomalously red Quaternary deposits in Denmark. *Clay Minerals* 39:85-98.
- Norton C. F. and Grant W. D. 1988. Survival of halobacteria within fluid inclusions in salt crystals. *Journal of General Microbiology* 134: 1365-1373.
- Okabe H. 1978. Photochemistry of triatomic molecules. In: *Photochemistry of small molecules*, edited by Okabe H. New York: John Wiley & Sons.
- Oren A. 2002. *Halophilic microorganisms and their environments*. 1st ed, edition by Seckbach J. Dordrecht: Kluwer Academic Press.
- Oró J. and Holzer G. 1979. The photolytic degradation and oxidation of organic compounds under simulated martian conditions. *Journal of Molecular Evolution* 14:153-160.
- Owen T. 1992. Composition and early history of the atmosphere. In *Mars*, edited by Kieffer H. H., Jakosky B. M., Snyder C. W., Matthews M. S. Tucson: University of Arizona Press. pp. 818-834.
- Oyama V. I. and Berdahl B. J. 1977. The Viking Gas Exchange Experiments results from Chryse and Utopia surface samples. *Journal of Geophysical Research* 82:4669-4676.
- Oyama V. I. and Berdahl B. J. 1979. A model of martian surface chemistry. *Journal of Molecular Evolution* 14:199-210.
- Parkinson W. H. and Yoshino K. 2003. Absorption cross-section measurements of water vapor in the wavelength region 181-199 nm. *Chemical Physics* 294:31-35.
- Patel M. R., Zarnecki J. C., and Catling D. C. 2002. Ultraviolet radiation on the surface of Mars and the Beagle 2 UV sensor. *Planetary and Space Science* 50(9):915-927.

Reference list

- Peeters Z., Botta O., Charnley S. B., Ruitkamp R., and Ehrenfreund P. 2003. The astrobiology of nucleobases. *Astrophysical Journal* 593(2): L129-L132.
- Pfennig N. and Lippert K. D. 1966. Über das Vitamin B12-Bedürfnis phototropher Schwefel-bakterien. *Archiv Für Mikrobiologie* 55(3):245-256.
- Pierazzo E. and Chyba C. F. 1999. Amino acid survival in large cometary impacts. *Meteoritics and Planetary Science* 34:909-918.
- Ponnamperuma C., Shimoyama A., Yamada M., Hobo T., and Pal R. 1977. Possible surface-reactions on Mars - Implications for Viking biology results. *Science* 197(4302):455-457.
- Quinn R. C. and Zent A. P. 1999. Peroxide-modified titanium dioxide: A chemical analog of putative martian soil oxidants. *Origins of Life and Evolution of the Biosphere* 29(1):59-72.
- Quinn R.C. 2005d. Experimental characterization and in-situ measurement of chemical processes in the martian surface environment. PhD thesis. Leiden University, Leiden, the Netherlands.
- Quinn R. C., Ehrenfreund P., Grunthaler F. G., Taylor C. L., Zent A. P., 2005b Aqueous decomposition of organic compounds in the Atacama desert and in martian soils. in prep.
- Quinn R.C., Zent A. P., Ehrenfreund P., Taylor C. L., McKay C. P., Garry J. R. C., and Grunthaler F. J. 2005c. Dry acid deposition and accumulation on the surface of Mars and in the Atacama desert, Chile. (abstract #2282). 36th Lunar and Planetary Science Conference. CD-ROM.
- Quinn R. C., Zent A. P., McKay C. P. 2005a. The photochemical stability of carbonates on Mars. in prep.
- Rieder R., Gellert R., Anderson R. C., Brückner J., Clark B. C., Dreibus G., Economou T., Klingelhöfer G., Lugmair G. W., Ming D. W., Squyres S. W., d'Uston C., Wänke H., Yen A., and Zipfel J. 2004. Chemistry of rocks and soils at Meridiani Planum from the Alpha Particle X-ray Spectrometer. *Science* 306:1746-1749.
- Robl T. L. and Davis B. H. 1993. Comparison of the HF-HCl and HF-BF₃ maceration techniques and the chemistry of resultant organic concentrates. *Organic Geochemistry* 20(2): 249-255.
- Rosado M. T., Duarte M. L. T. S., and Fausto R. 1998. Vibrational spectra of acid and alkaline glycine salts. *Vibrational Spectroscopy* 16: 35-54.
- Rothschild L. J. 1990. Earth analogues for martian life. Microbes in evaporites: A new model system for life on Mars. *Icarus* 88:246-260.
- Rozenberg M., Shoham G., Reva I., and Fausto F. 2003. Low-temperature Fourier transform infrared spectra and hydrogen bonding in polycrystalline L-alanine. *Spectrochimica Acta Part A* 59:3253-3266.
- Ruitkamp R., Halasinski T., Salama F., Foing B. H., Allamandola L. J., Schmidt W., and Ehrenfreund P. 2002. Spectroscopy of large PAHs - Laboratory studies and comparison to the diffuse interstellar

- bands. *Astronomy & Astrophysics* 390(3):1153-1170.
- Rummel J. D. 2001. Planetary exploration in the time of astrobiology: Protecting against biological contamination. *Proceedings of the National Academy of Sciences* 98(5):2128-2131.
- Rummel J. D. and Billings L. 2004. Issues in planetary protection: Policy, protocol and implementation. *Space Policy* 20:49-54.
- Russell M. J. 1996. The generation at hot springs of sedimentary ore deposits, microbialites and life. *Ore Geology Reviews* 10:199-214.
- Sagan C., Thompson W. R., and Khare B. N. 1992. Titan - a laboratory for prebiological organic-chemistry. *Accounts of Chemical Research* 25 (7):286-292.
- Schramm L. S., Brownlee D. E. and Wheelock M. M. 1989. Major element composition of stratospheric micrometeorites. *Meteoritics* 24:99-112.
- Schubert G., Solomon S. C., Turcotte D. L., Drake M. J., and Sleep N. H. 1992. Origin and thermal evolution of Mars. In *Mars*, edited by Kieffer H. H., Jakosky B. M., Snyder C. W., Matthews M. S. Tuscon: University of Arizona Press. pp. 818-834.
- Schuerger A. C., Mancinelli R. L., Kern R. G., Rothschild L. J., and McKay C. P. 2003. Survival of endospores of *Bacillus subtilis* on spacecraft surfaces under simulated martian environments: implications for the forward contamination of Mars. *Icarus* 165:253-276.
- Schorghofer N. and Aharonson O. 2004. Stability and exchange of subsurface ice on Mars. (abstract #1463). 35th Lunar and Planetary Science Conference. CD-ROM.
- Sephton M. A. 2002. Organic compounds in carbonaceous meteorites. *Natural Product Reports* 19(3):292-311.
- Sheehan W. and Dobbins T.A. 2002. *Sky & Telescope* 7&10:12-16.
- Shemansky D. E. 1972. CO₂ extinction coefficient 1700-3000 Å. *Journal of Chemical Physics* 56(4):1582-1587.
- Skelley A. M., Scherer J. R., Aubrey A. D., Grover W. H., Ivester R. H. C., Ehrenfreund P., Grunthaler F. J., Bada J. L., and Mathies R. A. 2005. Development and evaluation of a microdevice for amino acid biomarker detection and analysis on Mars. *Proceedings of the National Academy of Sciences* 102(4):1041-1046.
- Smith D. 1992. The ion chemistry of interstellar clouds. *Chemical Reviews* 92(7):1473-1485.
- Smith D. E., Zuber M. T., Solomon S. C., Phillips R. J., Head J. W., Garvin J. B., Banerdt W. B., Muhleman D. O., Pettengill G. H., Neumann G. A., Lemoine F. G., Abshire J. B., Aharonson O., Brown C. D., Hauck S. A., Ivanov A. B., McGovern P. J., Zwally H. J., and Duxbury T. C. 1999. The global topography of Mars and implications for surface evolution. *Science* 284:1495-1503.
- Soffen, G.A. 1977. The Viking project. *Journal of Geophysical Research* 82:3959-3970.

Reference list

- Sorokin D. Y., Tourova T. P., and Muyzer G. M. 2005. Oxidation of thiosulfate to tetrathionate by an haloarchaeon isolated from hypersaline habitat. *Extremophiles*. DOI 10.1007/s00792-005-0465-0
- Southworth B. A. and Voelker B. M. 2003. Hydroxyl radical production via the photo-Fenton reaction in the presence of fluvic acid. *Environmental Science & Technology* 37:1130-1136.
- Squyres S. 1984. The history of water on Mars. *Annual Reviews of Earth and Planetary Sciences* 12:83-106.
- Squyres S. W., Arvidson R. E., Bell III J. F., Brückner J., Cabrol N. A., Calvin W., Carr M. H., Christensen P. R., Clark B. C., Crumpler L., Des Marais D. J., d'Uston C., Economou T., Farmer J., Farrand W., Folkner W., Golombek M., Gorevan S., Grant J. A., Greeley R., Grotzinger J., Haskin L., Herkenhoff K. E., Hviid S., Johnson J., Klingelhöfer G., Knoll A. H., Landis G., Lemmon M., Li R., Madsen M. B., Malin M. C., McLennan S. M., McSween H. Y., Ming D. W., Moersch J., Morris R. V., Parker T., Rice Jr. J. W., Richter L., Rieder R., Sims M., Smith M., Smith P., Soderblom L. A., Sullivan R., Wänke H., Wdowiak T., Wolff M., and Yen A. 2004a. The Spirit Rover's Athena Science Investigation at Gusev Crater, Mars. *Science* 305:794-799.
- Squyres S. W., Arvidson R. E., Bell III J. F., Brückner J., Cabrol N. A., Calvin W., Carr M. H., Christensen P. R., Clark B. C., Crumpler L., Des Marais D. J., d'Uston C., Economou T., Farmer J., Farrand W., Folkner W., Golombek M., Gorevan S., Grant J. A., Greeley R., Grotzinger J., Haskin L., Herkenhoff K. E., Hviid S., Johnson J., Klingelhöfer G., Knoll A. H., Landis G., Lemmon M., Li R., Madsen M. B., Malin M. C., McLennan S. M., McSween H. Y., Ming D. W., Moersch J., Morris R. V., Parker T., Rice Jr. J. W., Richter L., Rieder R., Sims M., Smith M., Smith P., Soderblom L. A., Sullivan R., Wänke H., Wdowiak T., Wolff M., and Yen A. 2004b. The Opportunity Rover's Athena Science Investigation at Meridiani Planum, Mars. *Science* 306:1698-1703.
- Squyres S. W., Grotzinger J. P., Arvidson R. E., Bell J. F. III, Calvin W., Christensen P. R., Clark B. C., Crisp J. A., Farrand W. H., Herkenhoff K. E., Johnson J. R., Klingelhöfer G., Knoll A. H., McLennan S. M., McSween H. Y. Jr., Morris R. V., Rice J. W. Jr., Rieder R., and Soderblom L. A. 2004c. In situ evidence for an ancient aqueous environment at Meridiani Planum, Mars. *Science* 306:1709-1714.
- Stan-Lotter H., McGenity T. J., Legat A., Denner E. B. M., Glaser K., Stetter K. O., and Wanner G. 1999. Very similar strains of *Halococcus salifodinae* are found in geographically separated Permo-Triassic salt deposits. *Microbiology* 145:3565-3574.
- Sternovsky Z., Robertson S., Sickafoose A., Colwell J., and Miha'ly Hora'nyi, M. 2002. Contact charging of lunar and martian dust simulants. *Journal of Geophysical Research* 107 (E11):5105-5113.
- Stoker C. R. and Bullock M. A. 1997. Organic degradation under simulated Martian conditions. *Journal of Geophysical Research* 102(E5): 10881-10888.
- Stoks P. G. and Schwartz A. W. 1979. Uracil in carbonaceous meteorites. *Nature* 282(5740): 709-710.
- Stoks P. G. and Schwartz A. W. 1981. Nitrogen-heterocyclic

- compounds in meteorites - Significance and mechanisms of formation. *Geochimica et Cosmochimica Acta* 45(4):563-569.
- Stoks P. G. and Schwartz A. W. 1982. Basic nitrogen-heterocyclic compounds in the Murchison meteorite. *Geochimica et Cosmochimica Acta* 46(3):309-315.
- Tanaka K. L., Scott D. H., and Greeley R. 1992. Global stratigraphy. In *Mars*, edited by Kieffer H. H., Jakosky B. M., Snyder C. W., Matthews M. S. Tuscon: University of Arizona Press. pp. 345-382.
- ten Kate, I. L., Ruiterkamp R., Botta O., Lehmann B., Gomez Hernandez C., Boudin N., Foing B. H., and Ehrenfreund P. 2003. Investigating complex organic compounds in a simulated Mars environment. *International Journal of Astrobiology* 1(4):387-399.
- ten Kate I. L., Garry J. R. C., Peeters Z., Quinn R., Foing B., and Ehrenfreund P. 2005. Amino acid photostability on the Martian surface. *Meteoritics & Planetary Science* 40(8):1185-1193.
- ten Kate I. L., Garry J. R. C., Peeters Z., Foing B., and Ehrenfreund P. 2006. The effects of martian near surface atmospheric conditions on the photochemistry of amino acids [submitted].
- Thomas P. C., Malin M. C., Edgett K. S., Carr M. H., Hartmann W. K., Ingersoll A. P., James P. B., Soderblom L. A., Ververka J., and Sullivan R. 2000. North-south geological differences between the residual polar caps on Mars. *Nature* 404:161-164.
- Thomas-Keprta K. L., Clemett S. J., Bazylinski D. A., Kirschvink J. L., McKay D. S., Wentworth S. J., Vali H., Gibson E. K. Jr., McKay M. F., and Romanek C. S. 2001. Truncated hexa-octahedral magnetite crystals in ALH84001: Presumptive biosignatures. *Proceedings of the National Academy of Science* 98-5:2164-2169.
- Thomas-Keprta K. L., Clemett S. J., Bazylinski D. A., Kirschvink J. L., McKay D. S., Wentworth S. J., Vali H., Gibson E. K. Jr., and Romanek C. S. 2002. Magnetofossils from ancient Mars: a robust biosignature in the Martian meteorite ALH84001. *Applied and Environmental Microbiology* 68(8):3663-3672.
- Thompson B. A., Harteck P., and Reeves, R. R. Jr. 1963. Ultraviolet absorption coefficients of CO₂, CO, O₂, H₂O, N₂O, NH₃, NO, SO₂, and CH₄ between 1850 and 4000 Å. *Journal of Geophysical Research* 68(24):6431-6436.
- Tielens A. G. G. M., Hony S., van Kerckhoven C., and Peeters E. 1999. Interstellar and circumstellar PAHs. *ESA-Special Publication* 427:579-586.
- Titus, N., Kieffer, H. H., and Christensen, P. R. 2003. Exposed water ice discovered near the south pole of Mars. *Science* 299:1048-1051.
- Uvdal K., Bodö P., Ihs A., Liedberg B., and Salaneck W. R. 1990. X-Ray photoelectron and infrared spectroscopy of glycine adsorbed upon copper. *Journal of Colloid and Interface Science* 140(1):207-216.
- Veverka J., Noland M., Sagan C., Pollack J., Quam L., Tucker R., Eross B., Duxbury T., and Green W. 1974. Mariner 9 atlas of moons of Mars. *Icarus* 23(2):206-289.

Reference list

- Yamaguchi M., Miyamaru F., Yamamoto K., Tani M., and Hangyo M. 2005. Terahertz absorption spectra of L-, D-, and DL-alanine and their application to determination of enantiometric composition. *Applied Physics Letters* 86:053903-1-3.
- Yen A. S., Gellert R., Schröder C., Morris R. V., Bell J. F., Knudson A. T., Clark B. C., Ming D. W., Crisp J. A., Arvidson R. E., Blaney D., Brückner J., Christensen P. R., DesMarais D. J., de Souza P. A., Economou T. E., Ghosh A., Hahn B. C., Herkenhoff K. E., Haskin L. A., Hurowitz J. A., Joliff B. L., Johnson J. R., Klingelhöfer G., Madsen M. B., McLennan S. M., McSween H. Y., Richter L., Rieder R., Rodionov D., Soderblom L., Squyres S. W., Tosca N. J., Wang A., Wyatt M. and Zipfel J. 2005. An integrated view of the chemistry and mineralogy of martian soils. *Nature* 436:49-54.
- Yen A. S., Kim S. S., Hecht M. H., Frant M. S., and Murray B. 2000. Evidence that the reactivity of the martian soil is due to superoxide ions. *Science* 289:1909-1912.
- Yeomans D. 2000. Small bodies of the solar system. *Nature* 404(6780): 829-832.
- Yoder C. F., Konopliv A. S., Yuan D. N., Standish E. M., and Folkner W. M. 2003. Fluid core size of mars from detection of the solar tide. *Science* 300:299-303.
- Zent A. P. and McKay C. P. 1994. The chemical reactivity of the martian soil and implications for future missions. *Icarus* 108:146-157.
- Zent A. P., Quinn R. C., Grunthaner F. J., Hecht M. H., Buehler M. G., McKay C. P., and Ricco A. J. 2003. Mars atmospheric oxidant sensor (MAOS): an in-situ heterogeneous chemistry analysis. *Planetary and Space Science* 51:167-175.
- Zhao M. and Bada J. L. 1995. Determination of α -dialkylamino acids and their enantiomers in geological samples by high-performance liquid chromatography after derivatization with a chiral adduct of o-phthalaldehyde. *Journal of Chromatography A* 690:55-63.
- Zinner E. 1988. In *Meteorites and the Early Solar System*. Tuscon: University of Arizona Press. pp. 956-983.
- Zolotov M. Y. and Shock E. L. 2000. An abiotic origin for hydrocarbons in the Allan Hills 84001 martian meteorite through cooling of magmatic and impact-generated gases. *Meteoritics and Planetary Science* 35:629-638.

Curriculum vitae

Op vrijdagmiddag 30 april 1976, tijdens het koninklijk defilé ter ere van de 67^{ste} verjaardag van de toenmalige koningin Juliana, werd ik geboren in het Ikazia ziekenhuis in Rotterdam. Na het doorlopen van de Oranjeschool in Spijkenisse en het Marnix Gymnasium in Rotterdam, begon ik in 1993 aan de studie Luchtvaart- en Ruimtevaarttechniek aan de TU Delft. Een keuze ingegeven door mijn sterke voorliefde voor ruimtevaart. In 1998 heb ik 4 maanden gewerkt aan de performance analyse van de Ariane 4 en Ariane 5, als stageopdracht bij Arianespace, Evry, Frankrijk. Ik ben afgestudeerd bij de Baanmechanica/Astrodynamica vakgroep bij prof. ir. B. A. C. Ambrosius. Mijn afstudeeronderwerp betrof het ontwerp van een mathematisch model voor een 'aerocapture' manoeuvre rond de planeet Mars. Deze opdracht heb ik uitgevoerd onder leiding van prof. dr. K. D. Mease van het Flight Dynamics and Control Lab, Faculty of Mechanical and Aerospace Engineering, University of California, Irvine. Op 1 oktober 1999 heb ik mijn ingenieursdiploma behaald. Na het afronden van mijn studie heb ik bij het Nationaal Lucht- en Ruimtevaartlaboratorium (NLR) in de Noordoostpolder gewerkt. Hier heb ik meegewerkt aan de validatie van het Europese satellietnavigatiesysteem GalileoSat. Het werd mij echter duidelijk dat ik onderzoek wilde gaan doen op een ander vlak. In november 2001 ben ik begonnen aan mijn promotieonderzoek bij de Sterrewacht en het Leids Instituut voor Chemisch Onderzoek van de universiteit van Leiden. De resultaten van dit onderzoek staan in dit proefschrift beschreven. Tijdens mijn promotieonderzoek heb ik mijn werk gepresenteerd op verschillende wetenschappelijke congressen in Noordwijk, Potsdam (Duitsland), Nice (Frankrijk), Oaxaca (Mexico), Houston (VS), Graz en Wenen (Oostenrijk), Ischia en Sicilië (Italië), en Honolulu (Hawaii). Ook heb ik nog verschillende populair wetenschappelijke lezingen gegeven. Na mijn promotie hoop ik mijn werk voort te kunnen zetten in de vorm van postdoctoraal onderzoek.

Nawoord

Gelukkig bestaat er een nawoord om iedereen te bedanken die mij geholpen heeft de afgelopen 4 jaar. Zonder al die mensen om mij heen was het leven toch een stuk minder vrolijk geweest!

Fleur, bedankt dat je 4 jaar lang zo goed op mijn fietsje hebt gepast! Fijn dat ik toch altijd even langs kon waaien, ondanks dat onze vrijdagmiddagthee een beetje in de soep liep. Kees, naast alle morele support in de laatste 3 maanden, is het je ook nog eens gelukt om mij te bekeren tot je appeltjesgeloof! Bas H., 1,5 jaar wijze lessen heeft me helaas (nog) geen blik opgeleverd, maar wel een heldere kijk op roeien én op mijn promotie. Florian, I didn't know that halophiles could be that much fun! Bernard and Bernd thanks for the Mars chamber patience and support. Astrobio's (James, Nick, Richard, Oliver, Zan, Zita), could there be any better group? James, thanks for keeping up with my moderate temper and always sunny moods! Fortunately, you never had to experience flying water bottles. Zan, klaagmuur, wandelende encyclopedie, paranimf. Je hebt het er maar druk mee. Martine, samen kun je meer dan 1 alleen, zelfs in de skiff.

Letty, Wijnand, omi, pa en moe Rijkaart, Margreet en Ingver, bedankt dat jullie mij, naast jullie nooit aflatende interesse, ook met twee benen op de aardbodem hebben gehouden! Letty, mijn allerliefste zussie, fijn dat je mijn paranimf bent! Papa en mama, waar was ik geweest zonder jullie! Zonder mijn van papa geërfd interesses en mama's gevoel voor logische werktijden, zou ik het een stuk moeilijker gehad hebben de afgelopen 4 jaar.

Victor, zonder jou zou mijn ruimte om te varen maar leeg zijn.

Inge Loes, 2006

Additional publications

ten Kate I. L., Ruitkamp R., Botta O., Lehmann B., Gomez Hernandez C., Boudin N., Foing B. H., and Ehrenfreund P. 2002. Laboratory studies on complex organic molecules on Mars. Part I - Rationale. In: *Earth-like planets and moons. Proceedings of the 36th ESLAB Symposium, 3-8 June 2002, ESTEC, Noordwijk, The Netherlands*. ESA SP-514. Eds.: B. Foing, B. Battrick. Noordwijk: ESA Publications Division. pp. 293 - 296.

ten Kate I. L., Ruitkamp R., Botta O., Lehmann B., Gomez Hernandez C., Boudin N., Foing B. H., and Ehrenfreund P. 2002. Laboratory studies on complex organic molecules on Mars. Part II - Experimental set-up and related work. In: *Proceedings of the First European Workshop on Exo-Astrobiology, 16-19 September 2002, Graz, Austria*. ESA SP-518. Ed.: Huguette Lacoste. Noordwijk: ESA Publications Division. pp. 81-85.

ten Kate I. L., Ruitkamp R., Botta O., Lehmann B., Gomez Hernandez C., Boudin N., Foing B. H., and Ehrenfreund P. 2003. Simulations of martian surface and subsurface processes. (abstract #1313). 34th Lunar and Planetary Science Conference. CD-ROM

Garry J. R. C., ten Kate I. L., Ruitkamp R., Peeters Z., Lehmann B., Foing B. H., and Ehrenfreund P. 2004. Amino acid survival under ambient martian surface UV lighting (abstract #1686). 35th Lunar and Planetary Science Conference. CD-ROM

Garry J. R. C., ten Kate I. L., Ehrenfreund P., and Foing B. H. 2006. Response of organics to simulated martian conditions. In: *Microorganisms and the Martian Environment*. ESA SP. Submitted.

Lammer H., Wurz P., ten Kate I. L., and Ruitkamp R. 2002. Simulations of martian surface and subsurface processes. In: *Proceedings of the First European Workshop on Exo-Astrobiology, 16-19 September 2002, Graz, Austria*. ESA SP-518. Ed.: Huguette Lacoste. Noordwijk: ESA Publications Division. pp. 533-534.

